THE ISOTOPIC COMPOSITION OF Mg AND THE IMPLIED LIMITS ON ^{26}Al IN THE EARLY SOLAR SYSTEM; NUCLEOSYNTHESIS OF ^{26}Al; AND NUCLEOSYNTHETIC CHRONOLOGIES FOR THE GALAXY

Thesis by

David Norman Schramm

In Partial Fulfillment of the Requirements

for the Degree of

Doctor of Philosophy

California Institute of Technology

Pasadena, California

1971

(Submitted January 27, 1971)

ACKNOWLEDGEMENTS

I would like to thank G.J. Wasserburg for his constant advice and attention throughout this work. Among other things, he was able to show me that minute details can have gigantic results and that "snooping around" a problem can yield very exciting things. I would also like to thank W.A. Fowler for his ability to give me good psychological therapy as well as his readiness to give me inspiration and scientific advice throughout the course of this work. The author also wants to acknowledge every member of The Lunatic Asylum, past and present, and to repeat the acknowledgments of Sections 4, 5, and 6. In particular, D.S. Burnett, whose ability to be a walking, talking chart of the nuclides as well as a good friend, has proven to be invaluable. C. Bauman, P.C. Young, V. Derksen, and A. Massey were always available to diagnose and cure the ailments of the Lunatic. D.A. Papanastassiou did a great job in doctoring the Lunatic as well as giving sound scientific advice. F. Tera was able to teach me a knowledge and appreciation of chemical techniques that I never imagined existed before.

I would like to thank my co-authors, G.J. Wasserburg, J.C. Huneke, and F. Tera, for permission to use the published papers reproduced in Sections 4, 5, and 6 of this thesis.

The author was supported in part by a NDEA Fellowship for the years 1967-70 and by a NSF Fellowship for the year 1970-71. The research was supported by NSF grants GP-15911 and GP-9114. The

Lunatic was built under NSF grant GP-9114.

In addition, I would like to continue the long tradition in doctoral theses by dedicating this thesis to my wife and children for putting-up with the trials and tribulations of a student's family for all these years.

THE ISOTOPIC COMPOSITION OF Mg AND THE IMPLIED LIMITS ON ^{26}Al IN THE EARLY SOLAR SYSTEM; NUCLEOSYNTHESIS OF ^{26}Al; AND NUCLEOSYNTHETIC CHRONOLOGIES FOR THE GALAXY

By

David N. Schramm

ABSTRACT

A particular isotope pair of astrophysical interest, ^{26}Al-^{26}Mg, was investigated in detail. A high precision mass spectrometric technique was developed whereby Mg isotopic compositions could be analyzed to better than five parts in 10^4.

Feldspar (high Al, low Mg) mineral separates were carried out on several meteoritic and lunar samples. No anomalous ^{26}Mg values were found. Thus, there is no evidence for the existence of ^{26}Al at the formation of the solar system.

Upper limits on the possible amount of ^{26}Al at solidification in the extraterrestrial samples were calculated. These limits were used to estimate the maximum change in central temperature of a planetary object which could be produced by the ^{26}Al decay.

A review is given of the production mechanisms for ^{26}Al and it has been shown that a flux of at least 4×10^{18} protons/cm^2 is required to produce enough ^{26}Al to melt the cores of planetary objects.

The general problem of nucleosynthetic chronologies has been investigated. Nucleochronologies for the galaxy have been calculated using ^{235}U/^{238}U, ^{232}Th/^{238}U, ^{244}Pu/^{238}U (or preferably ^{244}Pu/^{232}Th),

and $^{129}I/^{127}I$. The systematics of the nucleochronologic equations are derived and it has been found that the mean age of the elements can be found from long-lived radioactive nucleii in a manner which is independent of the time dependent production rate. It has also been found that the interval between the termination of nucleosysthesis and the time of formation of solid bodies in the solar system can be determined model independently from the short-lived nucleii. In addition, some information on the time dependent shape of the production function can also be determined model independently.

TABLE OF CONTENTS

1. Introduction

Radioactive elements have for a long time given us information on astrophysical events (c.f. Rutherford, 1929, on the age of the earth). This present work investigates some of the details involved in finding information about the formation of the solar system and the age of the elements from radioactive nuclides. A particular isotope pair of astrophysical interest, ^{26}Al-^{26}Mg, is investigated in detail and the generalized problem is examined. To give a more logical development to the problem, the generalized problems of nucleosynthetic chronologies will be discussed first before going into the details of the ^{26}Al-^{26}Mg problem.

The main body of this thesis is in Sections 4, 5, and 6, which are unmodified versions of published papers. Sections 1, 2, and 3A are meant to be basically introductory material. Section 3B is a review of the nucleosynthesis of ^{26}Al. Section 6 is a complete discussion of experimental limits on the existance of ^{26}Al in the early solar system and the possible implications. The first appendix to Section 3 is a discussion of the calibration of the Lunatic I, mass spectrometer which was used for the ^{26}Al-^{26}Mg analysis. The second appendix to Section 3 goes into the mineral separation details of the ^{26}Al-^{26}Mg work reported on in Section 6.

In conjunction with the discussion of the generalized problems of nucleosynthetic chronologies, calculations were performed using the $^{235}U/^{238}U$, $^{232}Th/^{238}U$, $^{129}I/^{127}I$, and $^{244}Pu/^{238}U$ (or preferably $^{244}Pu/^{232}Th$), inferred to be present at the formation of the solar

system, to calculate the mean age of the elements, along with nucleochronologies for the galaxy. These calculations are summarized in Section 2 of this thesis with the details shown in Sections 4 and 5.

2. Summary of Nucleochronological Calculations

This section provides a brief summary of the results shown in Section 4, Nuclear Chronologies for the Galaxy by G.J. Wasserburg, David N. Schramm, and J.C. Huneke, published in The Astrophysical Journal (Letters) Vol. 157, (1969), p. L91-L96, and Section 5, Nucleochronologies and the Mean Age of the Elements, by David N. Schramm and G.J. Wasserburg, published in The Astrophysical Journal Vol. 162 (1970) p. 57-69. Section 4 shows detailed calculations of nucleochronologies using U^{235}/U^{238}, Th^{232}/U^{238}, Pu^{244}/U^{238}, and I^{129}/I^{127}; while Section 5 gives the systematics of the nucleochronologic equations and discusses model independent quantities.

The motivation for this work came from the work of Wasserburg, Huneke, and Burnett (1969 a,b), when they found a correlation between fission-like xenon anomalies and excess fission tracks in whitlockite, $Ca_3(PO_4)_5$, from the meteorite St. Severin. This observation, in conjunction with observations by other workers on excess fission tracks and anomalies in neutron-rich Xe isotopes, showed that a fissionable nucleus, R_x, existed at the time of formation of the solar system. This nucleus, R_x has tentatively been identified as Pu^{244} ($\tau_{1/2} = 8.18 \times 10^7$ yr.). This result also yielded that the $^{244}Pu/^{238}U$ ratio at the time when the whitlockite retained xenon was 1/30 assuming no Pu/U fractionation.

This data would not yield a consistant solution with the $^{235}U/^{238}U$ and $^{232}Th/^{238}U$ chronologies for the simple models of nucleosynthesis (e.g. YONI).

The work shown in Section 4 was then carried out to find what models would give consistant solutions for the new R_x data with the $^{235}U/^{238}U$ and $^{232}Th/^{238}U$ data as well as the $^{129}I/^{127}I$ data determined from the ^{129}Xe anomaly (Hohenberg, Podosek, and Reynolds, 1967).

In working out a variety of models, it was found that there were certain systematics to the relevant equations. These systematics are derived and discussed in detail in Section 5. The basic ideas are briefly discussed in the following few paragraphs. For a more complete, detailed discussion of these ideas and their qualifiers, see Sections 4 and 5.

It is assumed that a nucleus (radioactive or stable), has been produced in some time-dependent manner, but always in the same proportion to some other nucleus produced in the same process. This production presumably goes on throughout the history of the galaxy until the matter forming the solar system separates from the galactic gas. The time period from onset of nucleosynthesis until separation of the solar system is called T. The production rate ($p(\tau)$) during this period is assumed to vary with time.

Following the separation of the solar system and termination of nucleosythetic activity, there is a time period Δ followed by the separation and cooling of planetary objects in the solar system.

During this period Δ, there is no further production since the matter has been separated from the galactic gas; but, the radioactive nuclides will still be decaying. From meteorites, the relative abundances of some nucleii (radioactive and stable) can be determined at the time of solidification. From theoretical calculations, (e.g. Seeger, Fowler, and Clayton, 1965) estimates of the relative production rates can be made. Note the these calculations are rather uncertain as is demonstrated by Seeger and Schramm (1970), who showed that the mean production ratio for r-process calculations from various empirical mass laws was approximately the same as the ratio of progenitors.

For each radioactive species (taken relative to another species, preferably a stable or long-lived isotope), an equation is obtained with unknowns T, Δ , and the time dependent production function $p(\tau)$. (See Section 4, eq. 2 and, in more general terms, Section 5, eq. 3.) Several radioactive species yield a system of simultaneous equations in Δ , T and $p(\tau)$. Each equation in the system differs from the others in that it has different decay constants (λ_i) and different physical constants:

$$R(i,j,) \equiv \frac{P_i/P_j}{N_i(T+\Delta)/N_j(T+\Delta)}$$

where P_i/P_j is the relative production rate and $N_i(T+\Delta)/N_j(T+\Delta)$ is the relative abundance at the time of solidification of bodies in the solar system.

Section 5 derives certain general relations which can be obtained from the system of equations independent of $p(\tau)$. These relations fall into three catagories: long-lived isotopes ($\lambda T \leq 1$); short-lived isotopes ($\lambda T \gg 1$); and intermediate lived isotopes. It is shown that the long-lived isotopes, taken relative to stable isotopes determine $T - \langle\tau\rangle$ where:

$$\langle\tau\rangle = \frac{\int_0^T \xi P(\xi)\, d\xi}{\int_0^T P(\xi)\, d\xi}$$

Thus, $T - \langle\tau\rangle$ is the mean age of the elements at the time of separation of the solar system from the galactic gas. This average age is determined completely independent of $p(\tau)$ for $\lambda T \ll 1$. For most models studied $T - \langle\tau\rangle$ has only small dependence ($\sim$10%) on $p(\tau)$ even if $\lambda T \sim 1$. The actual value of T, however, has been found to be extremely model dependent.

Short-lived nucleii give information on the free decay time Δ and the value of $p(T)$ (production rate at the termination of nucleosynthesis) relative to the total integral of $p(\tau)$, $T \cdot \langle p \rangle$. If two or more short lived nucleii are used, these two quantities Δ and $p(T)/T \cdot \langle p \rangle$ can be determined independent of $p(\tau)$. (Note in determining these quantities an assumption must be made as to whether $p(\tau)$ is spiked or smooth in the neighborhood of $\tau = T$. See Section 5.)

From an expansion of $p(\tau)$ about T, it is found that the intermediate-life nucleii give information on the shape of $p(\tau)$. If a particular model is chosen and the equations examined for a consistant solution, a solution will be found only when the model has built into it the constraints found from the model independent analysis.

Section 4 is a discussion of the applicability of several models to the $^{129}I/^{127}I$, $^{244}Pu/^{238}U$, $^{235}U/^{238}U$, and $^{232}Th/^{238}U$ equations with selected R(i,j) values. These nucleii are all r-process nucleii. The r-process presumably takes place in supernovae, (Hoyle and Fowler, 1960); thus, the production function, $p(\tau)$, would be the distribution in time of supernovae.

The short-lived constraints affecting the end of nucleosynthesis

and the free decay time come from $^{129}I/^{127}I$ and $^{244}Pu/^{238}U$. (Note that it would be better to take ^{244}Pu relative to ^{232}Th rather than ^{238}U since ^{232}Th has a much longer half-life.) The long-lived constraint determining the mean age of the elements comes from $^{232}Th/^{238}U$. An intermediate-lived constraint comes from $^{235}U/^{238}U$.

Models are calculated for particular sets of parameters in Section 4. The reasons why the constraints yielded those particular results are discussed in Section 5. In particular, note the discussion in part IV of Section 5 where it is demonstrated that for models with $\lambda_{232}\, T \leq 1$, the mean age remains approximately constant while the total duration of nucleosynthesis, T, may vary considerably.

In part IV of Section 5, models are also discussed where $\lambda_{232}T \gg 1$. It is shown that there are no formal difficulties in constructing models where the dominant amount of nucleosynthesis took place over 100 billion years ago. Even with these long-time models, it is still necessary that the last few billion years before the formation of the solar system look approximately like the short-time, $\lambda_{232}T \leq 1$, models so that the radioactive parent-daughter constraints are satisfied.

A limit on these long-time models comes from the ratio of a radioactive nuclide to a stable nucleus. The stable nucleus acts as a total time integrator. As was shown by Wasserburg, Fowler, and Hoyle (1960), the $^{129}I/^{127}I$, thus can provide an upper limit of $\sim 3 \times 10^{13}$ yrs. Even this upper limit is not firm since in the preceeding discussion of models it has been assumed that the only way of reducing the density of a particular nuclide is by radioactive decay. To be more

general, the nucleochronologic model calculations should include the decay constant ω_g, representing gas loss due to astrophysical processes. (See discussion in part I, Section 5.) In particular, for these long-time models, the density of a nuclide would decrease due to the expansion of the universe. In Fowler and Hoyle (1960), it is shown that the effect of this expansion is equivalent to having $\omega_g = -3H$, where H is Hubble's constant $\sim 10^{-10}$ yr.$^{-1}$. Therefore, all nucleii, including stable ones, have effective decay times and so, there are no total time integrators. With no total time integrators, it is virtually impossible to put an upper limit on the age of elements from nucleochronologies. Any constraint on the upper limit to the age of the elements must therefore come from other astrophysical, cosmological or theological considerations. (In conjunction with non-zero values of ω_g, it should be noted that calculations have been performed for the exponential model, equation 19, Section 5, where the model decay constant ω_e, and the gas destruction constant ω_g combine to yield an effective decay constraint ω.)

The constraints of the calculations become much more strict if the R(i,j)'s are known accurately and if more nucleochronometers are used. At present, the uncertainities in the production ratios going into the R(i,j)'s are very great. (For example, the r-process production ratio for $^{129}I/^{127}I$ has been estimated to have values ranging from less than 1 all the way up to ~3 ; see Table 1, Sec. 5. Such a change, even for a short-lived isotope, has a profound effect on the possibility of nucleochronologic models.) Possibly

better methods for calculating these can be found.

Another current problem is the definite identification of R_x as ^{244}Pu. This can be done by measuring the Xe fission spectrum from the spontaneous fission of ^{244}Pu and comparing it with the spectrum of the observed fission Xe anomalies. It should be noted here, that the R_x is measured in meteorites only through its fission yield. It is also important to remember that in addition to the St. Severin fission Xe spectrum (Wasserburg, Huneke and Burnett, 1969 a,b) another fission type Xe spectrum has been reported (c.f. Rowe, 1968), and is called carbonaceous chondrite fission (CCF). It is possible that the St. Severin fission Xe spectra is not due to ^{244}Pu, but to some other fissioning nucleus with a half-life long enough so that it is still around after the interval Δ; for example, a long-lived superheavy ($Z \sim 114$).

Measuring elemental ratios which are representative of the solar system is a difficult problem. The uncertainities in the use of $^{232}Th/^{238}U$, are discussed in the appendix to Section 5. Along this line, there is also the problem of $^{244}Pu/^{238}U$ (assuming R_x is ^{244}Pu). Wasserburg,et. al. (1969 a,b), determined the $^{244}Pu/^{238}U$ ratio as 0.033 in the whitlockite mineral separate from the chondritic meteorite, St. Severin. Podosek (1970) determined the $^{244}Pu/^{238}U$ ratio for the same meteorite, but a whole rock sample. The ratio he obtained was 0.013, which agreed with whole rock measurements by Wasser-

burg, et. al. (1969 a,b). Whether the ratio in the mineral whitlockite, which retains Pu and U or the ratio in the whole rock, is representative of the solar system, is debatable. It also must be remembered that these are just measurements on a single meteorite. Work on the chondrite Guarena (Huneke et. al. 1970), seems to indicate results similar to those obtained for St. Severin. However, much more work needs to be carried out on many objects before a definite $^{244}Pu/^{238}U$ value for the solar system can be stated with confidence. It should be noted from the work shown in Sections 4 and 5, that $^{244}Pu/^{238}U$ ratios less than 0.033 make the nucleochronologic equations less restrictive with respect to allowed models. For example, for $^{244}Pu/^{238}U$ values near that of Podosek's 0.013, it is possible, within the uncertainities of the relative r-process production rates, to have a consistant solution for continuous uniform nucleosythesis. It should be remembered that the better ratio to determine would be $^{244}Pu/^{232}Th$ rather than $^{244}Pu/^{238}U$, since ^{232}Th has a much longer life, (see discussion in Section 5).

The addition of a new chronometer with a half-life much longer than ^{232}Th would, of course, be beneficial, since it could then be used to obtain the mean age of the elements in a model independent manner. One promising possibility is ^{187}Re-^{187}Os, (Clayton, 1964), which is discussed in Section 5. This would be a particularly good chronometer since all the quantities involved can be experimentally

determined, unlike the other chronometers investigated where the production ratio must be theoretically estimated. The ^{187}Re lifetime is much longer than the age of the universe for all cosmologies (other than steady state). Thus, the Re-Os chronology would make possible a determination of the mean age of the elements which is model independent.

The possibility of setting-up nucleochronologies for processes other than the r-process, should be more fully investigated. Sections 3 and 6 of this thesis investigate ^{26}Al-^{26}Mg which could possibly have yielded a chronology for a special p-process type event in the early history of the solar system, (see Section 3B for a discussion of ^{26}Al production). However, no evidence for ^{26}Al was found. The perennial question of using a ^{40}K/is chronology complicated by the fact that the production mechanisms for ^{40}K are not clear-cut. Clayton, (1964), discusses several other possible chronometers, including the lead isotopes and ^{87}Rb-^{87}Sr, as does Kohman, (1969). One possibility which has not been discussed, is ^{176}Lu ($\tau_{1/2} \approx 2.2 \times 10^{10}$yr.), which has p-process as well as s-process contributions which could possibly be separated to yield a chronometer.

In summary, it can be said that at present, with the four nucleochronometers, it is possible to obtain to fair approximation, the free decay separation time for the solar system and some information regarding the shape of the production function, $p(\tau)$, near the time of separation of the solar system; and, with the assumption that $\lambda_{232}\, T \leq 1$, it is also possible to get a good estimate for the mean age of the elements. It should also be noted that the numerical results are very sensitive to some of the relative production rates assumed.

Section 3. The Existence of ^{26}Al in the Early Solar System.

3A. Summary of ^{26}Al-^{26}Mg Problem

While the work of Sections 4 and 5 was being completed, Clarke et. al. (1970), reported finding an anomaly in ^{26}Mg which was interpreted to imply the existence of ^{26}Al ($t_{1/2}$ = 7.4 x 10^5 yr.), at the formation of solid bodies in the solar system. These workers attempted to define an early solar system chronology based on the $^{26}Al/Si$ ratio. Due to the short half-life of ^{26}Al, this would imply that nucleosynthesis occurred within a few million years of solidification of the meteorites. However, in Sections 4 and 5, it was shown that the time interval, Δ, between the end of galactic nucleosynthesis and the solidification of objects in the solar system was $\sim 10^8$ yrs. Thus, any ^{26}Al present in the solar system could not have been synthesized in galactic processes. Section 3B will review possible mechanisms for the production of ^{26}Al and discuss this assertion more thoroughly.

Due to the special production mechanisms and short-time scales involved, as well as the significance of ^{26}Al as a possible primordial heat source (c.f. Fish, Goles, and Anders, 1960), it was decided to check the results of Clarke, et. al. (1970).

The details of the experiment are given in Section 6. The basic idea is that ^{26}Mg produced by the decay of ^{26}Al will be associated with Al-rich areas in primitive matter (meteorites). The mineral phase feldspar is rich in Al with relatively little Mg, (see Section 6 on terrestrial feldspars). Thus, the experiment requires the separation

of very pure feldspar. (It must be very pure since other phases in meteorites are Mg rich.) Then, analyze the Mg isotopic composition to high precision and compare with the composition of terrestrial standards. It is important to note here, that if the ^{26}Mg from the decay of ^{26}Al equilibrated with the rest of the Mg in the solar system, it would then be impossible to detect any effect. An observation of a ^{26}Mg excess implies that the feldspar crystalized before all the ^{26}Al had a chance to decay. If the ^{26}Al decayed before crystalization, or if the feldspar melted after the decay, the excess ^{26}Mg would be equilibrated with the large amounts of common Mg present. It is worth remembering here that ^{26}Al is a heat source. If there were enough ^{26}Al to totally melt the object, it would equilibrate all the radiogenic ^{26}Mg up to the time of the melting. If a melt did occur, in order to see an effect, there would have to be enough ^{26}Al still around after the object cooled and re-crystalized to leave a measurable ^{26}Mg anomaly. Note that if only the core of an object melted, feldspars from the unmelted outer layers could still retain the evidence of ^{26}Al.

Clarke et. al. found ^{26}Mg anomalies as large as 4 to 6 parts per mil. Thus, in order to adequately carry out the experiment, it was necessary to run Mg isotopic

compositions to better than one part in a thousand. As is shown in Section 6, a technique of running Mg on a mass spectrometer was found such that the $^{26}Mg/^{24}Mg$ ratio could be determined to better than five parts in 10^4. This accuracy was verified using isotopically enriched standards, (see the part on enriched standards in Section 6). This procedure represents a major improvement in the method of carrying out isotopic abundance measurements on Mg, an element which in the past has proven notoriously difficult to analyze.

Feldspar separates were made for several classes of meteorites and three different lunar rocks. A brief discription of the separation procedure is given in Section 6. A more detailed description of the mineral separation procedure for each object is given in Appendix II of this section.

In addition to the separations performed at Caltech, Clarke et. al. (1970), were generous enough to send aliquots of some of their samples including the sample in which they obtained their largest effect.

It is shown in Section 6 that <u>no ^{26}Mg anomalies are found</u> for any samples including those received from Clarke et. al. (1970).

Limits on the maximum amount of ^{26}Al at the time of solidification are calculated for each object. From these limits, the maximum possible increase in central temperature due to ^{26}Al heating is

calculated for each object investigated. It is shown that there is no evidence for enough ^{26}Al to boil water, much less form a molten core , at the time when the feldspars solidified. This does not rule out the possibility that a few million years prior to solidification ^{26}Al could have been an effective heat source.

To further test the conclusions of Section 6 , it would be interesting to analyze other meteorites, particularly meteorites of other classes. Along this line of thought, an analysis of an unequilibrated (L3) chondrite Hallingeberg was attempted. It was found to be impossible to obtain a low Mg, high Al separate from this meteorite, see Appendix II. It therefore seems that the techniques used in this work will not apply to the more primitive unequilibrated meteorites.

It may be possible to improve the resulting limits by obtaining purer feldspar mineral separates. However, from the work with large single crystal terrestrial feldspars, (see Section 6), it appears that some feldspars have Mg in their lattice. The limit to a feldspar separate then would not have a Mg abundance of zero, but some finite value (probably about a few hundred to a thousand ppm).
The limits on ^{26}Al for the meteorites studied probably could not be improved by more than a factor of ~ 5 by means of better mineral separates even if all impurites were removed. (In the case of the silica inclusions in Colomera and the large crystalled achondrites

such as Moore County, the separates are probably already almost as pure as possible.) The most important experiments to be carried out in the future will probably revolve about finding somewhat more "primitive" planetary objects rather than a further refinement in technique. These objects would almost certainly have to be from small planetesimals or comets rather than large >100 km objects since the melting which would be generated by ^{26}Al in large objects would tend to destroy the evidence.

Further applications of the techniques discussed here might be to investigate integrated cosmic ray exposures. If objects exist with exposure age $\gtrsim 1.5 \times 10^9$ yrs., and feldspar separates with only a few hundred ppm Mg could be obtained, the exposure age could be determined, (see Section 6). In a slightly different vein, the precision mass spectrometric techniques developed here might be applied to the determination of nuclear reaction cross-sections when a Mg isotope is the final product. For the cases where the target was not Mg, it would be possible to detect the production of as few as 5×10^{12} atoms ^{26}Mg.

In conclusion, from the current state of knowledge given in Section 6, it can be stated that there is no evidence for the existence of ^{26}Al in the early solar system.

3B. Review of Methods of Producing ^{26}Al

Various estimates for the amount of ^{26}Al synthesized prior to the solidification of objects in the solar system have previously appeared in the literature. Clarke et. al. (1970) gave a brief review of some of these methods for estimating the ^{26}Al production. In this work, the problem will be discussed in somewhat greater detail.

The following are the reactions, based on solar system abundances, with their Q-values, which may be of importance in synthesizing ^{26}Al. The Q-values were computed using mass excesses tabulated by Lederer, Hollander and Perlman (1967).

^{26}Mg (p,n) ^{26}Al	Q = -4.8 MeV
^{27}Al (p,pn) ^{26}Al	Q = -13.1 MeV
^{28}Si (p,2pn) ^{26}Al	Q = -24.6 MeV
^{32}S (p,α2pn) ^{26}Al	Q = -31.6 MeV
^{27}Al (n,2n) ^{26}Al	Q = -13.1 MeV
^{28}Si (n,2np) ^{26}Al	Q = -24.6 MeV
^{32}S (n,α2np) ^{26}Al	Q = -31.6 MeV
^{23}Na (α,n) ^{26}Al	Q = -3.0 MeV
^{24}Mg (α,pn) ^{26}Al	Q = -14.7 MeV
^{25}Mg (α,p2n) ^{26}Al	Q = -22.0 MeV
^{26}Mg (α,p3n) ^{26}Al	Q = -33.1 MeV
^{27}Al (α,αn) ^{26}Al	Q = -13.1 MeV
^{27}Al (α,2p3n) ^{26}Al	Q = -41.4 MeV

$^{28}Si\ (\alpha,\alpha pn)\ ^{26}Al$ $\qquad$ Q = -24.6 MeV

$^{28}Si\ (\alpha,3p3n)\ ^{26}Al$ $\qquad$ Q = -52.9 MeV

It is important to note that reactions leading to $^{26}Si(\tau_{1/2}\approx 2$ sec.) are not included, since the ^{26}Si β^+ decays all lead to the 0^+ isomeric state of ^{26}Al rather than to the 5^+ ground state. The 0^+ isomer β^+ decays to ^{26}Mg (0^+) in ~6.4 sec. and thus, would contriute to ^{26}Mg rather than ^{26}Al, (see Fig. 1).

The above list of reactions includes p, n and α induced reactions. Due to the short-life of ^{26}Al relative to the $\sim 10^8$ yr. interval between the end of galactic nucleosynthesis and the solidification of objects in the solar system (see Sections 2, 4 and 5) the ^{26}Al searched for in the experiments of Section 6 would most likely have been made, if it ever existed, by reactions in the early solar system. These reactions would be primarily proton induced reactions from some high energy proton irradiation. Neutron reactions might also be of importance since secondary neutrons would be produced in substantial amounts by very high energy (greater than a few hundred MeV) protons. High energy secondary neutrons could interact since a 100 MeV neutron travels ~1 astronomical unit in a vacuum before decay. Alpha particle reactions, though probably not important in this type of early solar system irradiation ($\lesssim 10\%$), would be important for ^{26}Al production by spallation in cosmic rays and thus, have been included. Spallation reactions from iron group nucleii have also been investigated but are not shown above since contributions from the iron peak are found to be small.

As mentioned above, it is known from ^{129}I and ^{244}Pu that

there was an interval $\sim 10^8$ yr. between the last r-process nucleosynthesis and the retention of Xe gas in meteorites. The time of Xe retention is usually assumed to be the time of solidification of solid bodies in the solar system. In the heat source estimates made in Section 6, it was shown that it takes at least a $^{26}Al/Si$ ratio of 2×10^{-7} to melt the cores of a planetary object (radius $\geq$ 100 km.). It was also shown in Section 6 that it would be possible at best (the Moore Co. case), to detect $^{26}Al/Si > 10^{-8}$ by the techniques shown there. In Section 3A, it was mentioned that if an object totally melted, there would be no ^{26}Al record unless the object resolidified before $^{26}Al/Si$ was $<10^8$. Note that if the core melted, but the surface did not, then, the feldspars from the surface could still show ^{26}Mg anomalies, assuming no further equilibration occured. Since the ^{26}Al mean life is $\sim 10^6$ yrs., it would be impossible for there to be enough ^{26}Al around to melt objects or to detect at the time of Xe retention if the ^{26}Al were synthesized at the same time as the r-process nucleii. It therefore seems that ^{26}Al must be made by a local process in the solar system if it is to be detected by the method described in Section 6, or if it is going to melt the cores of objects near the time of final solidification.

It is possible, however, to invent models for the formation of the solar system which would allow ^{26}Al to be synthesized external to the solar system and still be an effective heat source. One possibility is to assume that final Xe gas retention occurs $\sim 10^8$ yrs. after objects solidified. Another is that the last r-process

contribution to the solar system occurred $\sim 10^8$ yrs. before the last nucleosynthetic event making ^{26}Al.

If ^{26}Al were made in an event prior to solar system formation, then planetary objects would have to solidify out of the ejecta from this event within a few million years, if ^{26}Al is to be an effective heat source. Since this time interval is so short, it seems to imply that for this model the planets formed during the contraction of the sun rather than being thrown out from the sun at some later time. If the event making the ^{26}Al did not make r-process nucleii, this could imply one of the following: 1. The interstellar gas, which mixed with the ejecta from the nucleosynthetic event to make the solar system,was enriched in the r-process elements relative to the current solar system abundances. Or, 2. The nucleosynthetic event also ejected r-process elements which had not been effected by the event, (e.g. an outer shell). This second case would imply the star formed with some r-process material and evolved to the time of the nucleosynthesis and ejection within $\sim 10^8$ yrs. in order to satisfy the r-process chronology constraint.

Assuming the interval implied from the Xe anomalies is representative of the time interval between the termination of galactic nucleosynthesis and the formation of solid objects in the solar system, then ^{26}Al, if present, would have to be synthesized locally. If the ^{26}Al is made in the solar system rather than out of it, it is then necessary to have a proton irradiation near the time when it is desired to use ^{26}Al as a heat source. Before going into these specialized mechanisms necessary to produce ^{26}Al in the early solar system, it is

interesting to review the production of ^{26}Al in other astrophysical situations. In conjunction with astrophysical production of ^{26}Al, it is interesting to note ratios can now be measured in stars using MgH lines (c.f. Branch, 1970). In fact, Branch indicates that $^{25}Mg/^{24}Mg$ and $^{26}Mg/^{24}Mg$ for sun spots seems to be greater than terrestrial and meteoritic values. If this isotopic composition is representative of the sun as a whole, the question then arises as to whether the sun spot mass spectrum for Mg or the meteoritic and terrestrial spectra is representative of the primordial gas out of which the solar system formed. A study of the nuclear processes which would be necessary to produce such a difference between the sun and planets has not been done. It is interesting to note, however, that if the sun spot isotopic composition was representative of the primordial gas, this might imply a massive (much greater than any heretofore proposed), homogeneous proton irradiation of the planetary material.

For most astrophysical circumstances, it is necessary to look into thermonuclear production processes. For most thermonuclear ^{26}Al production, the relevant reaction is:

$$^{26}Mg + p \rightleftarrows {}^{26}Al + n - 4.8 \text{ MeV},$$

since this reaction determines the relative abundance of ^{26}Al to the stable nucleus ^{26}Mg. In working out this reaction in detail, an interesting point to note is that the 0.229 MeV state of ^{26}Al decays to ^{26}Mg in 6.4 sec. (see Fig. 1). Thus, even with an infinite excess of protons, there will still be some ^{26}Mg in equilibrium with ^{26}Al. This can be seen from the equilibrium expression for the abundance of ^{26}Al relative to the abundance of ^{26}Mg after a few times the

half-life of the 0.229 MeV state:

$$\frac{[^{26}Al]}{[^{26}Mg]} = \frac{[p]}{[n]} \cdot \frac{G(^{26}Al)}{G(^{26}Mg)} \cdot \frac{\exp[-(4.8 \times 11.6/T_9)]}{\{1+\frac{[p]}{[n]} \exp[-(5.03 \times 11.6)/T_9]\}}$$

where T_9 is the temperature in 10^9°K and the G's are nuclear partition functions; that is, $G(^{26}Al) = 11 + 7 \exp\left(\frac{-0.418 \times 11.6}{T_9}\right) + \ldots$ and $G(^{26}Mg) = 1 + 5 \exp\left(\frac{-1.81 \times 11.6}{T_9}\right) + \ldots$ For cases of interest, the equilibrium expression reduces to:

$$\frac{[^{26}Al]}{[^{26}Mg]} \approx 11 \frac{[p]}{[n]} 10^{-24.2/T_9}$$

which is independent of the effect of the 0.229 MeV state.

Let us now look at some possible locations for the synthesis of ^{26}Al.

i. The Big Bang

The isotope, ^{26}Al, from the Big Bang would, of course, not be left over to the time when the solar system separated. (This duration would be the order of at least several billion years as can be seen from Sections 4 and 5.) However, if sufficiently large quantities were made in the Big Bang, there might be some remaining when the clusters formed $\sim 10^7$ yrs. after the Big Bang, (Peebles, and Dicke, 1968). It should, however, be impossible for any ^{26}Al left from the Big Bang to be around when the galaxies formed at $\sim 10^8$ yrs., (Peebles, 1967).

From Wagoner, Fowler, and Hoyle (1967), it is possible to determine the temperatures and relative neutron-proton abundance for nucleosynthesis in the Big Bang, so that the relative abundance of ^{26}Al to ^{26}Mg may be calculated using the equilibrium expression shown above. Assuming the 3° black body radiation is from the ex-

panded fireball, and that the deceleration parameter q_o is ≤ 3 (Sandage, 1961), we are then restricted to what Wagoner, Fowler, and Hoyle, (1967) refer to as "low density" universes and only the nuclei D, ^{3}He, ^{4}He, and ^{7}Li/(no Mg or Al) are produced in significant quantities. The temperature when most of nucleosynthesis occurs is then $\sim 0.5 < T_9 \lesssim 1$. The relative abundance of protons to neutrons is $10 \lesssim [p]/[n] \lesssim 10^7$, which yields $\frac{[^{26}Al]}{[^{26}Mg]} \lesssim 10^{-16}$. Thus, there is no ^{26}Al produced in the Big Bang.

ii. Little Bangs

Little Bangs are explosions from states of high temperature and density which may be associated with rapidly evolving supermassive stars and could have produced violent events during the formation and early history of the galaxy. These explosions are discussed by Wagoner, Fowler, and Hoyle, (1969), and by Wagoner, (1969). For these explosions, Wagoner (1969), finds that relative abundances of protons to neutrons of ~ 1 produce abundances of elements in rough agreement with those observed in most metal-weak stars and in our galaxy. For these more promising cases, Wagoner finds that the temperature (T_9), where nucleosynthesis of elements in the vicinity of Mg occurs, is ~ 2 to 3, which yields $\frac{[^{26}Al]}{[^{26}Mg]} \lesssim 10^{-7}$. Thus, as in the case of the Big Bang, though not as severe, no significant amount of ^{26}Al is produced in a little bang.

iii. Stellar Synthesis

a. Interiors - Synthesis of elements for $6 \lesssim Z \lesssim 14$, is thought to occur in explosive carbon burning as described by Arnett (1969).

This process occurring in exploding stars has been found to fit the elemental abundances in the above mentioned region. In addition, silicon burning as described by Bodansky, Clayton, and Fowler (1968), has been found to approximate the observed solar system abundances for $14 \lesssim Z \lesssim 26$. The combination of the two processes, which both occur in the same type of stellar explosion, can then explain the abundances for the nucleii which comprise 99% by mass of the elements heavier than He. The physical model is the following, according to Arnett (1969). In the late stages of the evolution of a massive star an instability causes explosive silicon burning. This silicon burning ignites the $^{12}C + {}^{12}C$ reaction in the surrounding region of the star composed of the products of helium burning. The release of of nuclear energy then causes a hydrodynamic expansion which disrupts the star, and ejects the products into the interstellar-medium.

Since ^{26}Al has Z=13, it is near the region where synthesis of elements by both explosive carbon burning and by silicon burning might be important, it seems logical to look at the production of ^{26}Al from both processes.

Arnett (1969), gives a range of temperatures, time scales, and the corresponding densities which would be characteristic conditions for explosive silicon burning. Bodansky, Clayton, and Fowler (1968), give a table relating the temperatures and densities which give the best match to the natural abundances of α-particle nucleii and the ratio $^{56}Fe/^{54}Fe$ for silicon burning. Bodansky et. al. (1968), also show the ratio [p]/[n] as a function of temperature and density. The optimum tem-

perature and density for silicon burning with regard to giving a good match to the abundances as well as fitting the characteristic conditions of explosive silicon burning (which in turn form the initial conditions for explosive carbon burning), is found to be $T_9 \approx 4.65$, $\rho \approx 10^9 g/cm^3$ and a time scale of ~ 0.03 sec. With this temperature and density, the proton-neutron ratio is $[p]/[n] = 10^{7.3}$ which yields for the quasi-equilibrium of silicon burning $\frac{[^{26}Al]}{[^{26}Mg]} \approx 1.4 \times 10^3$. Therefore, for this situation, almost all of mass 26 is made as ^{26}Al. Assuming a rapid expansion (supernova freeze-out) follows this quasi-equilibrium situation, it can be assumed that the relative abundance calculated above will be ejected into the interstellar media. This expansion must be rapid enough so that equilibrium is no longer maintained. Nuclear reactions during this freeze-out have been neglected.

Now let us see how much ^{26}Al there is relative to ^{28}Si following silicon burning. The equilibrium can be calculated as follows from

$$^{26}Al + p + n \rightleftarrows {}^{28}Si + 24.6 \text{ MeV}$$

The equilibrium abundance is

$$\frac{[^{26}Al]}{[^{28}Si]} = \frac{4 \; \frac{G[^{26}Al]}{G[^{28}Si]} \cdot \left[\frac{26}{28}\right]^{3/2}}{[n] \cdot [p]} \theta^2 \cdot \exp[-285/T_9]$$

where $\theta = \left[\frac{M_\mu \cdot kT}{2\pi\hbar^2}\right]^{3/2} = 5.94 \times 10^{33} \; T_9^{\,3/2} \; cm^{-3}$ (M_μ being the mass of 1 atomic mass unit), and $G[^{28}Si] = 1 + 5e^{-20.6/T_9} + \ldots \approx 1$. Thus,

$$\frac{[^{26}Al]}{[^{28}Si]} \approx \frac{1.4 \cdot 10^{70} \; T_9^{\,3} \cdot 10^{-124/T_9}}{[n] \; [p]}$$

From Bodansky et. al. (1986), for $T_9 = 4.65$, $\rho = 10^9$, our optimum case,

$[n] = 10^{21.7}$ cm^{-3} and $[p] = 10^{29}$ cm^{-3}. Thus, $\frac{[^{26}Al]}{[^{28}Si]} \approx 2.6 \times 10^{-6}$. It was mentioned previously that a ratio of $\frac{[^{26}Al]}{[^{28}Si]} \gtrapprox 2 \times 10^{-7}$ will melt the cores of planetary objects. This means that if terrestrial type planetary objects could form within 2.7×10^6 years out of the ejecta from a supernovae that had undergone Si-burning, the cores of these objects could be melted by ^{26}Al (assuming no reduction in the $^{26}Al/Si$ ratio by dilution).

In order to detect any ^{26}Al by the technique described in Section 6, it would be necessary for the feldspars to have solidified within ~6 million years of the supernovae explosion. The implications of this short time interval between galactic synthesis and solidification, were previously discussed in comparison with the $\sim 10^8$ yr. time interval implied by the Xe data.

For explosive carbon burning, Arnett (1969) has included ^{26}Al in his calculations. He indicates that $^{26}Al/^{26}Mg \sim 10^{-3}$ and $^{26}Al/^{28}Si \sim 10^{-3}$ for the ejecta from explosive carbon burning for the case that best fits solar system abundances ($T_9 = 1.8$, $\rho = 10^7$ g/cm^3). These results, however, cannot be reproduced with the simple equilibrium type calculation used above for silicon burning. The validity of Arnett's result is thus in question, however nonequilibrium freeze-out reactions may be involved. If the solar system were made entirely of the ejecta from Arnett's explosive carbon burning, objects could solidify $\sim 10^7$ yr. after the explosive carbon burning supernovae and still have ^{26}Al as an effective heat source. However, realistically, the ejecta from explosive

carbon burning would be diluted with the ejecta from Si-burning as well as outer unburned regions of the supernova and possibly interstellar gas before forming the solar system. If these other components to the solar system gas included Si, the $^{26}Al/Si$ ratio from carbon burning would be reduced by dilution before forming the solar system. Since Arnett (1969) has ^{28}Si under abundant with respect to the chondritic abundances of nearby elements by an order of magnitude in this $T_9 = 1.8$, $\rho = 10^7$ g/cm^3 event, it appears that the $^{26}Al/Si$ ratio would be reduced at least a factor of 10 by dilution prior to the solidification of solid bodies in the solar system.

b. Atmosphere of the stars- Nucleosynthesis of ^{26}Al in the outer envelope of stars would presumably take place by spallation reactions. There are no essential differences in regard to ^{26}Al production, between a proton irradiation of a gaseous pre-planetary nebula (as mentioned by Reeves and Audouze, 1968), and high energy proton reactions occurring in the outer envelope of the sun. Thus, discussions of spallation production of ^{26}Al in a gas will be postponed to the sections dealing with ^{26}Al synthesis in the solar system.

Note, if ^{26}Al is produced in the envelope of the early sun (possibly the T-Tauri phase), there is the problem of ejecting the material from the star and solidifing it within a few million years if the ^{26}Al

is to function as a significant heat source. The only other significant difference between the outer layers of the sun and the pre-planetary nebula, is that the sun would have much more hydrogen than the assumed chondritic composition pre-planetary nebula. This would mean that the target material may be somewhat shielded which would imply a higher flux in order to produce the same amount of ^{26}Al.

iv. Cosmic Rays

Before discussing the production of ^{26}Al in cosmic rays and in the solar system, it is important to look at the production cross-sections.

Various cosmic ray workers have tried to estimate the ^{26}Al production cross-sections. Little experimental data exist on the high energy production of ^{26}Al from the targets of interest. At high energy, $\gtrsim$100 MeV, there is little variation in spallation cross-sections with energy. Even at very high energy, $\gtrsim$1 GeV, the only significant effect is that there are larger contributions from target nucleii with large mass differences, ΔA, from the product, (see Miller and Hudis, 1959, for a discussion of this effect). In reference to ^{26}Al, this would mean a larger contribution from iron peak nucleii at extremely high energies. However, this additional contribution from the iron peak would still be small compared to the contribution from near-by targets. (See Rudstam, Stevenson and Folger, 1952, and Honda and Lal, 1960, for spallation cross-sections on iron.) Fuse and Anders (1969) have taken the observed ^{26}Al activity due to cosmic rays in meteorites and worked back to obtain estimates for the production rates on various target elements due to cosmic rays. Lavruhina, Kuznetsova and Satarova (1964) have taken a combination of what experimental data exist along with standard formulae for estimating spallation cross-sections to obtain a prediction of ^{26}Al activity in the center of a 10 cm radius chondritic meteorite due to cosmic ray production. The derived production cross-sections from the cosmic ray work can be used to estimate production of ^{26}Al

for any high energy flux since, as was already mentioned, the cross-sections should not vary substantially with energy. The semi-empirical formulae used by most workers for estimating spallation cross-sections are due to Rudstam (1956). (See Rudstam, 1966, for a more recent discussion.) The cross-section (σ) for an isotope (A,Z) is given by Rudstam as:

$$\ln \sigma (A,Z) = PA - Q - R (Z - SA)^2$$

where $P = 10.2\ E^{-0.63}$ (E in MeV), $R \approx 1.9$, and $S \approx 0.47$ are empirically determined parameters and the quantity Q can be estimated from the inelastic cross-section using the following relation;

$$e^{-Q} = P \cdot \sigma_{A_t} (\text{inelastic}) \left[\frac{E}{\pi}\right]^{1/2} \left\{e^{PA_t} - e^{PA_t/2}\right\}^{-1}$$

for cosmic radiations σ_{A_t}(inelastic) ≈ 0.75 times the geometrical cross-section for the target nucleus, A_t. If cross-section values are known at one or more energies, the shape of the excitation function can be obtained from the following relation (Arnold, Honda, and Lal, 1961),

$$\ln \sigma (E,A,Z) = \ln P - P\Delta A + C$$

where $\Delta A = A_t - A$ and C is the normalization constant. The above formulae are the ones used by Fuse and Anders (1969); Arnold, Honda and Lal, (1961); Honda and Lal, (1964); and most of the other workers who study ^{26}Al resulting from cosmic radiation. These formulae usually give results to within a factor of 2 of experimental values, where they exist. Lavruhina, et. al. (1964), use the following slightly different semi-empirical formulae (from Metropolis, et. al. 1956, and Dostrovsky et. al. 1958) to estimate the spallation cross-sections (σ) for the formation of an isobar, $A = A_t - \Delta A$;

$$\sigma(\Delta A, A_t) = \sigma_o A^{2/3} \frac{C_1 E^{-2/3}}{1+C_2 A} \cdot \exp\left[\frac{-C_1 E^{-2/3} \Delta A}{1+C_2 A}\right]$$

where σ_o = 60 mb, C_1 = 0.25, C_2 = 0.022, and E is in GeV. To determine the cross-section, for a particular nucleus (A,Z), they apply the following formula,

$$\sigma(A,Z) = \sigma(\Delta A\ ;\ A_t) \cdot \left(\frac{R}{\pi}\right)^{1/2} \exp\left[-R(Z-SA)^2\right]$$

where R and S are the Rusdtam parameters. (Note that ~1/2 of the mass 26 isobar goes to ^{26}Al.) Audouze, Ephere, and Reeves (1967) set-up a slightly different cross-section formula to be applied specifically to light nucleii, whereas the other formulae were derived for use with medium to heavy nucleii. Their formula explicitly puts in changes in isospin as well as changes in A. The results, however, are approximately the same as those obtained with the other formulae. (The Audouze, Ephere and Reeves, 1967, formula was used by Audouze and Reeves, 1968, for their estimate of the ^{26}Al production.)

Recently, Evans (1970) and Tanaka (1970) have experimentally measured the principle proton induced ^{26}Al production cross-sections at energies near threshold for the reactions studied. Evans was kind enough to release to me these unpublished preliminary data. The procedure used by Evans and Tanaka was to expose a thick target in a cyclotron; remove the target and take off various layers with a lathe. The energy is determined by the penetration depth. The layers are then counted for ^{26}Al using techniques similiar to those applied to meteorites. The cross-sections are evaluated relative to a ^{22}Na standard. These cross-sections are shown in Fig. 2 for ^{28}Si(p,2pn)^{26}Al, ^{27}Al(p,pn)^{26}Al, and ^{26}Mg(p,n)^{26}Al. (These lower

energy, experimental cross-section measurements are of particular significance to workers using the ^{26}Al observed in the lunar samples to determine the solar cosmic ray spectrum, S.H.R.E.L.L.D.A.L.F.F., 1970.) The high energy extrapolations shown there are based on curve shapes of analogous reactions.

It is interesting to compare the estimated cross-sections used in cosmic ray work with the high energy extrapolations of Figure 2. Fuse and Anders (1969) production is given in dpm/kg. These have been converted to an effective average cross-section in mb assuming a cosmic ray flux of 0.65 particles/cm^2·sec.·sr, (Wanke, 1960). The results are $\sigma_{Al} \approx 44$ mb, $\sigma_{Si} \approx 29$ mb, $\sigma_{Mg} \approx 0$, $\sigma_{S} \approx 4$ mb, $\sigma_{Fe+Ni} \approx 0.4$ mb. It should be noted that the Fuse and Anders calculations have implicitely built into them all forms of ^{26}Al production due to cosmic rays including effects of secondary neutrons. It is apparent that the high energy extrapolations of Figure 2 agree very well with the work of Fuse and Anders. The Fe cross-section has been measured by Lavruhina et. al. (1964) as 0.46 mb at 660 MeV and by Honda and Lal (1969) as 0.43 mb at 730 MeV, in good agreement with the above estimate. Lavruhina et. al. (1969) also give an estimate of $\sigma_{Al} \approx 44$ mb at 660 MeV.

For production of ^{26}Al in the cosmic ray flux, it should be noted that in these reactions, the heavy nucleus is the projectile, and interstellar hydrogen and helium are the targets. The relative abundance of Mg, Al and Si in the 50 to 200 MeV cosmic ray flux is $Mg/Si \approx 1.5$, and $Al/Si \approx 0.1$, (Meyer,1969). (It should be noted that a previous review, Ginzburg and Syrovatskii, 1964, give $Mg/Si \approx 2.9$ and $Al/Si \approx 0.6$.) Thus, the effective cross-section for ^{26}Al production

per silicon nucleus is,

$$(\sigma_{eff})_i \approx 1.5(\sigma_{Mg})_i + 0.1(\sigma_{Al})_i + (\sigma_{Si})_i$$

where i signifies either p or α. Using the high energy extrapolations shown in Figure 2, we can estimate $(\sigma_{eff})_p \approx 34$ mb. (Ginzberg and Syrovatskii's abundances would yield $(\sigma_{eff})_p \approx 53$ mb.) (Note that from Rudstam-type formulae, we know that the production of ^{26}Al in spallation reactions is about half of the mass 26 isobar.) From a determination of the stable secondary nuclear components, (e.g. Li, Be and B), in the cosmic ray flux, the amount of interstellar matter traversed by cosmic ray particles during their life time can be estimated. Meyer (1969) gave a value for this thickness of 3 to 5 g/cm^2. Using the above extimate for the cross-section, a thickness estimate of 3 g/cm^2, and neglecting ^4He which may induce an error of 25%, an estimate of the $^{26}Al/Si$ ratio in cosmic rays is $^{26}Al/Si \approx 0.06 \frac{\tau_{26}}{\tau_{C.R.}}$ where $\tau_{26}=1.07 \times 10^6$ yr. and $\tau_{C.R.}$ is the meanlife of the cosmic rays. (The above estimate assumes $\tau_{26} \ll \tau_{C.R.}$) As mentioned by Shapiro and Silberberg (1970), the importance of the production of ^{26}Al in cosmic rays is that if techniques were ever developed to resolve ^{26}Al, ^{27}Al, and ^{26}Mg in cosmic rays, it would then be possible to use the abundance of ^{26}Al to determine the age of the cosmic rays.

V. Solar System Synthesis

Most authors discussing the synthesis of ^{26}Al have used models involving a high energy proton irradiation in the early history of the solar system, (c.f. Fowler, Greenstein and Hoyle, 1962, here-

after referred to as FGH.) As mentioned previously, this type of production seems to be the most likely way to produce ^{26}Al during the early stages of the solar system.

These models usually assume the early sun was more active than the present sun and thus, could produce large numbers of high energy protons in the then frequent solar flares or disturbances. The magnitude of the flux is usually determined by normalization such that the observed abundance for some other nucleus (or nucleii) which is presumably produced in the same process would be fit. FGH and Reeves and Audouze (1968) use the light nucleii, (Li, Be, and B) for this purpose. Recent work, (Reeves, Fowler, and Hoyle, 1970), has shown that it is not necessary for Li, Be, and B to be produced in a special process in the formation of the solar system, but may, in fact, be produced by interstellar cosmic rays.

Anders (1964) normalizes the flux so as to produce the amount of ^{129}I (^{129}Xe anomaly) measured in the Abee meteorite. In Section 4 of this thesis it is shown that ^{129}I produced galactically in the r-process can explain the ^{129}Xe anomalies without any nucleochronologic difficulties. In fact, it is shown that if ^{129}I were produced locally, this would imply a time even longer than $\sim 10^8$ yr. between the end of r-process synthesis and the time of solidification.

Fish, Goles, and Anders (1960) did not bother to estimate a flux itself, but merely estimated the ^{26}Al abundance from the Suess and Urey (1956) element abundance table. Therefore, they do not specify any particular production model nor do they discuss

the time scale problems.

Since no ^{26}Al has been observed and all other isotopic effects observed can be explained without invoking some special process, it appears that there is no a priori reason to have such a flux. However, as mentioned previously, if there were ^{26}Al at the time of solidification of objects in the solar system, a high energy proton flux would be required to explain its existence so long after the termination of galactic nucleosythesis. This flux would have to be uniform throughout the region of the solar system producing the meteorites as well as the earth. (See Burnett, Lippolt and Wasserburg, 1966, on ^{40}K, Balsiger, Geiss, and Lipshutz, 1969, on ^{50}V and Eugster, Tera, Burnett and Wasserburg 1970, on Gd; where limits on the non-uniformity of integrated proton and neutron fluxes are obtained.)

The target material which is irradiated in the early solar system is assumed to be chondritic. [17%/Si, 1.1% Al, 14% Mg, (which is 11% ^{26}Mg), 28% Fe, 1.7% Ni, 2.1% S, and 1.4% Ca; Urey and Craig, 1953.] The effective total ^{26}Al production cross-section at a given energy is thus,

$$\sigma_{eff} = \sigma_{Si} + 0.068\sigma_{Al} + 0.107\sigma_{Mg} + 0.1\sigma_{S} + 1.85\sigma_{Fe} + \ldots$$

Therefore, the cross-section results of Fuse and Anders (1969) for the cosmic ray energy spectrum yield $\sigma_{eff} = 33$ mb. Lavruhina et. al. (1964) estimate $\sigma_{eff} \approx 24$ mb for a cosmic ray spectrum (not including secondary neutrons less than ~100 MeV). Another estimate of the production cross-section at high energy is that of FGH , where the target is assumed to be

75% ^{16}O and 25% Si group elements, a cross-section of 60 mb is estimated for production from the Si group with a 500 MeV flux. From the high energy extrapolations of Fig. 2 (with $\sigma_{Fe} \approx 0.4$ mb) the effective cross-section is $\sigma_{eff} \approx 36$ mb for high energies ($\gtrsim$100 MeV), which agrees quite well with the Fuse and Anders result and is within a factor of 2 of the FGH estimate. Reeves and Audouze (1968) estimate the effective cross-section for ^{26}Al production per Si atom as 56 mb for a flux of 50 MeV, which can be compared with the high energy extrapolations which yield $\sigma_{eff}(50\ MeV) \approx 61$ mb. For the rest of this discussion the experimental cross-sections of Fig. 2 with their high energy extrapolations will be used.

It is now necessary to investigate the energy spectrum the flux would have, dependent on the astrophysical situations under which the irradiation took place. Rather than propose any one particular model, a summary of various possibilities will be discussed. The acceleration of particles to make the flux would probably be due to a mechanism similiar to that of solar flares. To explore the flux problem, let us look at the effects of three different types of flux spectra from the early sun. The first would be a standard low energy solar flare type flux with a spectrum $\frac{dJ}{dE} \propto e^{-R/R_o}$, where J is the number of particles/cm^2, R is the magnetic rigidity, and $R_o \approx 100$ MV. This flux spectrum is similiar to an E^{-3} power law flux in the region of interest. This rigidity spectra was chosen since it best fits most current solar flare data. That, of course, does not mean that the early sun's flares necessarily followed this spectral shape. It would be very easy

to have large numbers of flares of this type since it would be highly possible for the early phases of the sun (e.g. T-Tauri) to be much more active than the present sun.

Another possibility would be some sort of mono-energetic flare. For the purposes of argument, let us choose the energy so as to reach the optimum effective cross-section for ^{26}Al production which can be seen from Figure 2 to be ~40 MeV. This type of flux is equivalent to the assumptions of Reeves and Audouze (1968) who assumed a 50 MeV flux. By choosing the optimum energy, it is possible to obtain a lower limit on the number of bombarding particles required to produce a specified amount of ^{26}Al.

The third type of flux considered will be a high energy flare flux similiar to that chosen by FGH with several hundred MeV particles traveling along magnetic field lines through the primordial matter. It is important to note that only this high energy flux will produce appreciable secondary neutrons. The neutron reaction cross-sections will be assumed to be similiar to the proton cross-sections. The secondary neutrons would have to have energies $\gtrsim$20 MeV to produce ^{26}Al. Thus they would travel (neglecting any scattering), $\gtrsim$ 1/2 an astronomical unit before decaying. If secondary neutrons are produced in large amounts, there must be some shielding so that nucleii with large thermal cross-sections will not be annihilated. This now brings us to a discussion of the state of the primordial matter at the time of the irradiations. Any shielding of the material from the flux depends on the g/cm^2

traversed. Thus, the same mass fraction of the primordial material was irradiated at a given time whether the material was in a solid or a gaseous state. It is very likely that a gas (or micron size dust particles), would become mixed, especially with an active early sun, however, solid objects could remain inhomogeneous with respect to the ^{26}Al distribution. If the irradiation took place in a turbulent gaseous state, it would still be necessary for solidification to occur within a few million years if the ^{26}Al is to have any effect on the solar system. If the irradiation takes place on solid planetesmals only the surface, penetration depth for that energy flux, would be irradiated. In order to have a homogeneous distribution to satisfy the ^{40}K, ^{50}V and Gd constraints, it would be necessary for the planetesmals to re-equilibrate either by collisions or melting. If this did not occur within a few million years of the irradiation, the ^{26}Al would only be on the surface and would not be an effective heat source for melting cores of objects. For the case of secondary neutrons, solid plantesmals would insure an opportunity for them to interact before decay, thus, increasing the effective cross-section for production of ^{26}Al. The effects of secondary neutrons are discussed quite thoroughly by Arnold, Honda and Lal (1960) for the case of cosmic rays on meteorites and the effect for the high energy flux discussed here would be practically identical. If the primordial matter were diffuse, the neutrons would die away after traveling ~1/2 to 1 A.U.

To produce a fixed amount of ^{26}Al, a certain "effective flux" is required to irradiate homogeneously all the primordial matter. Any shielding effects can be translated into a change in the total flux necessary to maintain the same effective flux. (e.g. If 90% of the matter is shielded this would mean that total flux would have to increase by a factor of 10 in order to produce the same amount of ^{26}Al as in the unshielded situation.) As was previously mentioned, it is known from K,V and Gd that if there were a flux, its effects were homogeneous. Therefore, any inhomogeneous effects due to shielding had to be wiped out before the meteorites formed. Since it is necessary to stir up the material at some time during or after the irradiation, it does not matter whether the pre-planetary matter is assumed to be gaseous or solid other than to change the total flux required to produce a fixed amount of ^{26}Al. The primary thing is that objects must form within a few million years if ^{26}Al is to have any effect. Note also, that if any effect is to be observed, there must be ^{26}Al left when the feldspars solidified. The homogeneous requirements for the effects of the flux eliminate the possibility that there could have been separate irradiations after the meteorites formed. That is, a meteorite such as the chondrite Guareña which is separated by 74 million yrs. from the Basaltic Achondrites according to Rb-Sr initial values (Wasserburg, Papanastassiou and Sanz, 1969), would be unlikely to show ^{26}Al effects unless all objects were irradiated uniformly near this 74 million

year time. Also, K, V, and Gd would have to be equilibrated in all objects after that time.

Now let us look at the effective flux requirements assuming no shielding. (As mentioned above, shielding changes the total flux, not the effective flux.) For the very high energy flux, the effective cross-section, neglecting neutron effects, was given before as ~36 mb. Thus, to produce 1 atom ^{26}Al on a Si = 10^6 scale, requires an integrated flux of ~3 x 10^{19} protons/cm^2. For the case of a 40 MeV flux, the effective cross-section is ~66 mb. Therefore, the flux is ~2 x 10^{19} protons/cm^2 to make 1 atom ^{26}Al/10^6Si. For the low energy flare spectrum with $R_o \approx 100$ MeV, the required flux is ~5 x 10^{20} p/cm^2 in the range 10 to 100 MeV. (This calculation of the ^{26}Al production from a low energy solar flare spectrum is based on work by R. Reedy, 1970.)

For all the above flux estimates, it was assumed that the irradiation took place over a time interval much less than the 10^6 yr. life of ^{26}Al. FGH use a time interval of 10^7 yr.; thus, their final production is reduced by a factor of 10. Their total estimated production is 28 atoms ^{26}Al/10^6 Si which is then reduced to 2.8 at the end of the irradiation. Other estimates of the primordial ^{26}Al/10^6Si are Reeves and Andouze (1968) with 0.56 atoms and Anders (1964) who estimated 6 atoms. The major difference in each of these models is the effective flux required. From the optimum 40 MeV flux, a lower limit on the effective flux necessary to melt the cores of planetary objects can be obtained. This limit is an integrated

flux $J > 4 \times 10^{18}$ p/cm^2, which comes from the unrealistic limit of zero time between the irradiation and solidification of planetary objects with radii $\gtrsim$ 100 km and a homogeneous ^{26}Al distribution.

Although models can be constructed to produce high fluxes, in no way can it be said, that it was mandatory for there to have been a high energy proton irradiation of greater than 4×10^{18} particles/cm^2. Since there is no a priori method of determining the magnitude of the flux from astrophysics, one must rely on nuclear physics; but, at the present time, there appears to be no experimental isotopic abundance evidence for the existence of this flux either. The production of stable and long-lived nuclides, once thought to require this flux for their existence, can now be explanined by other processes. This leaves ^{26}Al, for which there is no experimental evidence in the early solar system.

The only workers who have investigated the energy requirements associated with a model for the production of ^{26}Al are FGH. They mention that in the transfer of angular momentum from the sun to the planetary material, 5×10^{45} ergs of energy must be dissipated. They following Hoyle (1960) and Gold and Hoyle (1960) feel this energy will be stored as magnetic energy and dissipated through solar flares. They estimate that the conversion of magnetic energy to high energy particles has an efficiency of ~1/5. Thus, they have $\sim 10^{45}$ ergs to work with. For the flux spectra investigated in this present work, it would require from $\sim 10^{42}$ to $\sim 4 \times 10^{43}$ ergs depending on the spectral shape to make 1 atom ^{26}Al/10^6Si. This is well within the energy allowed by FGH.

Note that if a high flux exists, it would produce Li, Be, and B by spallation reactions (c. f. Reeves and Audouze, 1968, and FGH), and therefore, other explanations for Li, Be, and B would not be needed.

To summarize, let it be said that there are no nucleii presently observed which would have required some form of irradiation $> 4 \times 10^{18}$ protons/cm^2 in the early solar system in order to exist. However, that does not rule out the existence of such a flux. The energy spectrum chosen for the flux would depend on the particular model used. Whether the flux irradiates a pre-planetary gas, solid planetesmals, or for that matter, the outer layer of the sun, doesn't appreciably change things other than the scaling of the total flux due to shielding. The only way to avoid having this high flux and still have ^{26}Al, is to have the planetary objects solidify within a few million years of a carbon and silicon burning supernovae.

Section 3. Appendix I: Calibration of the Lunatic I

A calibration of the Lunatic I mass spectrometer (Wasserburg, Papanastassiou, Nenow, and Bauman, 1969) was carried out.

Figure 3 is a schematic of the Lunatic I system. During normal operation, the ion beam is collected in a Faraday Cup connected to a Cary 36 vibrating-reed electrometer with a 10^{11} Ω resistor. The signal is then measured with a Non-linear Systems digital voltmeter (DVM), and the result is sent to an on-line computer (at present an IBM 1800), for processing. The input impedance for the DVM varies with the range used, (ie. 100 K for 0.1 V range, 1 M for 1 V range, and 10 M for 10 V range). To compensate for this variation, an impedance matching circuit is used so that the signal leaving the Cary 36 always sees an impedance of 5 K in parallel with 100 K. (The recorder taps off of the 5 K part of the circuit.)

The purpose of the calibration was to observe the fractional deviations between the input signals and the DVM readings. To determine these fractional deviations, it is possible to use a varible voltage source (referred to as the Holy Cow), which can be connected into the Cary 36 feedback loop. In order to better interpret the calibration and remove any effects due to deviations in the Holy Cow from assumed input, the DVM and Holy Cow were calibrated relative to a Hewlett-Packard Model 740B differential voltmeter. In addition, a calibration was also made of the impedance matching network using the differential voltmeter. Thus, the total system as well as all the components (with the exception of the Cary 36 whose calibration is then implied), were calibrated relative to the differential voltmeter.

The DVM (see Fig. 4) was calibrated by disconnecting it from the system, then using the differential voltmeter as a direct input to the DVM. The spread in the data was $\leq \pm 1$ digit of the DVM. The results of this calibration are shown in column 2 of Table 2 and plotted in Fig. 5. The fractional deviations for all ranges have been normalized throughout this work so that 1 volt read on the 10 volt scale has zero deviation. With this normalization, it is seen that the full scale reading for each range has a fractional deviation of -3 parts in 10^4. For the DVM, it can be seen that to within the precision of the measurements:

$$f \equiv \frac{V_{out} - V_{in}}{V_{in}} \approx K \log(V_{in} / V_0)$$

where V_o and K are empirically determined for each range. The reading on the DVM is supposed to vary linearly with the frequency of the pulses coming out of the high gain amp. (see Fig. 4), with Z_{in} adjusted for each range such that full scale yields 10^5 pulses/sec. The calibration indicates that the DVM reading is not linear with the frequency, but in fact, detects low frequency pulses (low voltage) with greater efficiency than high frequency pulses (high voltage).

For an infinite gain amplifier, the time necessary to trigger the Schmidt trigger (see Figure 4) is

$$T = \frac{E_t \; Z_{in} \; C}{V_{in}}$$

where E_t is the trigger voltage and C ≈ 20 pf is the capacitance across the amp. The DVM output is proportional to 1/T (for infinite gain $V_{out} = V_{in}$). For finite gain, A, the trigger time goes

to: $T = (1+A)\cdot Z_{in}\cdot C\cdot \ln(1 + E_t/A\cdot V_{in})$

and thus the fractional deviation between V_{in} and V_{out} is $-1/A$ to first order. For this amplifier, the gain varies inversly with frequency. A high voltage would therefore, have a negative fractional correction, f, relative to a lower voltage on the same range. This result agrees qualitatively with the observed calibration, Figure 5. Quantitative agreement requires that the gain for full scale readings be $\sim 3 \times 10^3$, with the gain at one tenth scale $\gtrsim 10^5$. Discussions with A. Massey have indicated to me that it is quite possible for the high frequency gain to be as low as 3×10^3 even if the low frequency gain is $>10^5$. There is also an effect due to the fact that instead of an ideal op-amp, the DVM has a real amplifier with a finite input impedance. This effect would vary from range to range, which is different from the observed calibration behavior. Other possible effects (e.g. the effect of a residual charge on the capacitor or the effect of the peak shape of the reset pulse) also do not yield the observed behavior. It therefore appears that the dominant effect observed in the DVM calibration, is the variation of the amplifier gain with frequency.

The integration times for the DVM were also calibrated by again using the differential voltmeter as a direct input; then, taking readings with 1, 2, 4, and 8 second integration times. Deviations between readings using different integration times were found to be much less than deviations due to changes in input voltage within a range. The integration time circuit is independent of the range circuit and, it was found that the integration time calibration of

the DVM was independent of range.

Let

$$d_t \equiv \frac{V_t - tV_1}{tV_1}$$

where t is the integration time, V_1 is the reading for a 1 second integration time, and V_t is the reading for an integration time, t. The results for all ranges within the precision of the measurements are:

$$d_1 \equiv 0$$

$$d_2 \approx 0$$

$$d_4 \approx -2.5 \times 10^{-5}$$

$$d_8 \approx -2.5 \times 10^{-5}$$

To calibrate the impedance matching circuit, a fixed voltage source was made using a 1.5 volt battery connected in series with a 70 K resistor. The impedance matching network including the DVM was separated from the Cary 36 circuit. That is, a break in the system circuit was made at point A on the schmatic shown in Fig. 3. The fixed voltage source was connected between points B and C of Fig. 3. This yielded a voltage of ~100mv into the DVM. This voltage across B and C was measured with the differential voltmeter as well as the DVM using all combinations of ranges and integration times. It was found, using the differential voltmeter, that the 1 volt scale read ~4 parts in 10^4 higher than the 10 volt scale, and the 0.1 volt scale read ~1 part in 10^4 higher than the 10 V scale (see column 3 of Table 2).

The DVM reading showed the combined effect of this impedance matching calibration and the calibration of the DVM. No significant variation was found in the differential voltmeter readings using fixed range, but different time base. The differential voltmeter was then used as the voltage source in place of the battery with the output voltage now read only on the DVM. For various input voltages, the DVM again showed the combined effect of the DVM calibration and the impedance matching scale factors.

The Holy Cow was calibrated by disconecting it from the system, then measuring its output voltages with the differential voltmeter. The results, corrected for zeroes, are shown in column 4 of Table 2 and plotted in Fig. 6. Note in particular, that the deviations increase for lower voltages. This effect can be explained by the fact that thermal emf's become more significant for lower signals. The total system was then calibrated with the Holy Cow. This is done by con-

necting the Holy Cow into the Cary 36 feedback loop. Holy Cow voltages are set on all nine channels of the Lunatic and the system is cycled through the channels. The DVM results are sent to the computer, corrected for zeroes, and the ratios are calculated relative to 1 V measured on the 10 V scale with a 1 second integration time. Many sets of ratios are taken and the means of all the ratios are computed. The fractional deviations of the resulting means from the Holy Cow input settings are shown in column 5 of Table 2 and plotted in Figure 7. The error bars are two times the standard deviation of the mean for the ratios.

The system calibration was corrected for the Holy Cow calibration by subtracting column 4 from column 5 of Table 2. The resulting corrected system calibration is shown in column 6 of Table 2 and is plotted in Fig. 8. The dashed line in Fig. 8 is the 2σ counting statistics for an equivalent input signal due to ions using a $10^{11}\ \Omega$ resistor and integrated for 1 second.

The calibration shown in Fig. 8 represents the deviation of the total system from the differential voltmeter which is used as our standard. The calibration can be used to correct measured ratios as follows:

$$\text{for } f \cong \frac{V_{out} - V_{in}}{V_{in}},$$

$$\frac{(V_{in})_1}{(V_{in})_2} = \frac{(V_{out})_1}{(V_{out})_2} \cdot \frac{(1+f_2)}{(1+f_1)} \approx \frac{(V_{out})_1}{(V_{out})_2} (1+f_2-f_1).$$

That is, each ratio has a calibration correction f_2-f_1 where f_i is a

function of voltage as shown in Fig. 8.

For most analyses, mass spectrometer ratios are corrected for mass discrimination. For the magnesium case, the calibration correction for the $^{26}Mg/^{24}Mg$ ratio following the discrimination correction from the $^{25}Mg/^{24}Mg$ ratio is $2f_{25} - (f_{24} + f_{26})$. Another example is the Sr case where $^{88}Sr/^{86}Sr$ is used to correct $^{87}Sr/^{86}Sr$. The calibration correction for this case is $\frac{f_{86}+f_{88}}{2} - f_{87}$. For a typical Mg analysis ($^{24}Mg \approx 2$ V. See Sec. 6), the calibration correction would be ~1.6 parts in 10^4. However, all Mg analysis were done at approximately the same running conditions. They would, thus, all have the same calibration correction and therefore, relative effects (i.e. ^{26}Mg anomalies) would not contain a calibration error.

It is interesting to note that the Cary 36 vibrating-reed electrometer was the only component of the Lunatic I system not directly calibrated. An implied calibration for it can be obtained by subtracting the effects of the calibrations of all the other components from the total system calibration. The result is shown in column 7 of Table 2 and is plotted in Fig. 9.

In addition to the basic calibration described above, various other effects were investigated. It was found that the total system calibration using the Holy Cow was independent of whether the reed feedback resistor was 10^{10} or $10^{11}\ \Omega$. However, on the average, the noise as determined by the standard deviation of the ratios was less with the $10^{10}\ \Omega$ resistor.

It was found that the difference in results using an 8 second compared to a 1 second integration time, was ~7 parts in 10^5.

It was also found that there was no change in results (due to possible coupling), whether or not the Cary 401 vibrating-reed electrometer was on.

A check was made on the effect of the time delay setting in cycling through channels. It was determined that there was no variation in results with time delays $\gtrsim$ 1 second.

It is not possible to determine the linearity of the reed feedback resistor with the differential voltmeter. D.A.Papanastassiou, using precision Sr measurements, has found that the $10^{11}\Omega$ resistor begins to go non-linear for signals greater than ~3 V and deviates by a few parts in 10^4 at ~8 V. He is currently working to get this more quantative. With these results as well as the system calibration curve of Fig. 8, it appears that the optimum running conditions (with respect to minimum calibration corrections), would be signals between ~2.5 V and ~50 mV. It should be noted that there is practically no calibration correction for ratios where both peaks are measured on the 1 V range or where both peaks are measured between 1 and 2.5 V on the 10 V range.

Section 3. Appendix II: Mineral Separates

Although a brief description of the mineral separates is given in Section 6, it is important to provide a more detailed description here. Following the mineral separations, aliquots were processed through the chemistry, and the blank corrections calculated as shown in Table 1. The Al and Mg concentrations are shown in Table 6 of Section 6. Thus, Table 1 allows one to determine the amount of sample processed through each stage of the chemistry.

Colomera

Twelve milligrams of a large single crystal potassium feldspar inclusion, (Wasserburg, Sanz and Bence, 1968), from the iron meteorite Colomera were hand-picked for subsequent analysis. The grains, when picked, were covered with rust. The grains were gently crushed and the rust was removed by washing in warm 4N HCl. The grains were then water clear. A microprobe mount was made, and it was determined that the separate was 98% alkali-feldspar Or_{89}, 1% plagioclase feldspar, and 1% other.

Moore County

Two feldspar separates were made from the Achondrite Moore County. Both were crystals hand-picked after gentle crushing. The feldspar contained some pyroxene inclusions, and some small black inclusions. Some rust spots were noticed on the grains.

Separate I was prepared from 16.2 mg. of hand-picked crystals. It was first rinsed in warm 2N HCl for about 3 to 5 minutes, then

rinsed in H_2O and acetone. This procedure removed the rust spots. This separate was then crushed to -75$\mu$and put in 2.8 specific gravity methylene iodide and acetone solution, and centrifuged. The floats were then ground to less that 20μ . and again put through 2.8 g/cm^3 density methylene iodide and acetone. This sample was then hand-picked to remove impurities. This left 1.6 mg. of feldspar. Separate I was then processed as indicated by Table 1.

Separate II started from ~100 mg. of hand-picked plagioclase. This was put into 2.8 specific gravity liquid and centrifuged. Next the floats were ground to 25μ. (Sample was now 60 mg.) The sample was then put into 2.7 density liquid, and almost everything appeared to sink. This was put into 2.75 density liquid and centifuged. The 41 mg. of floats were reprocessed through the 2.75 liquid and hand-picked to remove impurities. This left 31.7 mg. of sample.

A 9.4 mg. fraction of this feldspar separate was put into solution in the usual manner with aliquots taken for analysis. A microprobe mount was made for both Moore County I and II. It was determined that the plagioclase was An_{92}. Moore Co.I feldspar separate contained 11% free SiO_2 phases, whereas no free quartz was found in the Moore Co. II feldspar separate.

Juvinas

A feldspar separate was made from the Achondrite Juvinas. Forty milligrams of feldspar were hand-picked from a feldspar-rich part of the specimen. This hand-picked feldspar was then gently ground

under acetone and centrifuged in 2.75 density methylene iodide and acetone. The impurites in the floats were hand-picked out and the floats were ground under acetone to -40μ and cycled through the 2.75 density liquid. Seven milligrams of the remaining 22 mg. sample were put through the normal chemistry. The Mg concentration was determined to be 1400 ppm. A microprobe mount was made, and it was determined that some grains had Mg-rich inclusions. It was also determined that the plagioclase feldspar was An_{91}. The remaining feldspar was then reground to less than 20μ and processed through 2.75 density liquid in an attempt to remove the Mg-rich impurities. The resulting separate still had 1400 ppm. No free SiO_2 phases were observed.

Pasamonte

Twenty-one milligrams of feldspar were hand-picked from the coarse grained portion, rather than the fine grained matrix, which was separated by passing through 75μ (200 mesh) screen wire.

This plagioclase was gently ground under acetone with an agate mortar and pestle. The plagioclase was then centrifuged in 2.75 density methylene iodide and acetone. The floats were carefully hand-picked, and then ground under acetone to less than 20μ size particles. The separate was then centrifuged again in 2.75 density liquid. The floats were again hand-picked to remove impurities. A microprobe grain mount was made. The plagioclase was determined to be An_{86}. The separate was determined to have 4% free SiO_2 phases. Approximately half (4.4 mg.) of the remaining 9.0 mg. of the

separate was processed through the chemistry.

St. Severin

The chondrite St. Severin was also investigated. The starting point for this feldspar separate was a feldspar-rich fraction left over from previous separates done on St. Severin in this laboratory, (Wasserburg et. al. 1969 a,b). It had been sieved such that it ranged in grain size from 70μ to 25μ , and had floated in 2.70 density liquid. An atomic absorption analysis determined the Mg concentration of this material to be 6200 ppm. A fraction of this material, 163.2 mg., was then ground under acetone until grain size was ~10μ . This was then centrifuged in 2.75 density methylene iodide and acetone. The floats were then centrifuged in 2.70 density liquid. The 27.0 mg. of floats were centrifuged in 2.67 density liquid, handpicked, and reprocessed through 2.66 density liquid. A 3.0 mg. aliquot of the remaining 17.1 mg. sample was then dissolved and the Mg concentration determined to be 3300 ppm. With such small grain size, some particles tended to remain in the acetone during washing and decanting. The particles that remained in the wash of the 2.7 floats were allowed to settle out overnight, and found to weigh 16.2 mg. These hyperfine grains were centrifuged in 2.67 density liquid, and the floats hand-picked for impurities. These floats were found to weigh 12.7 mg. Approximately half, 7.0 mg., of these hyperfines were then put through our standard chemistry and the Mg concentration was found to be 2000 ppm. A microprobe sample of these hyperfines was also made and determined to be

$Ab_{88}An_{12}$ with no free SiO_2 phases found. An aliquot of the hyperfines was processed through the chemistry.

Lunar Rock 12064, 26

This is a coarse grained holocrystalline gabroic rock. A portion of this rock was gently crushed and sieved to be 75 to 300μ in size. From this, 20 mg. of plagioclase were hand-picked, ground to less than 100μ and centrifuged through 2.75 density methylene iodide and acetone. Impurities were hand-picked from the floats. The floats were then ground to ~10μ and centrifuged again in 2.75 density liquid. The floats were hand-picked for impurities and a microprobe grain mount was made. The composition was determined to be An_{85} with less than 5% free SiO_2.

Guareña

The starting point for this separate was a feldspar-rich separate left over from earlier separates in this laboratory on Guareña (Huneke, Burnett, Schramm and Wasserburg, 1970). This 60 to 100μ starting material was found by atomic absorption to have 44000 ppm Mg. Approximately 50 mg. of this material was crushed to -70μ and centrifuged in 2.7 g/cm^3 liquid. At the conclusion, the grains were ground until particle size was less than 5μ. (This fine material tended to remain suspended in the acetone; thus, it was necessary to centrifuge the acetone to work with the separate.)

This fine material was contrifuged in 2.67 g/cm^3 liquid and

hand-picked to remove impurities. A microprobe analysis was carried out, and it was determined that the sample was $\sim Ab_{85}\ An_{15}$ with an Al concentration of 11.7%. No evidence of any free SiO_2 phases was found. Hot spots of Mg were found. The remaining 1.9 mg. of Guareña feldspar were dissolved using 1/3 ml. HF and 1/3 ml. $HClO_4$ and put through the chemical processing.

Lunar Rock 12013, 10

This sample was from a few milligrams of feldspar left over from previous mineral separates performed in this laboratory on Lunar Rock 12013 (Lunatic Asylum, 1970). It had been crushed to less than 75μ grain size and the floats were taken from centrifuging in 2.65 g/cm^3 liquid twice.

From a microprobe analysis, it was found that the separate had many Mg-rich impurities. It was also found that the sample was made up of several feldspar phases ranging from almost pure K feldspar to plagioclase with wide variation in Ca. The remaining 1.9 mg. of the sample were dissolved in 1/3 ml. HF and 1/3 ml. $HClO_4$ and processed through the chemistry.

Lunar Rock 10024, 24

This is a fine grained high-K rock, which was crushed and centrifuged in 2.4 g/cm^3 methylene iodide and acetone. The resulting sinks were centrifuged in 2.7 g/cm^3 density liquid. An aliquot of the floats, 1.9 mg., was dissolved using 1 ml. HF and 1 ml. $HClO_4$ and processed for analysis. A microprobe analysis indicated some Mg-rich impurities and ~10% cristobalite.

Hallingeberg

Hallingeberg is an unequilibrated condrite (L3) with little crystalized feldspar (Dodd, Van Schmus, and Koffman, 1967). This meteorite was the most primitive material analyzed in this work. (The only available matter more primitive than this would be C1 and C2 carbonaceous chondrites which have no feldspar.) An attempt was made to separate out the feldspar composition glass. A sink-float test in 2.75 g/cm^3 M.I. and acetone indicated that the white grains were probably feldspar glass.

The rock was gently ground to -75μ and put in 2.75 g/cm^3 liquid. The 9.7 mg. of floats were hand-picked for impurities and ground under acetone to -5μ. The acetone was centrifuged to remove the suspended particles. These grains were put in 2.70 g/cm^3 density liquid and then into an untra-sonic bath to break-up co-agulates. The 2.7g/cm^3 solution was then centrifuged. The floats were then hand-picked for impurities and a microprobe grain mount was made. This left less than a milligram of material to dissolve in 1/3 ml. HF and 1/3 ml. $HClO_4$ and analyze. The Mg concentation was found to be 7.2% which agreed with an average microprobe measurement of 7.3%. The microprobe analysis indicated the separate had ~10% Al. Thus, the separate was feldspar-like glass, but with Mg present as a major element which would rule out the use of this separate to find any ^{26}Mg anomaly due to ^{26}Al. To check the result that Al

rich areas had high Mg concentrations, micro-thin sections were made from 15 chondrules. A microprobe analysis indicated all Al areas had high Mg content, thus confirming our previous findings. This seems to indicate that the procedures used here are not applicable to the unequilibrated chondrites.

REFERENCES

This list contains the references for Sections 1 through 3, the references for the published papers of Sections 4 through 6 being included at the end of those sections.

Anders, E; 1964, Space Sci. Rev. 3, 583

Arnett, W.D.; 1969, Ap.J., 157, 1369

Arnold, J.R., Honda, M. and Lal, D.; 1961, J. Geophys. Res. 66, 3519

Audouze, J.; Ephere, M., and Reeves, H.; 1967, Nucl. Phys. A97, 144

Balsiger, H., Geiss, J., and Lipshutz, M.E.; 1969, Earth Planetary Sci. Lett., 6, 117

Bodansky, D., Clayton, D.D., and Fowler, W.A.; 1968, Ap.J. Supp. 16, 299

Branch, D.; 1970, Ap.J., 159, 39

Burnett, D.S., Lippolt, H.J., and Wasserburg, G.J.; 1966, J. Geophys. Res., 71, 1249

Clarke, W.B., De Laeter, J.R., Schwarcz, H.P., and Shane, K.C.; 1970 J. Geophys. Res., 75, 448.

Clayton, D.D.; 1964, Ap.J., 139, 637

Dodd, R.T., Van Schmus, W.R., Koffman, D.M.; 1967, Geochim. Cosmochim. Acta., 31, 921

Dostrovsky, J., Rabinowitz, P., and Biving, R.; 1958, Phys. Rev. 111, 1659

Eugster, O., Tera, F., Burnett, D.S., and Wasserburg, G.J.; 1970, J. Geophys. Res. 75, 2753

Evans, J.C.; 1970, Private Communication.

Fish, R.A., Goles, G.G., and Anders, E.; 1960, Ap. J., 132, 293

Fowler, W.A., Greenstein, J.L., and Hoyle, F.; 1962, Geophys. J. Roy. Astro. Soc., 6, 148, (referred to as FGH).

Fowler, W.A., and Hoyle, F.; 1960, Ann. Phys., 10, 280

Fuse, K., and Anders, E.; 1969, Geochim. Cosmochim. Acta. 33, 653

Ginzburg, V.L., and Syrovatskii, S.I.; 1964, The Origin of Cosmic Rays, MacMillan Co., New York

Gold, T. and Hoyle, F.; 1960, Mon. Not. R. Astro. Soc., 120, 89

Hohenburg, C.M., Podosek, F.A., and Reynolds, J.H.; 1967, Science, 156, 1211

Honda, M., and Lal, D.; 1960, Phys. Rev., 118, 1618

Honda, M., and Lal, D.; 1964, Nuc. Phys., 51, 363

Hoyle, F.; 1960, Quart. J. R. Astro. Soc., 1, 28

Hoyle, F., and Fowler, W.A.; 1960, Ap. J., 132, 565

Huneke, J.C., Burnett, D.S., Schramm, D.N., and Wasserburg, G.J.; 1970, In preparation

Kohman, T.P.; 1969, U.S. Atom. Ener. Com. Rep. NYO-844-76

Lavruhina, R.I., Kuznetsova, R. I., and Satarova, L.M.; 1964, Geokhimiya, 12, 1219

Lederer, C.M., Hollander, J.M., and Perlman,I.; 1967, Table of Isotopes, Wiley and Sons, New York

Lunatic Asylum; 1970, Earth Planetary Sci. Lett., 9, 137

Metropolis, N., Biving, R., Storm, M., Miller, J.M., and Friedlander, G.; 1958, Phys. Rev., 110, 185

Meyer, P.; 1969, Ann. Rev. Astron. Astrophys., 7, 1

Miller, J.M., and Hudis, J.; 1959, Ann. Rev. Nuc. Sci., 9, 159

Peebles, P.J.E.; 1967, J. R. Astro. Soc. Canada, 63, 1

Peebles, P.J.E., and Dicke, R.H.; 1968, Ap. J., 154, 891

Podosek, F.A.; 1970, Earth Planetary Sci. Lett., 8, 183

Reedy, R.C.; 1970, Private Communication

Reeves, H., and Audouze, J.; 1968, Earth Planetary Sci. Lett., 4, 135

Reeves, H., Fowler, W.A., and Hoyle, F.; 1970, Nature, 226, 727

Rowe, M.W.; 1968, Geochim. Cosmochim. Acta., 32, 1317

Rudstam, G.; 1956, Thesis, Univ. of Uppsala, Sweden

Rudstam, G.; 1966, Z. Naturforsch, 21, 1027

Rudstam, G., Stevenson, P.C., and Folger, R.L.; 1952, Phys. Rev., 87, 358

Rutherford, E.; 1929, Nature, 123, 313

Sandage, A.; 1961, Ap. J., 133, 355

Seeger, P.A., Fowler, W.A., and Clayton, D.D.; 1965, Ap. J. Supp. 11, 121

Seeger, P.A., and Schramm, D.N.; 1970, Ap. J. (Lett.), 160, L157

Shapiro, M.M. and Silberberg, R.; 1970, In Press, Ann. Rev. Nuc. Sci. Vol. 20.

S.H.R.E.L.L.D.A.L.F.F.; 1970, Proc. Apollo 11 Lunar Sci. Conf., 2, 1503

Suess, H., and Urey, H.C.; 1956, Rev. Mod. Phys., 28, 53

Tanaka, E.; 1970, Private Communication via J.C. Evans

Wagoner, R.V.; 1969, Ap. J. Supp., 18, 247

Wagoner, R.V., Fowler, W.A., and Hoyle, F.; 1967, Ap. J., 148, 3

Wänke, H.; 1960, Z. Naturforsch, 15a, 953

Wasserburg, G.J., Fowler, W.A., and Hoyle, F., 1960, Phys. Rev. Letters, 4, 112

Wasserburg, G.J., Huneke, J.C., and Burnett, D.S.; 1969a, J. Geophys. Res., 74, 4221

_____; 1969b, Phys. Rev. Letters, 22, 1198

Wasserburg, G.J., Papanastassiou, D.A. Nenow, E.V., and Bauman, C.A.; 1969, Rev. Sci. Instr., 40, 288

Wasserburg, G.J., Papanastassiou, D.A., and Sanz, H.G.; 1969, Earth Planetary Sci. Lett. , 7, 33

Wasserburg, G.J., Sanz, H.G., and Bence, A.E.; 1968, Science, 161, 684

Urey, H.C., and Craig, H.; 1953, Geochim. Cosmochim. Acta., 4, 36

Table 1 (See Sec.3,Appendix II.)

Sample	Run#	Blank Corrections: Mg Content of Dissolved Sample (μg)	Dissolution Blank[1] (%)	Amount Mg through columns (μg)	Column Blank[2] (%)	Amount loaded on filament (nanograms)	Filament Blank (%)	Total Blank[4] Corr. (%)
Kragero, Norway; Andesinde	47	1.0	2.0	1.0	2.4	250	0.20	4.6
Lakeview, Oregon; Bytownite	48	0.96	2.1	0.96*	1.3	480	0.10	3.5
Wyoming; Microcline	51	12.0	0.17	0.60	4.0	300	0.17	4.3
Bruderheim; Whole Rock	52	33500.0	~0	0.60	4.0	400	0.13	4.1
Colomera C-5; Feldspar	64	0.62	3.2	0.62	3.9	310	0.16	7.3
Wyoming; Microcline	65	12.0	0.17	0.60	4.0	300	0.17	4.3
Khortemiki; Soln. thru. Col.	66	——	——	~1.0*	1.2	~500	0.10	1.3
Moore Co.; Feldspar I	68	0.1	20.0	0.1	24.	100	0.50	44.5
Bruderheim; Feldspar III	69	2.6	0.77	0.97	2.5	320	0.16	3.4
Khortemiki; Soln.	73	——	——	——	——	~500	0.10	0.1
Moore Co.; Feldspar II	75	2.5	0.80	1.09	2.2	360	0.14	3.1
Bruderheim; Feldspar IV	76	2.2	0.91	1.06	2.3	530	0.09	3.3
Khortemiki; Feldspar	78	1.4	1.4	0.55	4.4	270	0.19	6.0
Lunar Rock 12064; Feldspar	79	3.1	0.65	2.04	1.2	510	0.10	2.0
Juvinas; Feldspar	80	6.3	0.32	1.74	1.4	430	0.12	1.8
St. Severin; Feldspar	81	14.0	0.14	4.48	0.54	550	0.09	0.8
Pasamonte; Feldspar	82	4.1	0.49	1.71	1.4	430	0.12	2.0
Clear Lake, Ore.; Bytownite	83	1.3**	1.0	1.3	0.92	430	0.12	2.0
Juvinas; Feldspar	84	6.3	0.32	1.74	1.4	430	0.12	1.8
Guarena; Feldspar	86	3.6**	0.36	1.7	1.4	560	0.09	1.9
Khortemiki; Soln. thru. Col.	87	——	——	~1.0*	1.2	~500	0.10	1.3
Bruderheim; Whole Rock	89	33500.0	~0	0.60	4.0	200	0.26	4.3
Lunar Rock 12013	90	8.6**	0.15	3.1	0.77	580	0.09	1.0
Lunar Rock 10024	92	4.5	0.45	1.7	1.4	420	0.12	2.0

1. Dissolution blank from 1 ml. HF and 1 ml. $HClO_4$ taken as 20 nanograms.
2. Column blank for 2 columns taken as 24 nanograms.
3. Filament loading blank taken as 0.5 nanograms.
4. Note-Blank corrections used are based on maximum blank measured for that operation. Variation in blanks was found to be ~25%. Total blank is taken as sum of dissolution plus column plus filament loading blanks. Measurements of total system blanks were made and found to agree with blank calculated by sum within a 25% variation.

* Only through one ion exchange column-blank taken as 12 nanograms.
** Dissolution ~1/3 ml. HF and ~1/3 ml. $HClO_4$ - blank taken as 13 nanograms.

Table 2 (See Section 4.)

Summary of the Calibration of The Lunatic I

			Fractional Deviations Normalized to 1 V(units of 10^4)			
INPUT	DVM	Range Switching Scale Factors	Holy Cow	Total System	Total System corrected for Holy Cow	Implied for Cary 36
10 V	-3.0		-0.48	+0.28	+0.76	+3.76
9 V	-2.7		-0.29			
8 V	-2.6		-0.28	-0.42	-0.14	+2.46
7 V	-2.4		-0.41	-0.40	+0.01	+2.41
6 V	-2.3	≡ 0	-0.24	-0.52	-0.28	+2.02
5 V	-2.0		-0.20	-0.60	-0.40	+1.60
4 V	-1.7		-0.15	-0.60	-0.45	+1.25
3 V	-1.3		-0.07	-0.34	-0.27	+1.03
2 V	-1.0		+0.10	-0.03	-0.13	+0.87
1 V(10VS)	0		≡0	≡0	≡0	≡0
1 V(1VS)			≡0	+1.39	+1.39	
0.9 V	-3.0		-1.20	+0.42	+1.62	-0.18
0.8 V	-2.8		-1.18			
0.7 V	-2.6		-0.99	+0.59	+1.58	-0.62
0.6 V	-2.5		-0.92			
0.5 V	-2.2	+4.8	-0.80	+0.60	+1.40	-1.20
0.4 V	-1.9		-0.93	+1.09	+2.02	-0.88
0.3 V	-1.3		+0.27	+1.81	+1.54	-1.96
0.2 V	-1.3		+0.60	+2.25	+1.65	-1.85
0.1 V(1VS)	0.0		+2.10	+3.40	+1.30	-3.50
0.1 V(0.1VS)	-2.9		+2.10	+2.10	0.0	+1.90
0.09 V	-2.8		+0.50			
0.08 V	-2.6		+2.00	+1.38	-0.62	+0.98
0.07 V	-2.2	+1.0	+2.50			
0.06 V	-2.2		+3.66	+1.67	-1.99	-0.79
0.05 V	-1.7		+5.09			
0.04 V	-1.3		+6.97	+5.2	-1.77	-1.47
0.03 V	-0.5		+11.8	+6.5	-5.3	-4.8
0.02 V	+0.3		+17.4			
0.01 V	+3.0		+47.4			

All measurements corrected for zeroes.

Figure 1. Mass 26 energy levels and decay scheme, from Lederer, Hollander, and Perlman, 1967; referred to in Section 3B.

DECAY SCHEME MASS 26

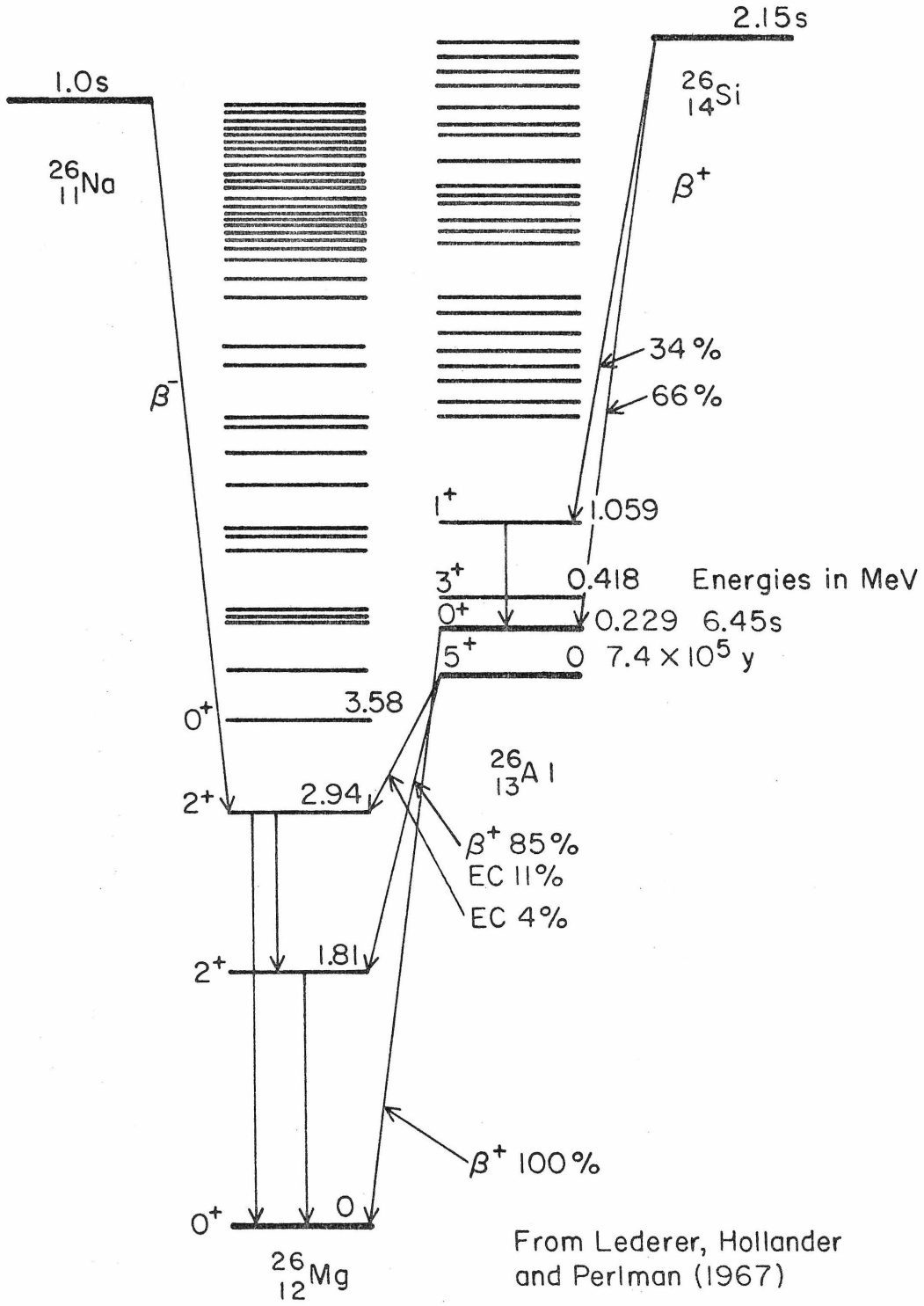

Figure 1.

Figure 2. Proton production cross-sections for ^{26}Al; $^{28}Si(p,2pn)^{26}Al$; and $^{26}Mg(p,n)^{26}Al$ data are from Tanaka (1970) and $^{27}Al(p,pn)^{26}Al$ data are from Evans (1970). Dashed lines are extrapolations based on excitation curves from analogous reactions. (Figure is referred to to in Section 3B.)

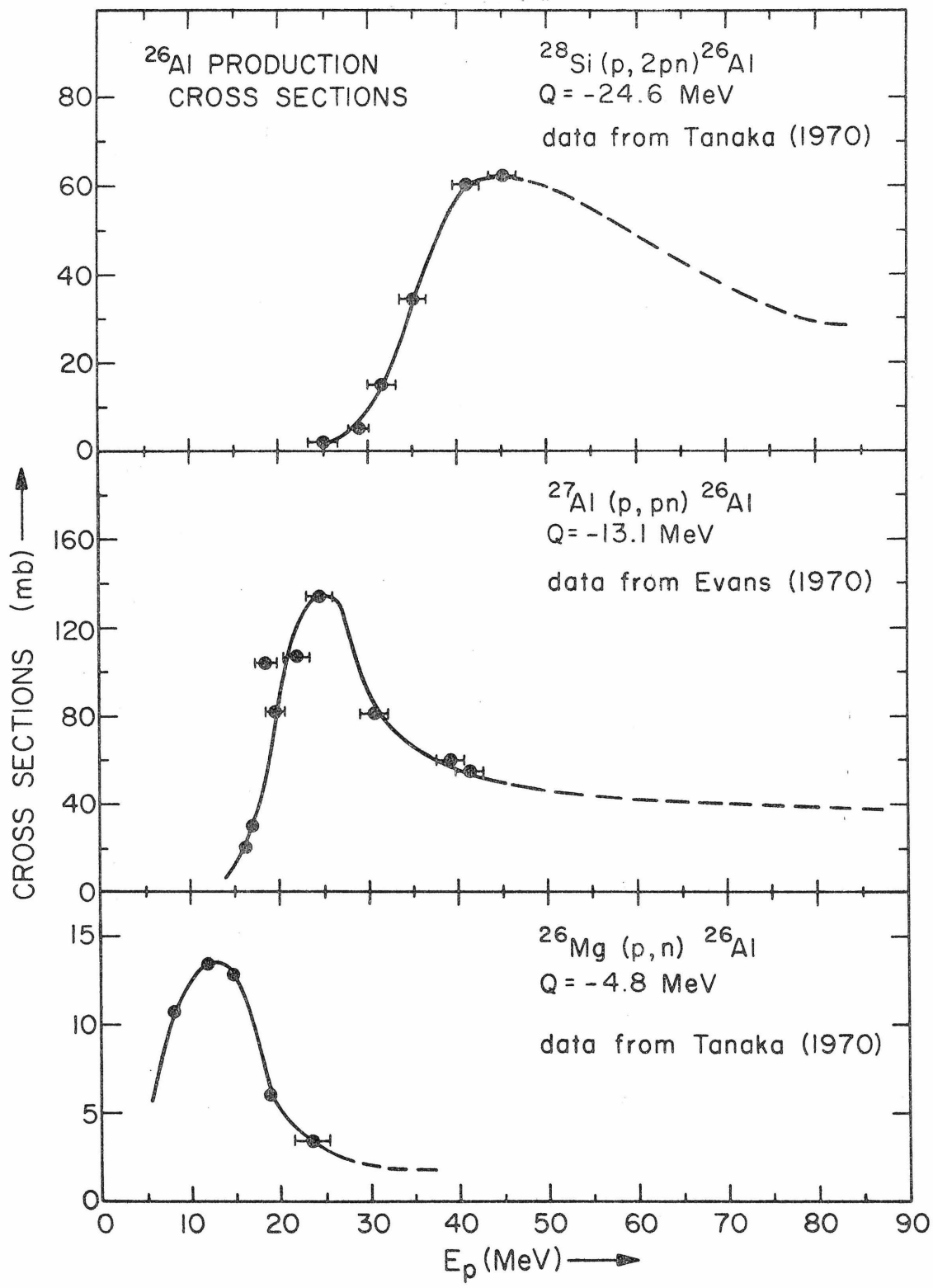
^{26}Al PRODUCTION
CROSS SECTIONS
^{28}Si (p, 2pn)^{26}Al
Q = -24.6 MeV
data from Tanaka (1970)
^{27}Al (p, pn) ^{26}Al
Q = -13.1 MeV
data from Evans (1970)
^{26}Mg (p, n) ^{26}Al
Q = -4.8 MeV
data from Tanaka (1970)
CROSS SECTIONS (mb)
E_p (MeV)

Figure 2.

Figure 3. Schematic of The Lunatic I (mass spectrometer) digital system. Points A, B, and C are places in the circuit referred to in Section 3, Appendix I.

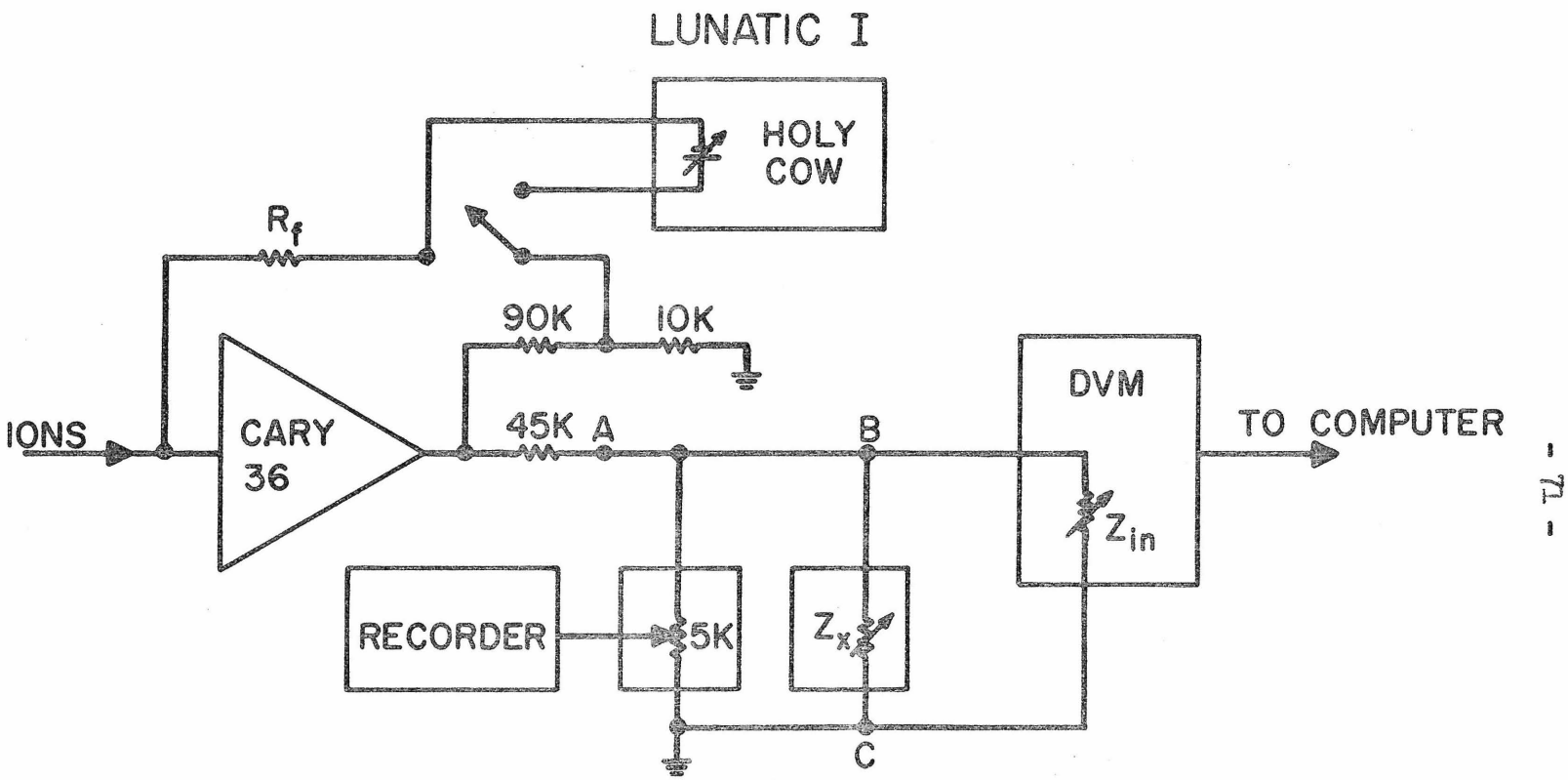

R_f is feedback resistor ($10^{10}\Omega$ or $10^{11}\Omega$)

Z_{in} is DVM input impedance

Z_{in} = 100K – 0.1 V range
1M – 1.0 V range
10M – 10.0 V range

Z_x is designed such that $Z_x \| Z_{in}$ = 100K

Figure 3.

Figure 4. Schematic of the Non-linear Systems Digital Voltmeter (DVM) referred to in Section 3, Appendix I.

DIGITAL VOLTMETER (DVM)

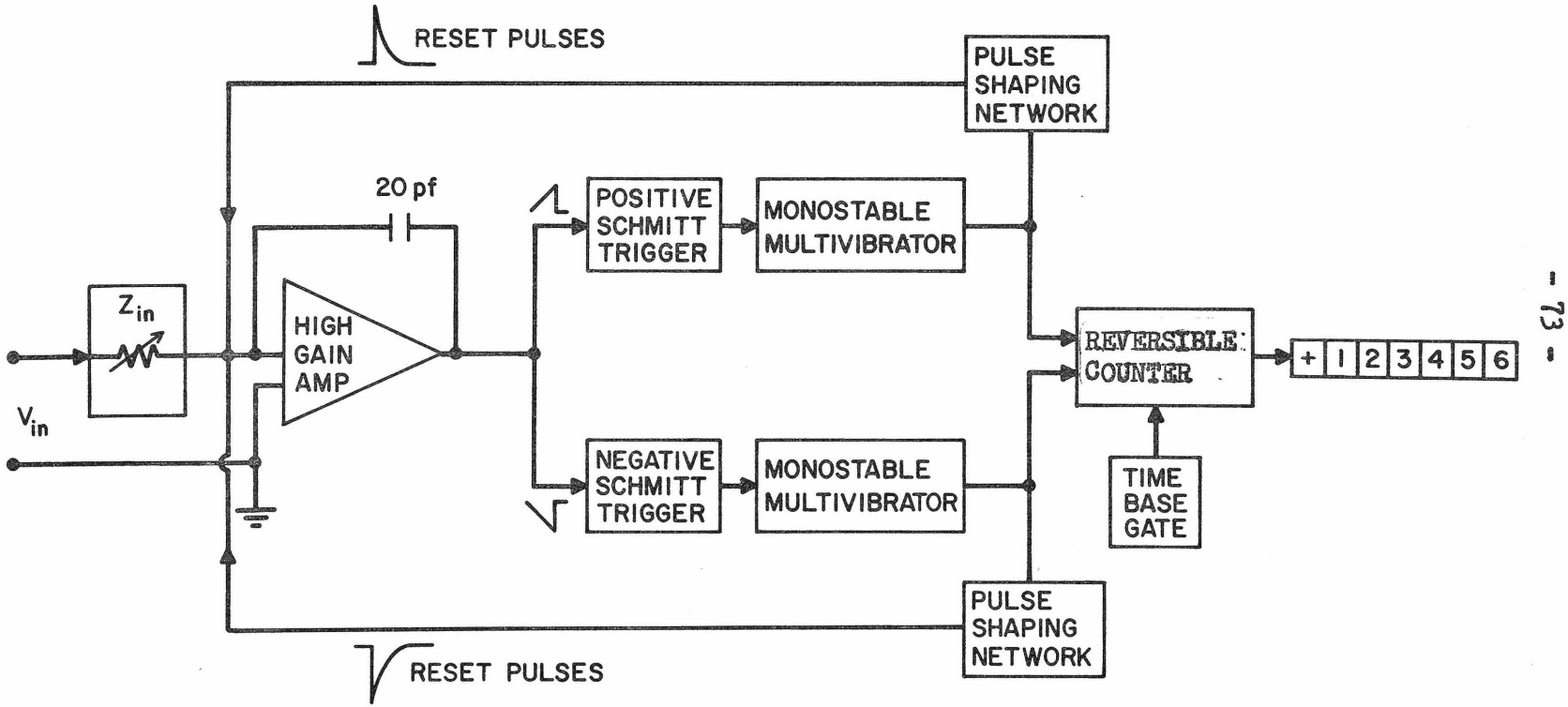

Figure 4.

Figure 5. Graph showing calibration of DVM with differential voltmeter; referred to in Sec.3, App.I. (Also see Table 2.)
The dashed curve represents the error bars on the calibration curve according to the manufacturers specifications, (fractional error=0.01 · V_{out} + 0.006 x full scale for 10 V and 1 V ranges and twice that for the 0.1 V range).

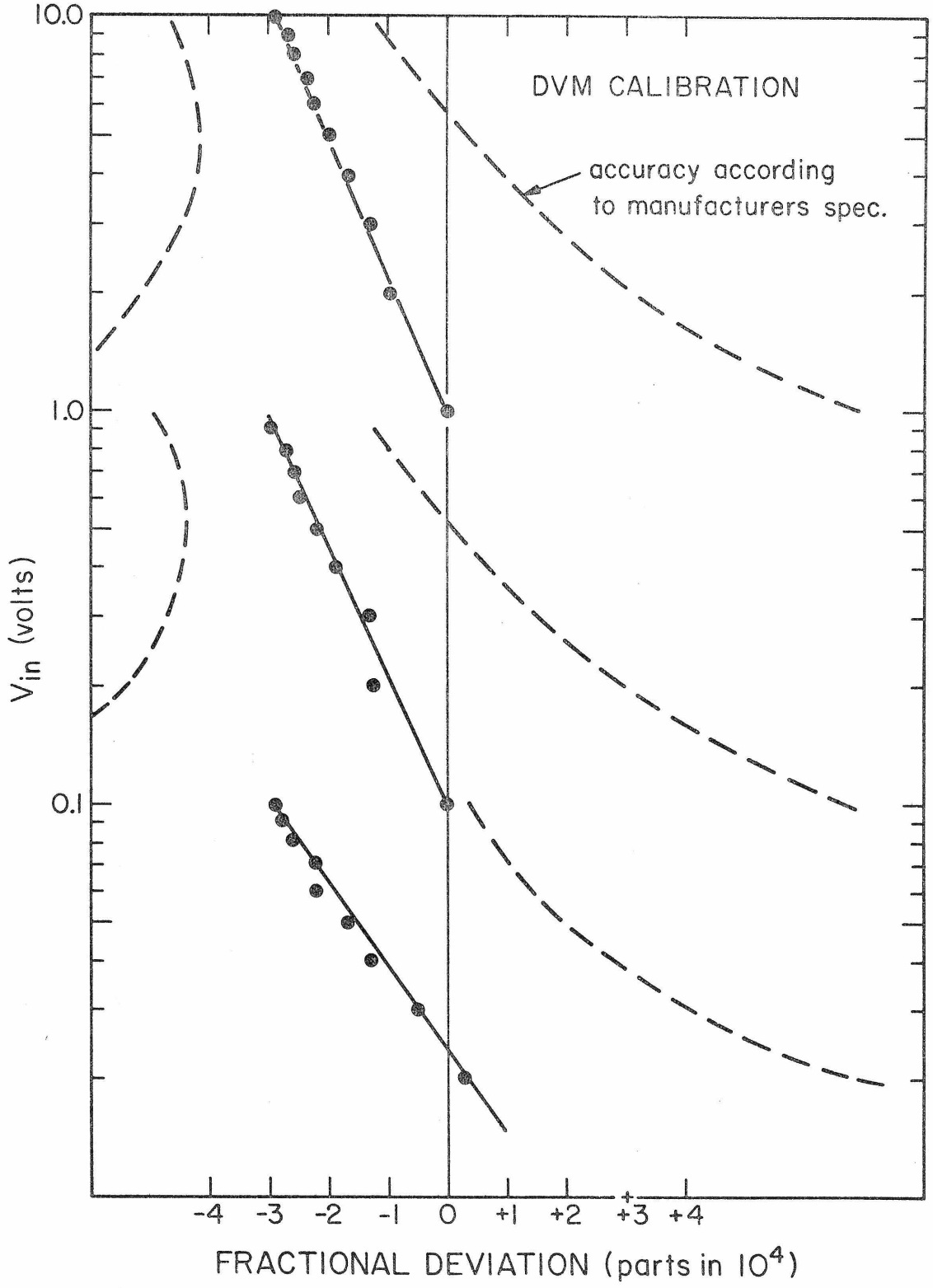
10.0
1.0
0.1
V_{in} (volts)
DVM CALIBRATION
accuracy according
to manufacturers spec.
-4
-3
-2
-1
0
+1
+2
+3
+4
FRACTIONAL DEVIATION (parts in 10^4)

Figure 5.

Figure 6. Graph showing calibration of the Holy Cow varible voltage source with the Hewlett-Packard Differential Voltmeter. The Figure is referred to in Sec.3, App.I. (Also see Table 2.)

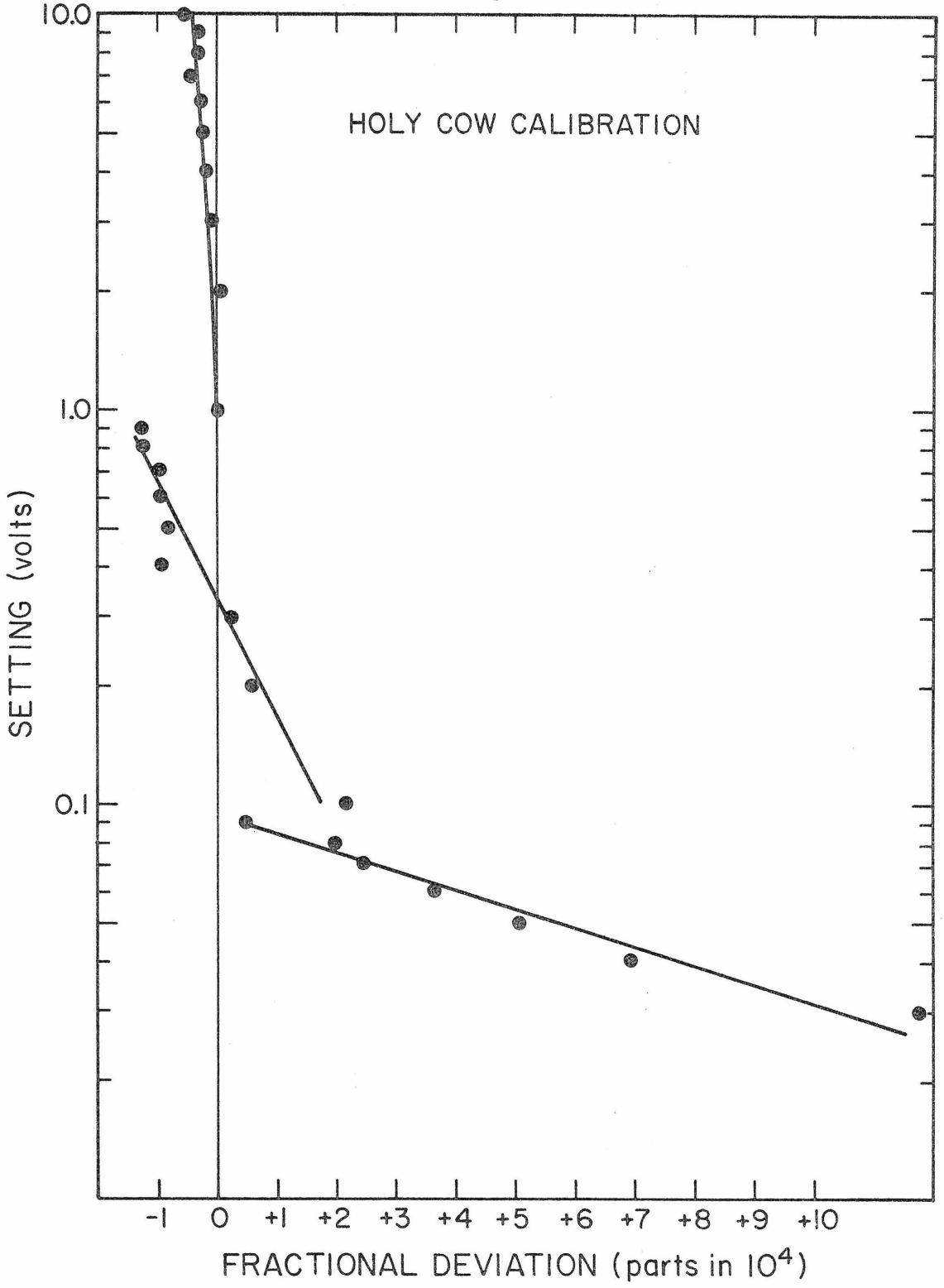
HOLY COW CALIBRATION
10.0
1.0
0.1
SETTING (volts)
-1
0
+1
+2
+3
+4
+5
+6
+7
+8
+9
+10
FRACTIONAL DEVIATION (parts in 10^4)

Figure 6.

Figure 7. Graph showing calibration of total system with Holy Cow. The Figure is referred to in Sec.3,App.I.(Also see Table 2.)

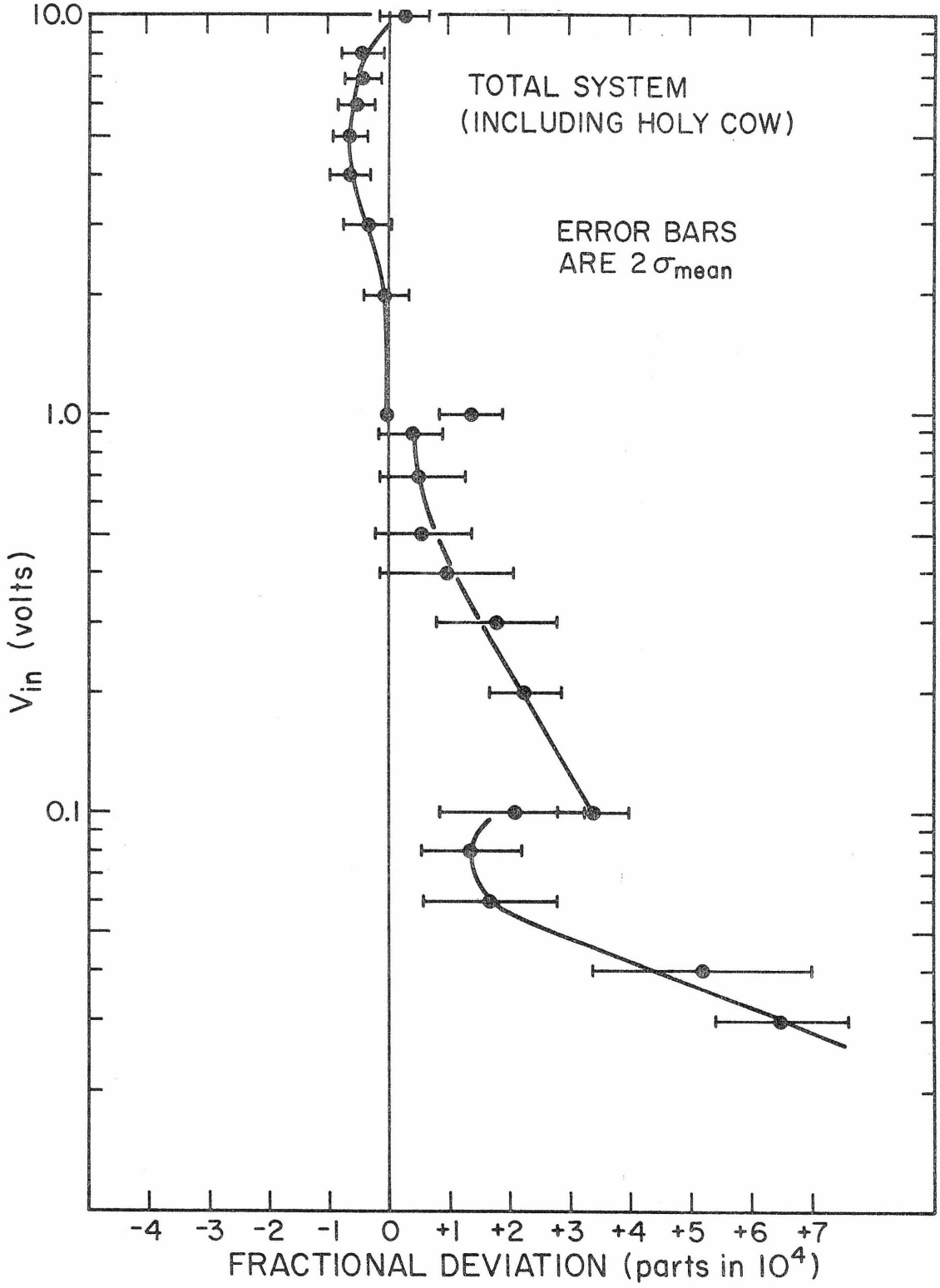
10.0
1.0
0.1
V_{in} (volts)
TOTAL SYSTEM
(INCLUDING HOLY COW)
ERROR BARS
ARE $2\sigma_{mean}$
-4 -3 -2 -1 0 +1 +2 +3 +4 +5 +6 +7
FRACTIONAL DEVIATION (parts in 10^4)

Figure 7.

Figure 8. Graph showing calibration of the total system corrected for the Holy Cow calibration shown in Figure 6. The Figure is referred to in Sec.3,App.I.(Also see Table 2.) The dashed curve is the 2σ counting statistics for an equivalent ion signal using a $10^{11}\Omega$ resistor.

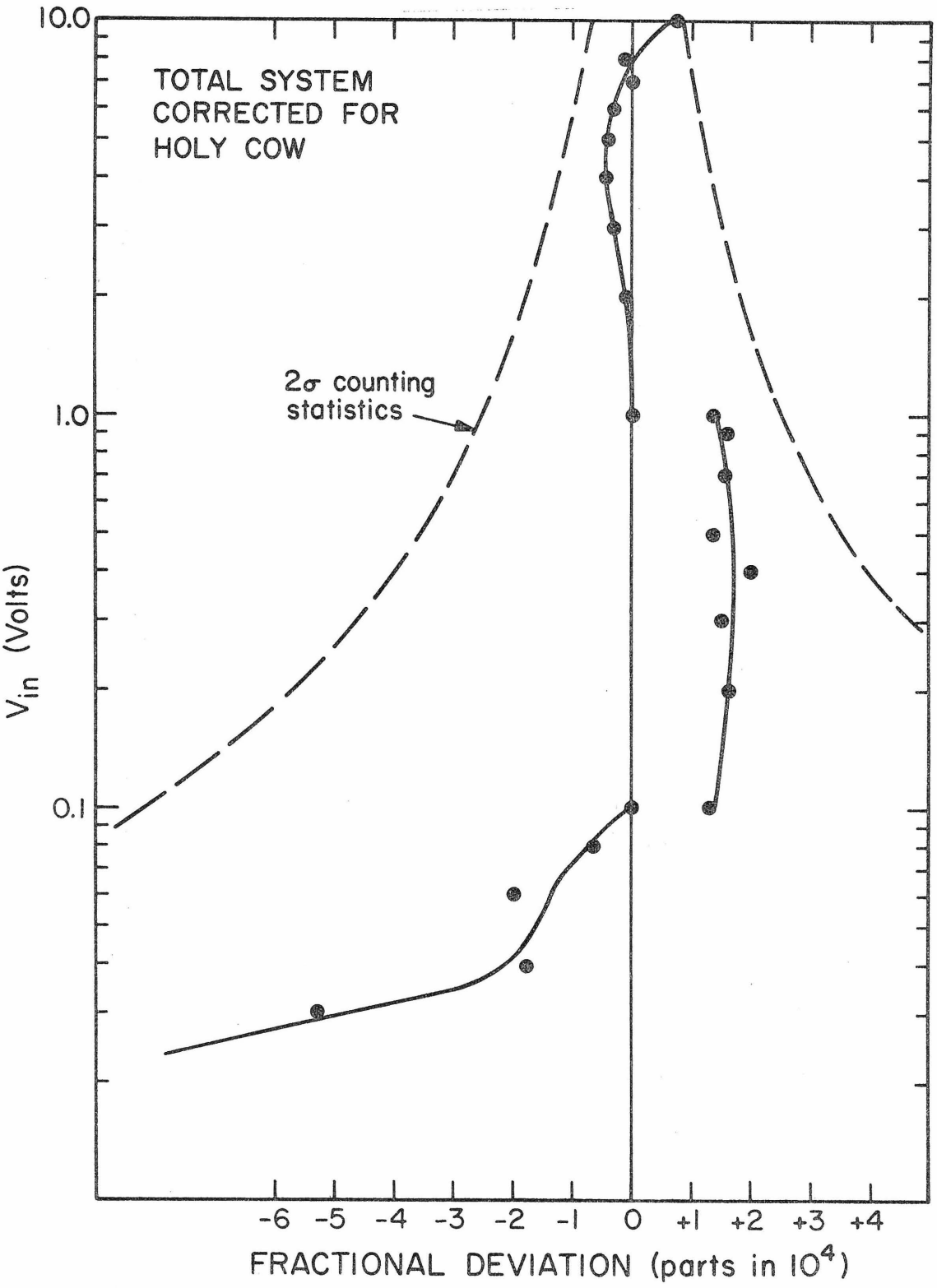
10.0
1.0
0.1
TOTAL SYSTEM
CORRECTED FOR
HOLY COW
2σ counting
statistics
V_{in} (Volts)
-6 -5 -4 -3 -2 -1 0 +1 +2 +3 +4
FRACTIONAL DEVIATION (parts in 10^4)

Figure 8.

Figure 9. Graph showing the implied calibration of the Cary 36 vibrating-reed electrometer as described in Sec.3,App.I. (Also see Table 2.)

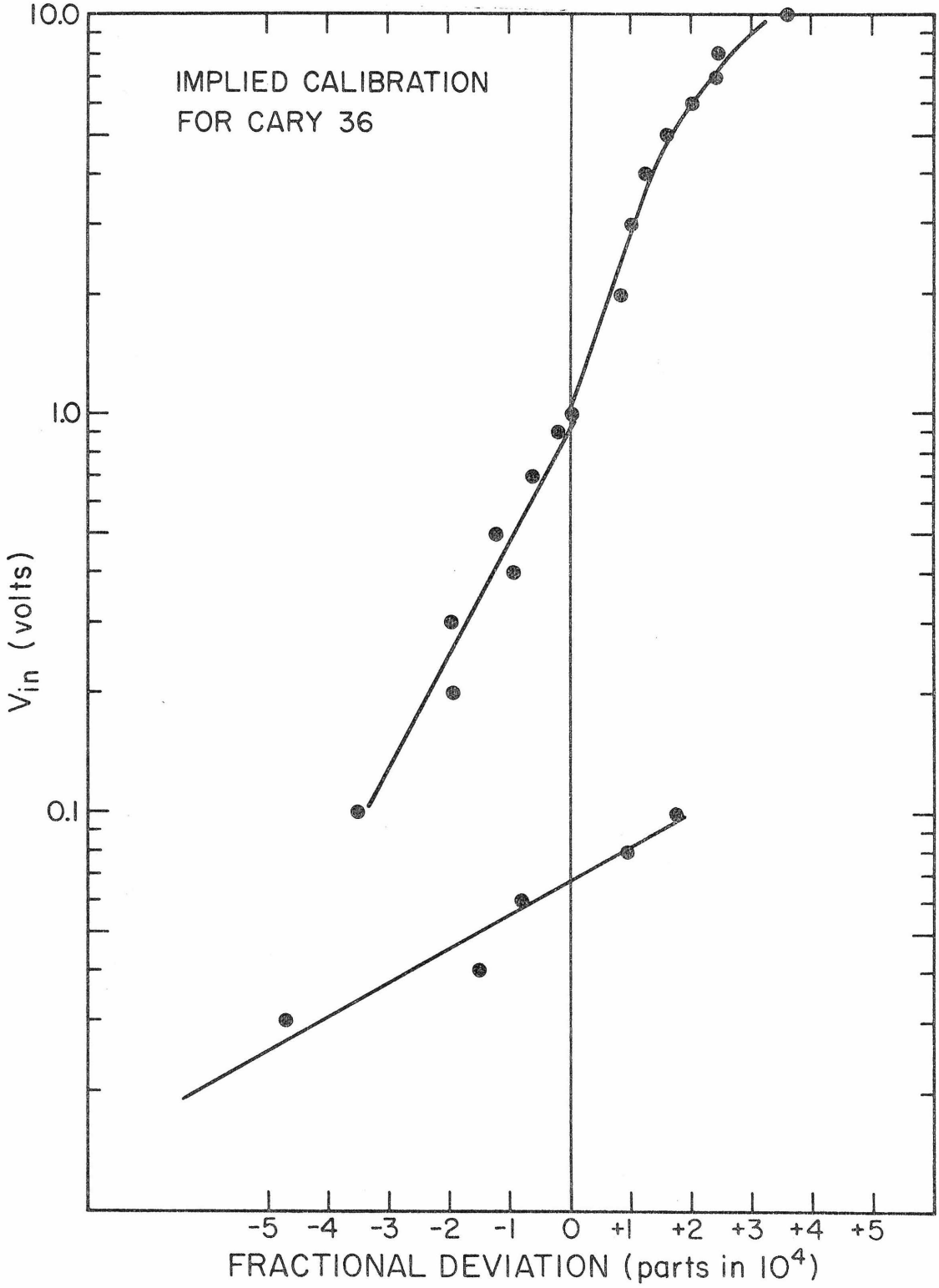
IMPLIED CALIBRATION
FOR CARY 36
10.0
1.0
0.1
V_{in} (volts)
-5 -4 -3 -2 -1 0 +1 +2 +3 +4 +5
FRACTIONAL DEVIATION (parts in 10^4)

Figure 9.

Section 4. Nuclear Chronologies for the Galaxy by G.J. Wasserburg, David N. Schramm, and J.C. Huneke. Published in The Astrophysical Journal, Vol. 157, (1969), pL91-L96.

THE ASTROPHYSICAL JOURNAL, Vol. 157, August 1969

NUCLEAR CHRONOLOGIES FOR THE GALAXY*

G. J. WASSERBURG, DAVID N. SCHRAMM, AND J. C. HUNEKE
The Charles Arms Laboratory of the Geological Sciences and The Kellogg Radiation Laboratory, California Institute of Technology, Pasadena

Received June 23, 1969

ABSTRACT

The ratios U^{235}/U^{238}, Th^{232}/U^{238}, Pu^{244}/U^{238}, and I^{129}/I^{127} have been used to obtain self-consistent solutions for the time evolution of r-process nuclei. Using $Pu^{244}/U^{238} = \frac{1}{30}$, the solutions all have a large amount of initial production, with a duration of from 0 to 10^{10} years, followed by a relatively quiescent period ($\sim 3 \times 10^8$ years) terminated by a nucleosynthetic event that possibly initiated the separation of the solar system. For values of Pu^{244} less than $\frac{1}{30}$, models of uniform synthesis terminated by a sharp nucleosynthetic event are possible.

The purpose of this Letter is to show that the relative abundances U^{235}/U^{238}, Th^{232}/U^{238}, I^{129}/I^{127}, and Pu^{244}/U^{238} at the time of formation of the solar system can provide rather severe restrictions on time scales for possible models of r-process element formation. We will further show that the existing data on the relative abundances and the relative production rates result in a very limited class of models. Previous studies have almost exclusively involved the pairs U^{235}/U^{238} and Th^{232}/U^{238} (Burbidge *et al.* 1957; Fowler and Hoyle 1960; Kohman 1961; Fowler 1962; Dicke 1969). The impetus for the present work has come from recent observations of fission products in meteoritic whitlockite produced by the decay of a transuranic element in existence at the formation of the solar system (Wasserburg, Huneke, and Burnett 1969). This isotope has been tentatively correlated with Pu^{244}. These authors point out that the ratio $Pu^{244}/U^{238} = \frac{1}{30}$ is incompatible with simple nucleosynthetic models.

The differential equation governing the abundance of isotope i with time τ is taken as $dN_i/d\tau = -\lambda_i N_i + P_i p(\tau)$, where P_i is a constant and $p(\tau)$ some function of τ; λ_i is the decay constant of species i and is zero for a stable nucleus. The integral of this equation is

$$N_i(\tau) = P_i \exp(-\lambda_i \tau) \int_0^\tau \exp(\lambda_i \xi) p(\xi) d\xi , \qquad N_i(0) = 0 . \quad (1)$$

Let the termination of nucleosynthetic activity be taken as T, the time interval between the termination and the formation of planetary objects in the solar system be taken as Δ (i.e., Δ is the period of free decay), and the time of formation of planetary objects be taken as t years ago. Then the relative abundance of two isotopes at the end of Δ is

$$\frac{N_i(T+\Delta)}{N_j(T+\Delta)} = \frac{P_i \exp[-\lambda_i(\Delta+T)] \int_0^T \exp(\lambda_i \xi) p(\xi) d\xi}{P_j \exp[-\lambda_j(\Delta+T)] \int_0^T \exp(\lambda_j \xi) p(\xi) d\xi} . \quad (2)$$

For the isotopic ratios enumerated earlier, we have four equations which must be simultaneously satisfied by T, Δ, and $p(\tau)$.

The different isotopes have very different mean lives and thus place different constraints on equation (2). The I^{129}/I^{127} ratio places a strong upper limit on Δ that is

* *Contribution* No. 1643.

virtually independent of the production ratio P_{129}/P_{127} and the choice of $p(\tau)$. The dependence of Δ on T is logarithmic and is very slowly varying (Wasserburg, Fowler, and Hoyle 1960).

Although I^{129} could possibly be formed in a process which does not produce U and Th, it is most reasonable to assume that U and Th must be made with Pu^{244}. Like I^{129}/I^{127}, the Pu^{244}/U^{238} ratio places a strong constraint on Δ; but, much more important, the abundance of U^{235} 4.6×10^9 years ago was still low enough so that the production of U^{235} associated with the necessary Pu^{244} production ($P_{235}/P_{244} = 2.2$) at times near the formation of the solar system would significantly alter the U^{235}/U^{238} ratio. The I^{129}/I^{127} and Pu^{244}/U^{238} equations in conjunction with the U^{235}/U^{238} equation constitute tight constraints on the function $p(\tau)$.

TABLE 1

VALUES OF CONSTANTS

	Standard Values	Range Explored
t	4.6×10^9 years	4.5–4.7×10^9 years
$(U^{235}/U^{238})_{now}$	1/137.8	
$(U^{235}/U^{238})_{T+\Delta}$	0.31298	0.2884–0.3397
$(Th^{232}/U^{238})_{now}$	3.8	3.0–4.4
$(Th^{232}/U^{238})_{T+\Delta}$	2.3573	1.88–2.70
$(I^{129}/I^{127})_{T+\Delta}$	1.091×10^{-4}*	$\leq 10^{-8}$
$(Pu^{244}/U^{238})_{T+\Delta}$	$\frac{1}{80}$†	$\frac{1}{75}$–$\frac{1}{150}$

PRODUCTION RATIOS EXPLORED‡

P_{235}/P_{238}	1.44 ± 0.29	P_{232}/P_{238}	1.67 (see Th/U range)
P_{244}/P_{238}	0.654 (see fractionation)	P_{129}/P_{127}	1 (see I range)

DECAY CONSTANTS USED ($year^{-1}$)

λ_{238}	1.537×10^{-10}	λ_{235}	9.72×10^{-10}
λ_{232}	4.99×10^{-11}	λ_{129}	4.077×10^{-8}
$\lambda_{244}{}^{\alpha}$	8.474×10^{-9}	$\lambda_{244}{}^{f}$	1.02×10^{-11}

* Hohenberg, Podosek, and Reynolds (1967).
† Wasserburg, Huneke, and Burnett (1969).
‡ Seeger, Fowler, and Clayton (1965).

The approach used was to examine various possible functional forms $p(\tau)$ for a simultaneous solution to equation (2) using the physical constants in Table 1 within the ranges shown. For a function $p(\tau,a,\beta,\ldots)$ with parameters a, β, . . . , we have determined the simultaneous solutions (Δ,T) to the three equations (2) (for I^{129}/I^{127}, Pu^{244}/U^{238}, and U^{235}/U^{238}) for all values of the parameters. The Th^{232}/U^{238} equation is used as an ancillary constraint to exclude models which give ratios outside the acceptable range (3.0–4.4).

For any function $p(\tau)$ a single nucleosynthetic event corresponds to the case $T = 0$. This case is illustrated in both Figures 1*a* and 1*b*. Because of the Pu^{244}/U^{238} and I^{129}/I^{127} constraints, no solution exists within the possible range of the constants.

We then consider cases of $p(\tau) = K + S\delta(\tau) + d\delta(T - \tau)$, with $K = 0$ or 1, corresponding to a model of continuous nucleosynthesis ($K = 1$) with contributions from single events at the beginning ($S > 0$) and/or the end ($d > 0$) of nucleosynthesis.

Curves for $d = 0$ and $d = 10^9$, $S = 0$, are shown in Figure 1*a*. Note that all the curves are raised with increasing d and that the concordant solutions at points A and B for $d = 0$ with the I^{129}/I^{127} curves move upward and to the right as d increases. The large displacement of B' with increasing d is due to the concomitant addition of U^{235} with Pu^{244} (for $d = 10^9$ the intersection B' does not exist).

Point B in Figure 1*a* is a triple intersection at $\Delta = 8.37 \times 10^7$ years and $T = 7.39 \times 10^9$ years. If we demand that the Pu^{244}/U^{238} curve also pass through point B, this requires that the ratio of $\frac{1}{30}$ from the whitlockite be larger than the average solar-system value by a fractionation factor of 3.8. The complete trajectories for these two intersections are

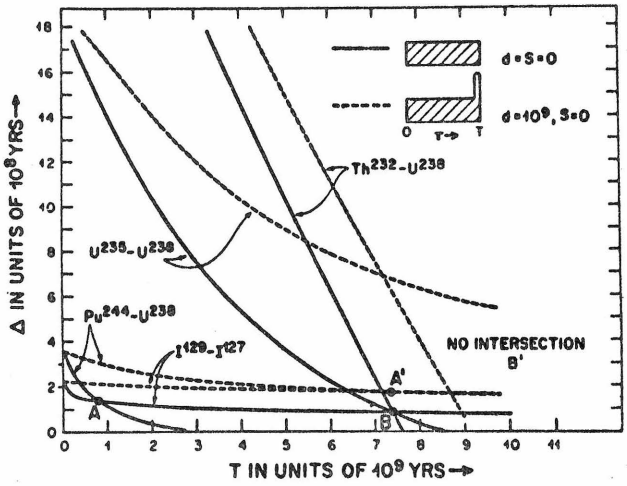

FIG. 1*a*.—(Δ,T) trajectories for each of the four isotope ratios for $\rho(\tau) = K + d\delta(\tau - T)$. Full curves are for uniform production (YONI model); dashed curves are for uniform production terminated by a spike. Points A and B are for concordance of Pu^{244}/U^{238} and I^{129}/I^{127} and of U^{235}/U^{238} and I^{129}/I^{127}, respectively. (Note concordance of the Th^{232}/U^{238} curve at point B as well.)

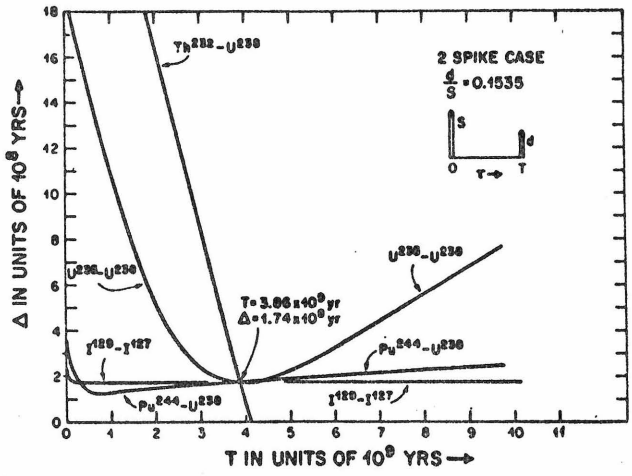

FIG. 1*b*.—Trajectories for each of the four isotope ratios for the model $\rho(\tau) = S\delta(\tau) + d\delta(T - \tau)$. Note the completely concordant point and the double intersection of Pu^{244}/U^{238} and I^{129}/I^{127} curves.

shown in Figure 2 for all values of d (curves *1* and *A*) as well as for fractionation factors of 1, 2, 3, and 4. The intersection of two curves, (U^{235}/U^{238}, I^{129}/I^{127}) and (Pu^{244}/U^{238}, I^{129}/I^{127}), is a solution to the three pertinent equations. Note that no intersection exists between curves *1* and *A* or curves *4* and *A*. Fractionation by more than 3.8 permits no solutions. Fractionations of less than 1.5 yield an unreasonable ratio $Th^{232}/U^{238} \geq 5.1$ and $T \geq 18 \times 10^9$ years. Thus any fractionation less than 1.5 or greater than 3.8 will not yield a solution. A decrease in P_{235}/P_{238} by 20 percent with a Pu^{244}/U^{238} fractionation of 1.20 will, however, yield a solution with $Th^{232}/U^{238} = 4.1$. Let us ignore the I^{129}/I^{127} constraint for this model and consider the concordance curve of Pu^{244}/U^{238} and U^{235}/U^{238}. The Th^{232}/U^{238} values along this curve are high and range from a minimum of 4.3 at $\Delta = 0$ to the maximum allowed value of 4.4 at $\Delta = 2.7 \times 10^7$ years. The fraction made in the final event, $\lambda d/(1 - e^{-\lambda T} + \lambda d)$, is 1.5 percent for a stable isotope and 14 percent for U^{235} if iodine is neglected.

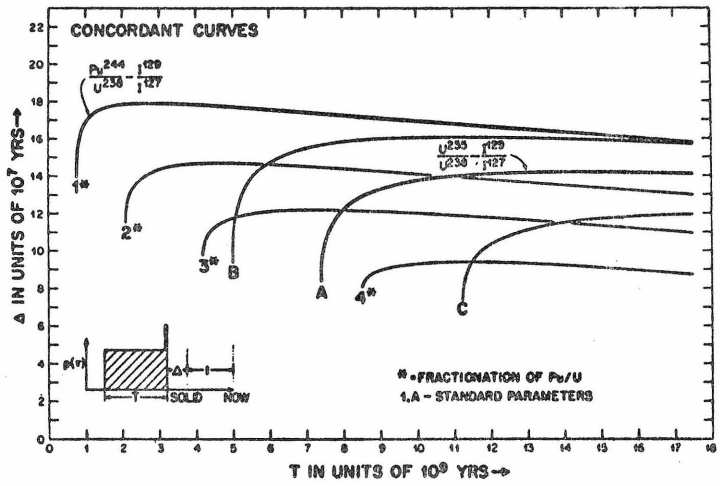

FIG. 2.—Concordant solutions of Pu^{244}/U^{238} and I^{129}/I^{127} (*1*) and concordant solutions of U^{235}/U^{238} and I^{129}/I^{127} (*A*) for $p(\tau) = K + d\delta(\tau - T)$. Curves *1*, *2*, *3*, *4*, are for $Pu^{244}/U^{238} = \frac{1}{80}$, $\frac{1}{90}$, $\frac{1}{100}$, and $\frac{1}{120}$, respectively. Curves *B* and *C* are for $P_{235}/P_{238} = 1.152$ and 1.728, respectively. This is equivalent to a shift in t of $\pm 2.7 \times 10^8$ years.

For the standard parameters used, there is no solution for uniform, continuous nucleosynthesis terminated by an event of arbitrary strength. A solution may be found at the extreme limits of all of the constants or more easily with Pu/U fractionation or some mechanism of nuclear destruction which preferentially destroys U^{235}. A ratio $Pu^{244}/U^{238} \leq \frac{1}{80}$ allows solutions for uniform synthesis with a spike at the end.

We now explore the case for $S \geq 0$. It is found that a concordant point for U^{235}/U^{238}, I^{129}/I^{127}, and Pu^{244}/U^{238} exists for $K = 0$, $d/S = 0.1535$, $T = 3.86 \times 10^9$ years, and $\Delta = 1.74 \times 10^8$ years, as shown in Figure 1*b*. This point yields $(Th^{232}/U^{238})_{now} = 3.8$. Thus it is a solution for all four isotope pairs. For $K = 1$, $S \geq 0$, and $d \geq 0$ the locus of triple concordance can be approximated by

$$\Delta(S/K,d/S) = 17.4 \times 10^7 - 3.36 \times 10^{-3}[T(S/K,d/S) - 3.86 \times 10^9] . \quad (3)$$

The case $K = 0$ is the low-T endpoint of the curve described by equation (3).

The ratio $(Th^{232}/U^{238})_{now}$ has been calculated along the curve and yields the values 3.8, 4.1, 4.4, 5.0, and 7.1 for $T = 3.9$, 4.9, 6.2, 8.2, and 13.4×10^9 years, respectively.

Solutions for this ratio greater than 4.4 are rejected, since they exceed the possible assigned limit. It follows that $3.86 \times 10^9 \leq T \leq 6.15 \times 10^9$ years, $S/K \geq 3.5 \times 10^{10}$ years and that the relative intensities are virtually fixed at $0.1535 \geq d/S \geq 0.124$. It also follows that the maximum contribution of continuous nucleosynthesis for a stable element is less than 14 percent. Note that solutions exist only for $d > 0$. Thus models without terminal events (e.g., Dicke 1969) do not yield solutions. Variations of the constants do not fundamentally alter the qualitative nature of the solutions presented here. It should be noted that values of $(Pu^{244}/U^{238})_{T+\Delta}$ less than $\frac{1}{30}$ yield a wider class of allowed solutions, whereas no solutions exist for $(Pu^{244}/U^{238})_{T+\Delta} \geq \frac{1}{15}$.

As an extension of this production model, we have examined the case

$$p(\tau) = \begin{cases} 1, & 0 \leq \tau \leq S, \\ k + d\delta(\tau - T), & S \leq \tau \leq T. \end{cases}$$

This model corresponds to a period of continuous, uniform nucleosynthesis for $\tau \leq S$ followed by a second period of continuous synthesis of a different intensity for $S \leq \tau \leq T$, and terminated by an event of strength d. For $k = 0$ there are compatible solutions for all equations for $S \leq 10^{10}$ years, $T - S \geq 1.5 \times 10^9$ years. There are sets of compatible solutions for both $k = 0$ and $k \neq 0$. In all these solutions $k(T - S)/[k(T - S) + S + d] \leq 0.14$. This is analogous to the other concordant models in which the dominant element production occurs in the first stage. For $k \neq 0$ the maximum fraction of stable elements made in the interval $S \leq \tau \leq T$ decreases with increasing S and is always less than that for the two-spike model $p(\tau) = K + S\delta(\tau) + d\delta(\tau - T)$.

Models with $dN_j/d\tau = -\lambda_j N_j + P_j \exp(-\omega_e \tau) + \omega_g N_j + P_j d\delta(\tau - T)$ were studied following Fowler (1962). For $d = 0$ no solutions exist for all values of ω_e and ω_g. For $\omega_g = 0$ solutions exist for $1/\omega_e < 2 \times 10^9$ years, with $\omega_e d \sim 0.1$ and $(Th^{232}/U^{238})_{now} < 4.4$.

For this investigation of a variety of production functions $p(\tau)$, using the "standard" values of the constants, we conclude that a nucleosynthetic model is required that has at least two distinct peaks separated by a time of low production. This time interval is about 3×10^9 years and is virtually model-independent. The first peak is an order of magnitude larger than the last peak or the integrated intervening continuous production. More subtle details of the production function are not determined, the initial peak possibly being a very rapid event or a long-time-scale continuous event. The time interval with low production is necessary in order for the U^{235} produced earlier to decay sufficiently so that the U^{235} produced with the Pu^{244} in the terminal event yields the required U^{235}/U^{238} ratio.

The values Δ are about $1\text{–}2 \times 10^8$ years for all the models in which the last event is represented as a delta function. A finite duration for this last event would reduce Δ. If this cannot be drastically decreased, then it is necessary that the Al^{26} (produced by a p-process) reported by Clarke *et al.* (1969) be produced in a later, separate event because of the short Al^{26} half-life.

The simplest interpretation may be obtained for the two-spike model. In this case the time scales are $3.86 \times 10^9 \leq T \leq 6.15 \times 10^9$ years and $1.66 \times 10^8 \leq \Delta \leq 1.74 \times 10^8$ years, the total time being $8.63 \times 10^9 \leq t + \Delta + T \leq 10.9 \times 10^9$ years. We may associate the initial event with the collapse of the proto-Galaxy and the creation of r-process nuclei in a phenomenon of short duration. This was followed by a low level of r-process element formation terminated by another sudden event, which initiated the formation of the solar system and contributed most of the Pu^{244} and I^{129} and 80 percent of the U^{235}. This type of model is in accord with the observation that the abundance of heavy elements in population I stars is independent of age. This observation has caused some workers (e.g., Unsöld 1969) to suggest that major element synthesis took place on a short time scale during the collapse of the Galaxy. If it is assumed that the astronomi-

cally observed elements may be considered as representing r-process nucleosynthesis, it would appear that these independent approaches are in good agreement.

Alternatively, we may consider the long-time-scale, steady element production with a total time $t + \Delta + T \leq 16.3 \times 10^9$ years and $S \leq 10^{10}$ years. The quiescent time is from 1.5×10^9 to less than 3.86×10^9 years. The sequence is the same as for the double-spike case, but the "initial event" is a period of uniform element synthesis.

Unless there is significant chemical fractionation of Pu, we must conclude that an event took place almost immediately prior to the formation of the solar system. This suggests that a local event (e.g., a supernova) could possibly have initiated the formation of the solar system as suggested, among other things, by Cameron (1962).

We wish to thank our colleagues D. S. Burnett, W. A. Fowler, J. L. Greenstein, Maarten Schmidt, R. F. Christy, P. J. E. Peebles, and J. W. Truran for their enthusiastic interest in our work. We have profited greatly from discussion with all of them. This work was supported by National Science Foundation grants GP9433 and 9114. One of us (D. N. S.) was supported by an NDEA Fellowship.

REFERENCES

Burbidge, E. M., Burbidge, G. R., Fowler, W. A., and Hoyle, F. 1957, *Rev. Mod. Phys.*, 29, 547.
Cameron, A. G. W. 1962, *Icarus*, 1, 13.
Clarke, W. B., de Laeter, J. R., Schwarcz, H. P., and Shane, K. C. 1969, *Trans. A.G.U.*, 50, 226.
Dicke, R. H. 1969, *Ap. J.*, 155, 123.
Fowler, W. A. 1962, in *Proceedings of the Rutherford Jubilee International Conference*, ed. J. B. Birks (London: Heywood & Co., Ltd.), p. 640.
Fowler, W. A., and Hoyle F. 1960, *Ann. Phys.*, 10, 280.
Hohenberg, C. M., Podosek, F. A., and Reynolds, J. H. 1967, *Science*, 156, 202.
Kohman, T. P. 1961, *J. Chem. Education*, 38, 73.
Seeger, P. A., Fowler, W. A., and Clayton, D. D. 1965. *Ap. J. Suppl.*, 11, 121.
Unsöld, A. O. J. 1969, *Science*, 163, 1015.
Wasserburg, G. J., Fowler, W. A., and Hoyle, F. 1960, *Phys. Rev. Letters*, 4, 112.
Wasserburg, G. J., Huneke, J. C., and Burnett, D. S. 1969, *Phys. Rev. Letters*, 22, 1198.

Section 5. Nucleochronologies and the Mean Age of the Elements by David N. Schramm, and G.J. Wasserburg. Published in The Astrophysical Journal, Vol. 162, (1970), p57-69.

THE ASTROPHYSICAL JOURNAL, 162:57–69, October 1970

NUCLEOCHRONOLOGIES AND THE MEAN AGE OF THE ELEMENTS

DAVID N. SCHRAMM AND G. J. WASSERBURG
The Charles Arms Laboratory of Geological Sciences and The Kellogg Radiation Laboratory, California Institute of Technology, Pasadena
Received 1969 December 18; revised 1970 March 16

ABSTRACT

The equations for a nucleosynthetic chronology are shown to be separable with the equations for extremely long-lived and stable nuclei yielding the mean age of the elements. This result is independent of the time-dependent production model used. This mean age is a lower bound on the age of the elements. The age of the elements is critically model-dependent. The short-lived isotopes are shown to yield the formation interval for the solar system which also is essentially model-independent. The short-lived and intermediate-lived isotopes taken relative to stable isotopes are shown to yield information on the rate of r-process nucleosynthesis with time and thus may provide the distribution of supernovae in time within the Galaxy.

I. INTRODUCTION

In a recent paper by Wasserburg, Schramm, and Huneke (1969) it was shown that information on the time dependence as well as the time scale of r-process nucleosynthesis could be extracted from the phenomenological equations for the radioactive elements produced in this process. The coupled equations involve the time duration T of nucleosynthesis, the rate of nucleosynthesis $p(\tau)$ $(0 \leq \tau \leq T)$, and the time Δ between the termination of nucleosynthesis and the formation of "cold" solid bodies (see Fig. 1).

We will show here that the functional dependence on T and Δ are separable and that to first order the time scale T depends only on the first two moments of the function $p(\tau)$. These results give a clear physical meaning to the possible solutions and permit precise rapid calculations for various models essentially by inspection.

The general differential equation describing the rate of change of the abundance of a nuclear species N_i with decay constant λ_i is

$$dN_i/d\tau = -\lambda_i N_i + \mathfrak{P}_i(\tau, N_i)\,, \tag{1}$$

where $\mathfrak{P}_i(\tau, N_i)$ is the generalized production function which may include terms representing destruction as well as production. These terms may, in general, depend on both the time τ and the abundance N_i. We assume the initial abundance $N_i(0)$ for each r-process nucleus to be zero and take this to be the origin in time.

For the present calculations we have restricted ourselves to equations of the form

$$dN_i/d\tau = -\lambda_i N_i + \omega_g N_i + P_i p(\tau) \tag{2}$$

for $\tau \leq T$, where $P_i p(\tau) + \omega_g N_i$ is the net time-dependent production function and $\omega_g N_i$ is usually a negative term representing gas loss due to stellar processes which are dependent on the gas density (see Schmidt 1963). Since $p(\tau)$ represents the rate of r-process production, which presumably takes place in supernovae (Hoyle and Fowler 1960), and ω_g represents the rate of gas loss due, for example, to trapping in remnant stars (white dwarfs, neutron stars, blackholes), then it may be that ω_g is not a constant but a time-dependent function proportional to $p(\tau)$. In these calculations it is assumed that ω_g is a constant and that the relative production rates of species i and j are constant (e.g., $P_i p(\tau)/P_j p(\tau) = P_i/P_j$ = constant). In all calculations we will use the relative number of two nuclear species (N_i/N_j). These ratios apply to the appropriate "interstellar" medium out of which the material of the solar system formed (see Fowler 1970).

We will utilize general indices to indicate a nuclear species. In practice the actual isotopes usually under consideration are ^{235}U, ^{238}U, ^{232}Th, ^{129}I, ^{127}I, and ^{244}Pu.

The integral of equation (1) from $\tau = 0$ to $\tau = T$ followed by free decay over the interval Δ is

$$N_i(T + \Delta) = P_i T\langle p\rangle \exp(-\lambda_i\Delta) \exp[-(\lambda_i - \omega_0)T] \int_0^T \exp[+(\lambda_i - \omega_0)\xi]\rho(\xi)d\xi\,, \quad (3)$$

where

$$\langle p\rangle = \frac{1}{T}\int_0^T p(\xi)d\xi \quad \text{and} \quad \rho(\xi) = p(\xi)/T\langle p\rangle \quad \text{with} \quad \int_0^T \rho(\xi)d\xi = 1\,.$$

Notice that N_i is proportional to P_i; thus, the relevant physical parameter is P_i/N_i. Note that this would not be the case if $\mathfrak{P}_i(\tau, N_i)$ in equation (1) contained a nonlinear term in N_i. For nonlinear gas-density dependence (cf. Schmidt 1963), when this term is large it may be possible to develop solutions which have a completely different behavior from those investigated here.

II. LONG-LIVED ISOTOPES

If $p(\xi) \geq 0$, we may consider $\rho(\xi)$ to be a probability-density function with the moments μ_n about the mean $\langle\tau\rangle$ as

$$\mu_n = \langle(\xi - \langle\tau\rangle)^n\rangle = \int_0^T (\xi - \langle\tau\rangle)^n \rho(\xi)d\xi\,, \quad (4)$$

where

$$\langle\tau\rangle = \int_0^T \xi\rho(\xi)d\xi \quad \text{and} \quad \mu_1 = 0\,.$$

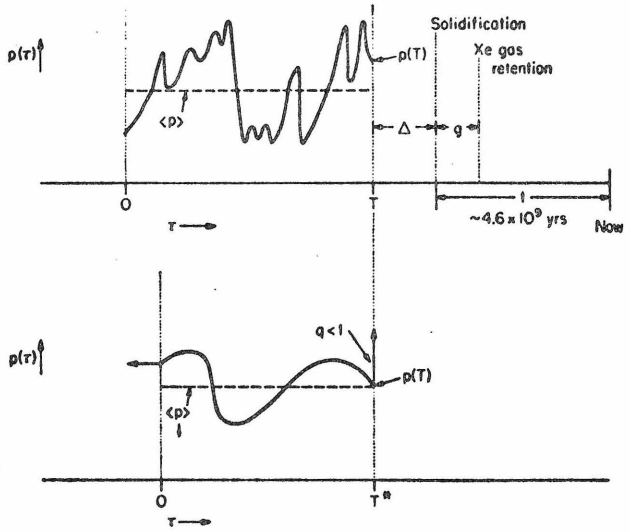

FIG. 1 (*top*).—Schematic showing duration T of r-process nucleosynthesis; formation interval Δ for solid bodies in the solar system; the Xe gas retention time g; the age t of solid bodies in the solar system; production function $p(\tau)$; average production rate $\langle p\rangle$; and final production rate $p(T)$.

FIG. 2 (*bottom*).—Schematic showing the case for $T = T^* \equiv T\langle p\rangle/p(T)$, $\langle p\rangle = p(T)$. Note that if T is increased such that $T > T^*$, then $p(T)$ becomes greater than $\langle p\rangle$ as the arrows indicate. Note also that the point $p(T)$ may be a local minimum (as illustrated) or a local maximum, even when $p(T) = \langle p\rangle$. Top figure shows the case where $T > T^*$, $p(T) > \langle p\rangle$, and $p'(T) < 0$.

Rewriting equation (3) in more convenient form, we have

$$N_i(T+\Delta) = P_i T\langle p\rangle \exp(-\lambda_i\Delta)\exp[-(\lambda_i-\omega_0)(T-\langle\tau\rangle)] \times \int_0^T \exp[(\lambda_i-\omega_0)(\xi-\langle\tau\rangle)]\rho(\xi)d\xi \tag{5}$$

$$= P_i T\langle p\rangle \exp(-\lambda_i\Delta)\exp[-(\lambda_i-\omega_0)(T-\langle\tau\rangle)][1+\beta_i],$$

where

$$\beta_i \equiv \sum_{n=0}^{\infty}\frac{(\lambda_i-\omega_0)^{n+2}}{(n+2)!}\mu_{n+2} = \frac{(\lambda_i-\omega_0)^2}{2!}\mu_2 + \frac{(\lambda_i-\omega_0)^3}{3!}\mu_3 + \cdots.$$

The ratio of two stable isotopes is simply the ratio of the production rates. The stable isotopes are total production integrators and do not themselves determine time. It is basically the ratio of an unstable isotope r (with $\lambda_r T \lesssim 1$) to a stable isotope s which determines time by the relative decay of the radioactive isotope r as compared with the stable one s.

Defining

$$R(i,j) \equiv \frac{P_i/P_j}{N_i(T+\Delta)/N_j(T+\Delta)} \quad \text{and} \quad \Delta_{ij}^{\max} \equiv \frac{\ln[R(i,j)]}{\lambda_i-\lambda_j}$$

we have from equation (5)

$$\text{a)}\quad T\left(1-\frac{\langle\tau\rangle}{T}\right) = \Delta_{ij}^{\max} - \Delta + \frac{1}{\lambda_i-\lambda_j}\ln\left(\frac{1+\beta_i}{1+\beta_j}\right),$$

$$\text{b)}\quad T = \frac{1}{1-\langle\tau\rangle/T}\left[\Delta_{ij}^{\max} - \Delta + \frac{1}{(\lambda_i-\lambda_j)}\ln\left(\frac{1+\beta_i}{1+\beta_j}\right)\right]. \tag{6}$$

The quantity $\Delta_{ij}^{\max}$ is the age for the sudden-synthesis solution ($T = \langle\tau\rangle = \beta_i = \beta_j = 0$) for isotopes i and j. We note that the quantity $R(i,j)$ is bounded by $1 \geq R(i,j)\exp[(\lambda_j-\lambda_i)\Delta] \geq \exp[-(\lambda_j-\lambda_i)T]$ for $\lambda_i < \lambda_j$.

For $\beta_i \lesssim 2$, we get to a good approximation

$$T(1-\langle\tau\rangle/T) = \Delta_{ij}^{\max} - \Delta + \frac{1}{\lambda_i-\lambda_j}\left[\frac{\beta_i}{1+\frac{1}{2}\beta_i} - \frac{\beta_j}{1+\frac{1}{2}\beta_j}\right]; \tag{7}$$

or to the first nonvanishing term in λ:

$$T(1-\langle\tau\rangle/T) \cong \Delta_{ij}^{\max} - \Delta + \tfrac{1}{2}(\lambda_i+\lambda_j-2\omega_0)\mu_2. \tag{8}$$

In the simplest case when $\lambda_r T \ll 1$, we have from equation (8)

$$T - \langle\tau\rangle + \Delta \cong \frac{1}{\lambda_r}\ln[R(r,s)] = \Delta_{rs}^{\max}. \tag{9}$$

Ignoring Δ for the moment, it follows that the *mean age* (as measured backward from T) of r-process elements is given by $\Delta_{rs}^{\max}$. This is *independent* of the rate of nucleosynthesis $p(\tau)$ and ω_0. Insofar as the quantities on the right-hand side are known and the condition $\lambda_r T \ll 1$ is satisfied, we may calculate $T - \langle\tau\rangle$. This must be the same for all such pairs of elements. If, therefore, $R(r', s')$ is unknown for one pair, it may be calculated from another pair $\{(\lambda_r)^{-1}\ln[R(r,s)] = (\lambda_{r'})^{-1}\ln[R(r',s')]\}$. If two pairs of isotopes do not have the same "mean age," it follows that either the data are wrong or the basic model is in error.

It is important to note that, although for the limit $\lambda_r T \ll 1$ the mean age $(T - \langle\tau\rangle)$ is obtained without any assumption about the production function $p(\tau)$, information on the

duration T of nucleosynthesis is model-dependent regardless of the number of isotopic pairs. Of course, T is always greater than $T - \langle\tau\rangle$. To zero order in λ, T depends only on the distribution function through the normalized first moment. If $\rho(\tau)$ is symmetric, then $\langle\tau\rangle/T = \frac{1}{2}$ and $T \cong 2[\Delta_{ij}{}^{\max} - \Delta]$. If $\rho(\tau)$ is strongly peaked at $\tau = 0$, then $\langle\tau\rangle/T \cong 0$ and $T \cong \Delta_{ij}{}^{\max} - \Delta$. If $\langle\tau\rangle/T \to 1$ or $T \to 0$, then $\Delta \to \Delta_{ij}{}^{\max}$ (the single-event sudden-synthesis case). If higher-order moments begin to make significant contributions, then for $\rho(\tau)$ symmetric, $T \geq 2(\Delta_{ij}{}^{\max} - \Delta)$. The contribution of $\jmath$ may be evaluated for a test case to see if $T - \langle\tau\rangle$ is model-insensitive. For continuous uniform nucleosynthetic theory $\rho = 1/T$ and

$$\jmath_i = \frac{2\{\sinh[\frac{1}{2}(\lambda_i - \omega_0)T] - \frac{1}{2}(\lambda_i - \omega_0)T\}}{(\lambda_i - \omega_0)T};$$

and for a two-spike model $\rho(\tau) = (1 - C)\delta(\tau) + C\delta(\tau - T)$

$$\jmath_i = C\left\{\exp\left[(\lambda_i - \omega_0)\frac{(1-C)}{C}\langle\tau\rangle\right] - 1 - (\lambda_i - \omega_0)\frac{(1-C)}{C}\langle\tau\rangle\right\}$$

$$+ (1 - C)\{\exp[-(\lambda_i - \omega_0)\langle\tau\rangle] - 1 + (\lambda_i - \omega_0)\langle\tau\rangle\}.$$

The case having maximum even moments is the two-spike case with $C = \frac{1}{2}$, which reduces to $\jmath_i = \cosh[\frac{1}{2}T(\lambda_i - \omega_0)] - 1$. For $(\lambda_i - \omega_0) \leq 1/(5\langle\tau\rangle)$, the correction in $T - \langle\tau\rangle$ for $\jmath_i$ corresponds to less than 10 percent in the worst case.

The isotopes used for determining $\langle\tau\rangle$ and the model-dependent T are ^{238}U and ^{232}Th (Fowler and Hoyle 1960). The ^{232}Th basically acts like a stable isotope with a small correction for radioactive decay and the time scale is governed by ^{238}U. As the time scale T is comparable with $1/\lambda_{238} = 6.5 \times 10^9$ years, the approximation $\lambda\langle\tau\rangle \ll 1$ is inaccurate, and it is necessary to include the quadratic term in order to obtain a precise root T. Specifically, the time T is given from equation (8),

$$T = \frac{2(\Delta_{ij}{}^{\max} - \Delta)}{1 - (\langle\tau\rangle/T) + \{[1 - (\langle\tau\rangle/T)]^2 - 2(\Delta_{ij}{}^{\max} - \Delta)(\lambda_i + \lambda_j - 2\omega_0)(\mu_2/T^2)\}^{1/2}}. \quad (10)$$

For parameters such that $2(\Delta_{ij}{}^{\max} - \Delta)(\lambda_i + \lambda_j - 2\omega_0)(\mu_2/T^2) > [1 - (\langle\tau\rangle/T)]^2$, the specific model does not permit a solution. Notice that large deformations in $\rho(\tau)$ near $\langle\tau\rangle$ will not change $\langle\tau\rangle$, and thus will only affect T through the second-order term (see eq. [8]).

From the standard value for $R(232, 238)$ shown in Table 1, $\Delta_{232,\,238}{}^{\max} = 3.2 \times 10^9$ years, which means that all symmetric production functions $p(\tau)$ would from equation (9) have a duration $T \sim 6.4 \times 10^9$ years and a highly peaked production function would have a duration $T \sim 3.2 \times 10^9$ years. Unfortunately, at present $R(232, 238)$ is not precisely known due to uncertainties in both the relative production rates and the Th/U ratio (see Appendix). The range of $\Delta_{232,\,238}{}^{\max}$ corresponding to the range shown in Table 1 for $R(232, 238)$ is 1.1×10^9 years $< \Delta_{232,\,238}{}^{\max} < 5.7 \times 10^9$ years.

For most models the second-order terms as given in equation (10) contribute less than $\sim$10 percent; thus the mean age $T - \langle\tau\rangle \approx (\Delta_{232,\,238}{}^{\max} - \Delta)$. Notice that for a range of values of $\Delta_{232,\,238}{}^{\max}$ the larger values of $\Delta^{\max}$ yield larger values of T, resulting in larger values for the terms in $\jmath_i$. Thus, from the range of values of $\Delta^{\max}$ for ^{238}U and ^{232}Th, it is clear that the mean age is not fully model-independent because of the contributions from $\jmath$. A superior chronometer for the mean age $T - \langle\tau\rangle$ would be made by an isotope such as ^{232}Th, which has a mean life 3 times longer than ^{238}U, taken relative to a stable isotope, under the assumption that the physical constants are precisely known.

In conjunction with this long-lifetime limit, the pair ^{187}Re-^{187}Os is particularly important (Clayton 1964), since the half-life of ^{187}Re is $\sim 4 \times 10^{10}$ years.

For the ^{187}Re case higher-order terms will definitely be negligible, thus the mean age $T - \langle\tau\rangle$ equals $\Delta_{187}^{max} - \Delta$, where Δ_{187}^{max} is given by

$$\Delta_{187}^{max} = \frac{\ln [1 + (^{187}Os_{rad}/^{187}Re)]}{\lambda_{187}}.$$

Here $^{187}Os_{rad}$ is the ^{187}Os produced by the decay of ^{187}Re. Using the available data on Re-Os, relative abundances and isotopic compositions, as well as an estimate from nuclear systematics of the ratio of neutron-capture cross-sections $\sigma(^{186}Os)/\sigma(^{187}Os)$, Clayton (1969) has estimated $(^{187}Os_{rad}/^{187}Re)$ to be $\sim$0.12.

It is important to note that all quantities used in calculating the Δ^{max} for ^{187}Re are measurable whereas the Δ^{max} from $^{232}Th/^{238}U$ requires a theoretical calculation of P_{232}/P_{238}.

Unfortunately, the cross-sections have not been measured and the half-life of ^{187}Re is not very well known. The best determination is that of Hirt *et al.* (1963), who took a mean of 4.3×10^{10} years from the data ranging from $3.2 \pm 0.5 \times 10^{10}$ to $5.5 \pm 1.0 \times 10^{10}$ years. Thus, taking the range of half-lives and $(^{187}Os_{rad}/^{187}Re)$, we obtain $4 \times$

TABLE 1

VALUES OF CONSTANTS

A. $t = 4.6 \pm 0.1 \times 10^9$ years

Decay Constants (in yr^{-1})	Decay Constants (in yr^{-1})
$\lambda_{238} = 1.537 \times 10^{-10}$	$\lambda_{235} = 9.72 \times 10^{-10}$
$\lambda_{232} = 4.99 \times 10^{-11}$	$\lambda_{129} = 4.077 \times 10^{-8}$
$\lambda_{244}{}^{a} = 8.474 \times 10^{-9}$	$\lambda_{246}{}^{f} = 1.02 \times 10^{-11}$

B. STANDARD VALUES WITH ESTIMATED RANGES

Relative Abundances	Production Ratios[a]
$(^{235}U/^{238}U)_{now} = 1/137.8 \rightarrow (^{235}U/^{238}U)_{T+\Delta} = 0.31298$	$P_{235}/P_{238} = 1.46(+0.40, -0.30)$
$(^{232}Th/^{238}U)_{now} = 3.9(+0.5, -0.2)$	
$(^{232}Th/^{238}U)_{T+\Delta} = 2.42(+0.35, -0.14)$†	$P_{232}/P_{238} = 1.74(+0.30, -0.20)$
$(^{129}I/^{127}I)_{T+\Delta+g} = 1.09 \times 10^{-4}$‡	$P_{129}/P_{127} = 2.93(+1.00, -2.00)$
$(^{244}Pu/^{232}Th)_{T+\Delta+g} = 0.014(+0.003, -0.010)$§	$P_{244}/P_{232} = 0.388 \pm 0.1$

C. $R(i, j)$'s AND THEIR ALLOWED RANGES

$R(i,j) = (P_i/P_j)/(N_i/N_j)_{T+\Delta}$	Standard	Range	$\Delta_{i,j}^{max}$ for Standard $R(i, j)$'s (years)
$R(235, 238)$	4.665	3.706–5.943	1.9×10^9
$R(232, 238)$	0.719	0.556–0.895	3.2×10^9
$R(129, 127)$	26880.0	8532.0–36060.0	2.5×10^8
$R(244, 232)$	27.7	16.9–122.0	4.0×10^8

NOTE.—The quantity g is normally taken as zero.

[a] Seeger, Fowler, and Clayton (1965); range estimate includes work of Seeger and Schramm (1970). It should be noted that these numbers are theoretical numbers since they are impossible to measure experimentally, and thus the range is merely a theoretical estimate of the validity of the numbers.

† See Appendix.

‡ Hohenberg, Podosek, and Reynolds (1967).

§ Wasserburg, Huneke, and Burnett (1969*a*, *b*); range estimate includes work of Podosek (1970).

$10^9 \leq \Delta_{187}^{\max} \leq 11 \times 10^9$ years. When the $\Delta^{\max}$ for ^{187}Re is compared with that for ^{232}Th/^{238}U, it is found that it is possible to get identical mean ages $T - \langle\tau\rangle$ within the ranges of uncertainty, but the current "best" values are different by more than a factor of 2 (see Clayton 1969). As pointed out by Bahcall (1961) and Clayton (1969), it is still possible that this conflict may be resolved by the enhanced ^{187}Re decay in stellar atmospheres.

III. SHORTER-LIVED ISOTOPES

Returning to equation (3) and integrating by parts, we obtain the series

$$N_i(T + \Delta) = P_i \exp(-\lambda_i\Delta) \sum_{n=0}^{\infty} \frac{(-1)^n}{\lambda^{n+1}} \left[\frac{d^n p(\tau)}{d\tau^n}\bigg|_{\tau=T} - \frac{d^n p(\tau)}{d\tau^n}\bigg|_{\tau=0} \exp(-\lambda_i T) \right]. \quad (11)$$

For large λ_i, if $p^{-1}dp/d\tau \ll \lambda_i$ and the terms attenuated by $\exp(-\lambda_i T)$ are negligible, we have

$$N_i(T + \Delta) \cong \frac{P_i}{\lambda_i} p(T) \exp(-\lambda_i\Delta).$$

If the ratio of two such isotopes were known at $T + \Delta$, then this would determine Δ directly:

$$\Delta = \frac{1}{\lambda_i - \lambda_j} \ln [R(i, j)\lambda_j/\lambda_i].$$

This is simply the time for the isotopic ratio to go from $(P_i/\lambda_i)/(P_j/\lambda_j)$ to $N_i(T + \Delta)/[N_j(T + \Delta)]$ by free decay. In general, the direct ratio to a long-lived or stable nucleus is determined (for example, ^{129}I and ^{127}I or ^{244}Pu and ^{238}U). Using the subscript L for a long-lived or stable nucleus, we have for $\lambda_i \gg \lambda_L$

$$N_L \cong P_L T\langle p\rangle[1 - (T - \langle\tau\rangle)\lambda_L].$$

Thus,

$$\frac{N_i(T + \Delta)}{N_L(T + \Delta)} \cong \frac{P_i \exp[-(\lambda_i - \lambda_L)\Delta]}{\lambda_i P_L} \frac{p(T)}{T\langle p\rangle[1 - (T - \langle\tau\rangle)\lambda_L]}. \quad (12)$$

In this equation there is a direct dependence on T. This may be particularly strong for the case of the pair ^{244}Pu and ^{238}U, where the dependence on T is strong because of the fact that $\lambda_{238}T \sim 1$. It is thus preferable to use the pair ^{244}Pu-^{232}Th in which the ^{232}Th virtually behaves as a stable isotope (for $T - \langle\tau\rangle = 3 \times 10^9$ years, $\lambda_{232}(T - \langle\tau\rangle) \approx 0.15$). For two equations of the form (12) for isotopes i, L and j, L', we have, upon taking the ratio and transposing,

$$\Delta_{i,j} \cong \frac{1}{\lambda_i - \lambda_j} \left\{ \ln \left[\frac{\lambda_j R(i, L)}{\lambda_i R(j, L')} \right] + \ln \left[\frac{1 - (T - \langle\tau\rangle)\lambda_L}{1 - (T - \langle\tau\rangle)\lambda_{L'}} \right] \right\}. \quad (13)$$

For stable or very long-lived isotopes, the second term on the right-hand side is negligible. This is independent of T and $p(\tau)$ to very high order and is a direct determination of Δ. If we had not assumed the production function to be smooth but instead allowed a spike at time T (e.g., $p(\tau) = p_0(\tau) + d\delta(\tau - T)$ where $p_0(\tau)$ is smooth, we would obtain

$$\Delta_{ij} \cong \frac{1}{\lambda_i - \lambda_j} \ln \left[\frac{\lambda_j R(i, L)}{\lambda_i R(j, L')} \frac{p_0(T) + \lambda_i d}{p_0(T) + \lambda_j d} \right]. \quad (14a)$$

The range in Δ is thus between that given by equation (13) and

$$\Delta_{ij} \cong \frac{1}{(\lambda_i - \lambda_j)} \ln \left[\frac{R(i, L)}{R(j, L')} \right]. \quad (14b)$$

For the case of ^{129}I and ^{244}Pu, it is important to note that these nuclides are inferred from anomalies in Xe gas in meteorites, whereas the other abundances used are from nonvolatile or less volatile elements. Throughout this discussion we have assumed that all relative abundances are representative of the same time, $T + \Delta$; however, a gas may not be retained in a solid body the same time as other elements. Thus, the relative abundances for the Xe-related elements may actually be representative of some other total time, $T + \Delta + g$, where g is the time difference between the formation of solid objects and the time when Xe is retained. Thus, for ^{129}I and ^{244}Pu, $\Delta + g$ should be substituted for Δ in all of the above equations pertaining to the short-lived isotopes. Using ^{129}I/^{127}I and ^{244}Pu/^{232}Th, our standard $R(i, j)$ values give $\Delta + g = 2.1 \times 10^8$ years for a pure spike model (eq. [14b]) varying down to $\Delta + g = 1.5 \times 10^8$ for an unspiked model (eq. [13]). The total range in Δ, including uncertainties in $R(i, j)$, is 7.5×10^7 years $\leq \Delta + g \leq 2.5 \times 10^8$ years. Throughout the rest of our discussion, we will assume $g = 0$.

Another point is that iodine is not a transuranic element, thus processes can occur which would produce iodine but not the transuranics (cf. Fowler, Greenstein, and Hoyle 1962). If a fraction f of the ^{129}I were made in a special process, then the correct value of $R(129, 127)$ from the r-process would increase by the factor $1/(1 - f)$ from the observed value. The new $R^*(129, 127) = R^0(129, 127)/(1 - f)$ can then be used in the above equations. It should be noted that the change in Δ resulting from the use of $R^*(129, 127)$ rather than $R^0(129, 127)$ is $[-\ln (1 - f)]/\lambda_{129}$. Thus, even if 90 percent of the ^{129}I were made in a special process, the resulting change in Δ would be an increase of only 5.6×10^7 years. For the rest of this discussion, we will assume that no such process occurred and thus set $f = 0$ in the calculations.

When ^{244}Pu is used, it is important to remember that this nucleus is inferred to be present from the presence of fission xenon and fission tracks in meteorites. Although the existence of a fissionable transuranic element at the formation of the solar system appears certain (Wasserburg, Huneke, and Burnett 1969*a*, *b*), the fission Xe spectrum of ^{244}Pu has not been determined, and thus no definitive identification of the fissioning nucleus as ^{244}Pu has been made. If the fission Xe is due not to ^{244}Pu but to some other nucleus R, then for a given model $p(\tau)$, it is possible to calculate limits on the R half-life. In this case Δ becomes indeterminate, and it is only possible to conclude that $\Delta \leq \Delta_{129,\,127}{}^{\max}$.

Returning to equation (13), we note that (similar to the case for $T - \langle\tau\rangle$ in eq. [9]), the result for Δ is independent of which appropriate pair of isotopes is used. This may be used to calculate relative production rates from the value of Δ determined by another isotope pair.

When $p(\tau)$ is smooth, we see that for two pairs of short-lived nuclei, both Δ and $p(T)/T\langle p\rangle$ are determined. From equation (12)

$$\frac{1}{T^*} \equiv p(T)/T\langle p\rangle = \frac{\lambda_i}{R(i, L)} \exp\left[(\lambda_i - \lambda_L)\Delta\right]\left[1 - (T - \langle\tau\rangle)\lambda_L\right], \qquad (15)$$

and Δ was determined from equation (13). The time scale T^* is 1.1×10^9 years for the standard values of Table 1. Notice that spiked models decrease T^* due to the increase in Δ (see eq. [14]). Thus, $T^* \leq 1.1 \times 10^9$ years.

To gain an understanding of $p(T)/T\langle p\rangle$, it is interesting to compare T^* (which is the duration obtained from eq. [15] when $p(T) = \langle p\rangle$) with the mean age $T - \langle\tau\rangle$ obtained from a long-lived pair. This duration T^* represents the duration if the final production rate is equal to the average production rate (see Fig. 2). If the age T as determined by equation (6) is greater than this duration, it indicates that $p(T)$ is greater than $\langle p\rangle$ (the final rate of nucleosynthesis is larger than the average rate). If $p(\tau)$ is thought of as the relative contribution of supernovae throughout the history of the Galaxy, then

$p(T) > \langle p \rangle$ would mean that the final supernova events just prior to formation of the solar system contributed more material to the solar system than the average event, and thus at least one of the final events may be thought of as occurring in the near vicinity of the proto-solar nebula.

Let us consider the sensitivity of equation (13) to a change in parameters. If Δ_0 is a solution to equation (13) for the parameters $R^0(129, 127)$ and $R^0(244, 232)$, then the solution for $R(129, 127) = KR^0(129, 127)$ and $R(244, 232) = kR^0(244, 232)$ is $\Delta = \Delta_0 + (\lambda_i - \lambda_j)^{-1} \ln (K/k)$ and

$$q \equiv \frac{p(T)/T\langle p \rangle}{p_0/T_0\langle p_0 \rangle} = \frac{K^{\lambda_j/(\lambda_i-\lambda_j)}}{k^{\lambda_i/(\lambda_i-\lambda_j)}}, \qquad \text{where } j = 244 \text{ and } i = 129. \quad (16)$$

Notice that Δ changes slowly with changes in K/k. Changes in the character of the production function as a result of a change in parameters is shown by deviations of the quantity q from unity. The production function is most sensitive to changes in $R(i, j)$ for the nuclide with the longer mean life (in our case ^{244}Pu) because of the form of the exponents. Thus, differences due to chemical fractionation between the true average solar-system value of (^{244}Pu/^{232}Th) or (^{244}Pu/^{238}U) and the measured values in particular materials will result in large changes in $p(T)/T\langle p \rangle$.

IV. INTERMEDIATE-LIVED NUCLEI

Let us now consider the case of nuclei with slightly longer mean lives (e.g., ^{235}U) assuming $p(\tau)$ is smooth. From equation (11) we have

$$N_i(T + \Delta) \cong P_i \exp(-\lambda_i \Delta) \frac{p(T)}{\lambda_i} \left[1 - \frac{p'(T)}{\lambda_i p(T)} + \ldots\right], \quad (17)$$

where

$$p'(T) = \left.\frac{dp(\tau)}{d\tau}\right|_T.$$

Normalizing to a stable or very long-lived nuclide, we have

$$\left.\frac{N}{N_L}\right|_{T+\Delta} \cong \frac{P_i \exp(-\lambda_i \Delta)}{\lambda_i P_L} \frac{p(T)}{T\langle p \rangle} \left[1 - \frac{p'(T)}{\lambda_i p(T)} + \ldots\right]. \quad (18)$$

Using the value of Δ and $p(T)/T\langle p \rangle$ as determined by the short-lived nuclei, we may determine $p'(T)/T\langle p \rangle$. From considerations of a series of short-lived and intermediate-lived isotopes, we may determine $p(T)/T\langle p \rangle$, $p'(T)/p(T)$, $p''(T)/p(T)$, . . . , and determine the shape of the production function in the neighborhood of T.

To investigate the effects of change in the parameters $R(i, j)$ for the short-lived nuclides on the shape of the production function, let us consider a "neutral point" indicated by the subscript 0 for which a solution exists for the short-lived isotopes determining Δ_0 and $p_0/T_0\langle p \rangle_0$ and an intermediate-lived isotope yielding $p'_0 = 0$ (where higher-order terms are assumed to be negligible). Then for changes in the parameters $R(i, j)$ for the short-lived isotopes we see that, relative to this neutral point, if $q > 1$, then $p' > 0$; and conversely, if $q < 1$, then $p' < 0$. Relative to the neutral point, increases in $p(T)/T\langle p \rangle$ require that the rate of nucleosynthesis increase just before termination. A decrease in $p(T)/T\langle p \rangle$ relative to the neutral point requires the rate to decrease. Note that if $T = T^e$ (eq. [15]), $p(T) = \langle p \rangle$, but $p(\tau)$ still has a local maximum (or minimum) at $\tau = T$ if $p'(T)$, from equation (18), is positive (or negative).

For particular models where the shape of the distribution function is explicitly given, the intermediate-lived cases (e.g., ^{235}U) may then give us information on T; however,

this information must be consistent with the mean-age determination from the long-lived isotopes or else the model is invalid. The ^{235}U-^{238}U constraint is particularly critical because of the fact that the ratio ($^{235}U/^{238}U$) is precisely known and the mean life of $^{235}U(1/\lambda_{235} = 1.03 \times 10^9$ years) is intermediate in comparison with T. From these considerations, we can analyze the results of Wasserburg, Schramm, and Huneke (1969), where it was shown that for certain values of $R(244, 238)$ it was necessary to have a peak in $p(\tau)$ at the termination of nucleosynthesis. The high value of $p(T)$ came from the low value of $R(244, 232)$ and the comparison of $T^* \leq 1.5 \times 10^9$ and $(T - \langle\tau\rangle) = 3.7 \times 10^9$ years for their standard parameters. The fact that the distribution was sharply peaked rather than a gradually rising function came from the ^{235}U constraint.

Let us examine the constraints imposed by our present standard parameters. It has been shown that independent of model $T - \langle\tau\rangle \approx 3.2 \times 10^9$ years; the formation interval Δ lies in the range 1.5×10^8 years $\leq \Delta \leq 2.1 \times 10^8$ years and $T^* \leq 1.1 \times 10^9$ years. By the use of equation (17) it can also be shown from using the $^{235}U/^{238}U$ constraint that $p'(T) > 0$; thus $p(T)$ is a local maximum. When T^* is compared with $T - \langle\tau\rangle$, it becomes clear that $p(T) > \langle p\rangle$. With the above in mind, it appears that a model with a spike at $\tau = T$ would be appropriate.

As an example of a model-dependent calculation, let us, utilizing the above discussion, investigate the exponential model of Fowler and Hoyle (1960) with a terminal event added just prior to the formation of the solar system. Equation (2) then reads

$$dN_i/d\tau = -\lambda_i N_i + \omega_0 N_i + P_i[A \exp(-\omega_e \tau) + B\delta(\tau - T)], \qquad (19)$$

where A and B are constants. Before discussing the results, it should be noted that large values of $1/\omega_e$ ($\omega_e T \ll 1$) would yield continuous uniform nucleosynthesis with an additional terminal event and small values ($\omega_e T \gg 1$) would yield "two-spike" solutions, an initial event and a final event with nothing in between. In solving for N_i/N_j, it is found that ω_e and ω_0 always appear in the sum $\omega_e + \omega_0 = \omega$, and the normalization can be made so that the only additional parameter is C, the fraction of a stable nucleus synthesized in the final event. This parameter C is the model parameter related to $p(T)/\langle p\rangle T$. Thus, the model has two parameters, ω and C, as well as the times T and Δ. The $^{129}I/^{127}I$ and $^{244}Pu/^{232}Th$ constraints can be combined as shown by equation (14) to yield the value of $\Delta \sim 2 \times 10^8$. This is consistent with our above discussion for our standard parameters if it is assumed that $C \geq 1/(\lambda_{244} T)$. Substituting this value of Δ into equation (12) for either $^{129}I/^{127}I$ or $^{244}Pu/^{232}Th$ determines C, analogous to the determination of $p(T)/\langle p\rangle T$ as shown in equation (15). The quantity C will be very sensitive to $R(244, 232)$ as was seen in equation (16). Our standard value yields $C \sim 0.2$ which is self-consistent with the assumptions used in calculating Δ. It was shown above that $T - \langle\tau\rangle$ is known, independent of the model, from the $^{232}Th/^{238}U$ constraint to about 10 percent. For the particular model under discussion $\langle\tau\rangle$ is a function of ω, C, and T. Since C is known, ω and T can then be found from the $^{235}U/^{238}U$ and $^{232}Th/^{238}U$ constraints.

For a given value of C, it can easily be seen that the two-spike case gives the smallest value of $\langle\tau\rangle$ and thus the smallest value of T.

If the standard $R(i, j)$ values in Table 1 are used, it is found that there is no solution because the T's demanded by the $^{232}Th/^{238}U$ constraint are always less than the T from the $^{235}U/^{238}U$ equation, even for the two-spike case. However, small changes in the $R(i, j)$ values well within the allowed ranges do yield solutions. It is possible to obtain solutions by using higher $R(244, 232)$ values, lower $R(129, 127)$ values, lower $R(235, 232)$ values, lower $R(232, 238)$ values, or some combination of the above. This type of behavior comes from the fact that the limiting two-spike solutions for T from the $^{235}U/^{238}U$ equation appear in the following form:

$$T \sim \text{const.} + \frac{1}{\lambda_{235}} \ln \{[R(129, 127)]^{-\lambda_{244}/(\lambda_{129}-\lambda_{244})}[R(244, 232)]^{\lambda_{129}/(\lambda_{129}-\lambda_{244})} - R(235, 232)\} \quad (20)$$

$$\sim \text{const.} + \frac{1}{\lambda_{235}} \ln \{R(129, 127)^{-1/4} R(244, 232)^{5/6} - R(235, 232)\} ,$$

where the $R(129, 127)$ and $R(244, 232)$ enter from the solution for C. The $R(232, 238)$ value is important because the T from $^{235}U/^{238}U$ must agree with the T from $^{232}Th/^{238}U$. Notice that the existence of a solution is extremely sensitive to the $R(244, 232)$ value and moderately sensitive to $R(235, 232)$ (see eq. [20]). In the selection of a particular model, the intermediate-lived ^{235}U constraint tells about the acceptability of the model since the model itself specifies the shape of $p(\tau)$. The $^{235}U/^{238}U$ equation is a relatively strong constraint since it involves a precisely known isotopic ratio and $1/\lambda_{235} \sim 10^9$ years.

In the region of $R(i, j)$ values where solutions exist, it is found that T and ω are extremely sensitive to $R(244, 232)$ and $R(235, 232)$. Solutions obtained for small variations (<30 percent) of our parameters about these standard values yield values of $1/\omega \lesssim 3 \times 10^9$ years and $T \sim (4\text{–}9) \times 10^9$ years.

It is important to note that T is highly model-dependent. Most models considered in the literature (Fowler and Hoyle 1960; Hohenberg 1969; Dicke 1969; Wasserburg, Schramm, and Huneke 1969) have large values of $p(\tau)$ at $\tau = 0$ which thus restricts T.

Production functions which start with low production rates ($p(0) \ll \langle p \rangle$) permit large values of T. For long times, the intermediate-lived nuclei produced in the region $\tau < \langle \tau \rangle$ contribute very little to the abundance at time $\tau = T$.

As an example of two models with the same mean age but with very different time scales, consider the following production function:

$$p(\tau) = \begin{cases} 1 & (0 \leq \tau < S) , \\ \sigma\delta(\tau - S) + d\delta(\tau - T) & (\tau \geq S) . \end{cases} \quad (21)$$

This model is a two-spike model which is preceded by continuous, uniform nucleosynthesis over a time S. For $S = 0$ it reduces to the simple two-spike case.

Let us take the physical parameters used by Wasserburg, Schramm, and Huneke (1969) for the production rates and relative abundances of ^{232}Th, ^{238}U, ^{235}U, ^{244}Pu, and ^{129}I. These differ only slightly from the standard physical parameters of the present paper and permit a two-spike solution for the reasons shown for equation (20).

Let us first consider models for which the exact mean age $T - \langle \tau \rangle$ approximately equals $\Delta^{max} = 3.3 \times 10^9$ years according to equation (9). Examples of two solutions are (1) a two-spike model ($S = 0$) with $d/(d + \sigma) = 0.13$ and $T = 3.86 \times 10^9$ years; and (2) a model with $S = 2.50 \times 10^9$ years, during which 14.7 percent of the total production takes place, and with $T = 6.20 \times 10^9$ years and the fraction $d/(d + \sigma + S) = 0.13$. For both models Δ is 1.74×10^8 years. These two cases differ by 60 percent (2.3×10^9 years) in the duration of nucleosynthesis and in that significant production takes place over the early period of continuous production. The total duration T is seen from the above example to be very model-dependent whereas the mean age remains constant.

In contrast to these solutions for which $\lambda_{232}T \lesssim 1$, we may consider *long-time* solutions for the identical physical parameters and the same form for the production function (eq. [21]). A solution exists for $S = 197 \times 10^9$ years, during which 46 percent of the total production takes place. The total duration of nucleosynthesis is $T = 200 \times 10^9$ years, with a mean age of 48.2×10^9 years. The other model parameters are $d/(\sigma + S + d) = 0.07$ and $\Delta = 1.58 \times 10^8$ years. The limiting case for such long-time models

is $T = 3 \times 10^{10}$ years, which occurs when $\Delta = 0$ (see Wasserburg, Fowler, and Hoyle 1960) and $d/(S + \sigma + d) = 1.09 \times 10^{-4} = 1/R(129, 127)$. The fraction made during the continuous early nucleosynthesis is 99.7 percent.

In considering such long-time solutions, it is illuminating to consider a three-spike model $p(\tau) = \delta(\tau) + \sigma\delta(\tau - S) + d\delta(\tau - T)$. For the physical parameters used in the preceding paragraph, we have a class of solutions which range from the two-spike case with $1/(1 + \sigma + d) = 0$ and $S = 0$, to a model with $1/(1 + \sigma + d) = 0.997$, $d/(1 + \sigma + d) = 1/R(129, 127) \sim 1 < 10^{-4}$, $S = 155 \times 10^9$ years, and $T - S = 2.1 \times 10^9$ years; the fraction $1/(1 + \sigma + d)$ increases with an increase in S. The spike at S and the time interval $T - S$ are similar in character to the two-spike solution. For $\lambda_{232}T \gg 1$, the fraction $1/(1 + \sigma + d)$ increases and becomes very large; however, the characteristics of the final two spikes remain basically the same, with a separation of the final spikes $(T - S)$ remaining the order of a few billion years. This type of behavior is similar to that found for the production function of equation (21). These examples clearly show that the time T is highly model-dependent, and that it is even possible to construct long-time solutions ($\lambda_L T \gg 1$) for which early production contributes a large fraction of the element production.

The above result can be generalized in the following manner. Consider a given set of physical parameters and the possible types of solutions with high initial nucleosynthetic production and $\lambda_L T \lesssim 1$. These different models will yield different time scales which are nevertheless commensurate. If we attempt to extend the time scales with some initial production at a low rate, we find that we cannot produce a sizable fraction of the r-process elements prior to the time scale defined with $\lambda_L T \lesssim 1$. The mean age is thus not greatly increased over what can be obtained for models with high initial production. If we now consider time scales for which $\lambda_L T \gg 1$, then all of the radioactive isotopes made during the early stages will have decayed and the only r-process isotopes remaining will be the stable ones. This can yield both time scales and an average age approaching infinity for the r-process elements. The models corresponding to such solutions will have production functions which, for the time interval near the termination of nucleosynthesis corresponding to $\sim 1/\lambda_{232}$, are basically of the same type as given for the models where $\lambda_L T \lesssim 1$. The change in structure corresponds to an equivalent shift in the physical parameters for the stable isotopes (in this case, ^{127}I). It is evident that all nuclear chronologies are, in this limiting manner, only chronologies for the radioactive elements. The only constraints on extremely long-time solutions with significant early synthesis of elements can come from detailed consideration of the relative abundances of radioactive progenitors to stable daughter isotopes (e.g., Pb, see Clayton 1963). When one considers the limited number of constraints presently available from nuclear abundances, it is necessary to use purely astrophysical arguments in formulating the time scale and the general characters of the production function—particularly with regard to early production of elements for time scales much longer than $1/\lambda_{232} \sim 2 \times 10^{10}$ years.

V. CONCLUSION

It has been shown that the nucleochronological equations can be decoupled such that the long-lived isotopes yield the mean age of the elements (prior to formation of the solar system) regardless of the time-dependent model used (if it is assumed that $\lambda_L T \lesssim 1$). All long-lived species must yield the same mean age; thus, checks on the r-process calculation can be made with these long-lived species.

The short-lived species yield the formation interval Δ almost independent of the model used. The short-lived species relative to a stable (or long-lived) isotope yields the value of the production function at the end of nucleosynthesis $p(T)$, relative to the total nucleosynthesis $T\langle p \rangle$. If no assumption is made regarding $p(\tau)$, then the intermediate-lived species can be used to obtain the derivatives of $p(\tau)$ evaluated at T; thus, if enough intermediate nuclei can be found, the entire shape of $p(\tau)$ can be determined.

If a particular model is assumed, then the intermediate-lived nuclei also may yield a duration T, and this duration must agree with that obtained for the long-lived nuclei. If there is no agreement, the model must be wrong. In order for the model to agree, it must have the appropriate derivatives of $p(\tau)$ evaluated at T. Once a model-dependent duration T is determined, then, if it is assumed that no r-process nucleosynthesis took place prior to galactic formation, an age for the Galaxy can be calculated:

$$\text{age} = T + \Delta + t ,$$

where $t = 4.6 \times 10^9$ years is the age of solid bodies in the solar system.

Since T is model-dependent, the age is model-dependent. A lower limit to the age of the Galaxy comes from the mean age of the elements which is a model-*independent* number. Age of Galaxy > mean age of stable r-process elements $= (T - \langle\tau\rangle) + \Delta + t$, which for a long-lived isotope is just $\Delta^{\max} + t$.

The authors wish to acknowledge stimulating and valuable discussions with their colleagues D. S. Burnett, R. F. Christy, T. Lauritsen, F. A. Podosek, M. Schmidt, and P. A. Seeger. The continuing interest of W. A. Fowler as well as his willingness to discuss these problems critically has been of great importance in the development of this work.

This work was supported by the National Science Foundation (grants GP 9114 and GP 15911). One of us (D. N. S.) was supported, in part, by an NDEA fellowship.

APPENDIX

The present solar-system value for $^{232}Th/^{238}U$ will be taken as 3.9. As this quantity is not an isotopic ratio of the same chemical element, there is some uncertainty in the value. This has led to some confusion in the literature, due to the variability of this ratio in terrestrial samples and in meteorites. The most powerful arguments pertaining to this ratio are:

1. Terrestrial Pb of all ages shows that it evolved from a characteristic $^{232}Th/^{238}U$ ratio of between 3.7 and 4.1, the best estimate from terrestrial leads being 3.9. The results for lead integrate over the variations which are found in the directly measured Th/U ratios of diverse rock types. The constancy of this ratio for almost all rocks of all ages strongly argues that this value is characteristic of the Earth as a whole and is not simply the sample of a small fragment of a planetary object.

2. The lead in the meteorite Nuevo Laredo shows it to have evolved from a $^{232}Th/^{238}U$ ratio almost identical with that of terrestrial lead.

3. Many meteorites show directly measured $^{232}Th/^{238}U \sim 4.0$. There are some values considerably lower and a few somewhat higher, the most common values being about 4.0. No evidence exists from meteorites for directly measured values as high as 5.0 or lower than 2.0. Arguments for values as low as 3 have been presented by Lovering and Morgan (1964) and pursued by Dicke (1969). These workers have, in their consideration, neglected to consider the more cogent arguments outlined above.

4. In addition, the recent data on lunar samples from the *Apollo 11* and *Apollo 12* missions (Lunar Sample Preliminary Examination Team 1969, 1970) give $^{232}Th/^{238}U = 4.2$. The lunar rocks certainly show that chemical fractionation has taken place on the Moon and has resulted in a significant differentiation of lunar crust and interior (based on heat-balance arguments and consideration of the chemical abundances). While it is quite possible to obtain Th-U fractionation in this process, it is remarkable that the Th/U ratios which are observed coincided closely with the best estimates for the solar-system value mentioned above.

Due to the possible uncertainties in the solar-system value of $^{232}Th/^{238}U$ as well as the uncertainties in P_{232}/P_{238}, we have considered the range of values shown in Table 1.

REFERENCES

Bahcall, J. N. 1961, *Phys. Rev.*, 124, 495.
Clayton, D. D. 1963, *J. Geophys. Res.*, 68, 3715.
———. 1964, *Ap. J.*, 139, 637.

———. 1969, *Nature*, 224, 56.
Dicke, R. H. 1969, *Ap. J.*, 155, 123.
Fowler, W. A. 1962, in *Proceedings of the Rutherford Jubilee International Conference*, ed. J. B. Birks (London: Heywood & Co.), p. 640.
———. 1970, *Gamow Memorial Volume* (in press).
Fowler, W. A., Greenstein, J. L., and Hoyle, F. 1962, *Geophys. J. R.A.S.*, 6, 148.
Fowler, W. A., and Hoyle, F. 1960, *Ann. Phys.*, 10, 280.
Hirt, B., Tilton, G. R., Herr, W., and Hoffmeister, W. 1963, in *Earth Science and Meteoritics*, ed. J. Geiss and E. D. Goldberg (New York: Interscience Publishers), p. 273.
Hohenberg, C. M. 1969, *Science*, 166, 212.
Hohenberg, C. M., Podesek, F. A., and Reynolds, J. H. 1967, *Science*, 156, 202.
Hoyle, F., and Fowler, W. A., 1960, *Ap. J.*, 132, 565.
Lovering, J. F., and Morgan, J. W. 1964, *J. Geophys. Res.*, 69, 1979.
Lunar Sample Preliminary Examination Team. 1969, *Science*, 165, 1211.
———. 1970, *ibid.*, 167, 1325.
Podosek, F. A. 1970, *Earth Planetary Sci. Letters*, 8, 183.
Schmidt, M. 1963, *Ap. J.*, 137, 758.
Seeger, P. A., Fowler, W. A., Clayton, D. D. 1965, *Ap. J. Suppl.*, 11, 121.
Seeger, P. A., and Schramm, D. N. 1970, *Ap. J.* (*Letters*), 160, L157.
Wasserburg, G. J., Fowler, W. A., and Hoyle, F. 1960, *Phys. Rev. Letters*, 4, 112.
Wasserburg, G. J., Huneke, J. C., and Burnett, D. S. 1969*a*, *J. Geophys. Res.*, 74, 4221.
———. 1969*b*, *Phys. Rev. Letters*, 22, 1198.
Wasserburg, G. J., Schramm, D. N., and Huneke, J. C. 1969, *Ap. J.* (*Letters*), 157, L91.

Section 6. The Isotopic Abundance of ^{26}Mg and Limits on ^{26}Al in the Early Solar System by David N. Schramm, F. Tera, and G.J. Wasserburg. In press-Earth and Planetary Science Letters, December, 1970.

THE ISOTOPIC ABUNDANCE OF ^{26}Mg AND LIMITS ON ^{26}Al IN THE EARLY SOLAR SYSTEM*

David N. Schramm, F. Tera, and G. J. Wasserburg

Lunatic Asylum, The Charles Arms Laboratory of
The Geological Sciences, and the Kellogg
Radiation Laboratory
California Institute of Technology, Pasadena, California

" .... it is pretty sure to be a crime to examine the laws of heat"

Viscount Morley

ABSTRACT

The isotopic composition of Mg is investigated in meteoritic, lunar and terrestrial feldspar samples and standard reagents using a mass spectrometer with on-line data processing. Isotopically enriched standards were run demonstrating a resolution of better than five parts in 10^4 for the $^{26}Mg/^{24}Mg$ ratio. No $^{26}Mg/^{24}Mg$ anomalies are found in any samples analyzed to within experimental errors. (These analyses include some samples run by Clarke, deLaeter, Schwarcz and Shane (1) and found by them to have $^{26}Mg/^{24}Mg$ anomalies of 4-6 parts in 10^3 relative to terrestrial values.) There is at the present time no positive evidence indicating the existence of ^{26}Al in the early solar system.

From these results, limits are placed on the amount of ^{26}Al ($\tau_{\frac{1}{2}} = 7.4 \times 10^5$ yrs.) and the resulting heating effects in the solar system at the time of crystallization of the meteorites. It is clear that when the meteorites solidified, ^{26}Al was not an important heat source; however, this would not rule out the possibility that a few million years prior to solidification ^{26}Al was a major heat source.

* Contribution Number 1916, Division of Geological Sciences

In Press: December 1970 issue, Earth and Planetary Science Letters

1. INTRODUCTION

Clarke, de Laeter, Schwarcz and Shane [1] have reported that there exists an anomalous amount of ^{26}Mg in meteoritic feldspars which they attribute to the decay of ^{26}Al ($\tau_{\frac{1}{2}} = 7.4 \times 10^5$ years). The implications of this observation have profound significance because of: the possible importance of ^{26}Al as a primordial heat source [2, 3, 4, and 5]; the problems with regard to nucleosynthesis of ^{26}Al [6,7], and the consequences on nucleosynthetic time scales for different processes [8]. In addition to the astrophysical importance of the ^{26}Al problem, the question of variations in the Mg isotopic abundances due to fractionation processes occurring in nature is also of interest [9,10]. Thus, it was decided that high precision measurements of the Mg isotopic composition is required to check the validity of the observed anomaly to furnish a firm limit for the amount of ^{26}Al. As pointed out by Clarke, de Laeter, Schwarcz and Shane [1], the most logical place to see a ^{26}Mg anomaly due to ^{26}Al decay would be in a phase of primitive matter with high Al concentration and low Mg concentration. For this reason, feldspar samples from meteorites were investigated by these workers, and a similar strategy has been followed by us. Clarke et al. [1] reported ^{26}Mg anomalies as great as six parts in 10^3. In this work it is shown that we are capable of easily resolving differences of five parts in 10^4 as established by using enriched standards; thus, any effect as large as that reported by these workers

2

should be easily seen by us. Measurements were carried out on a variety of extra-terrestrial and terrestrial samples. Feldspar separates were obtained from the Ca-rich achondrites, Moore Co., Juvinas and Pasamonte and the chondrites St. Severin and Guareña. A potassium-feldspar inclusion from the iron meteorite Colomera was also run. Feldspar separates from lunar samples #10024, #12064 and #12013 were also investigated. In addition, Clarke, de Laeter, Schwarcz and Shane were generous enough to send us their feldspar separates from Khor Temiki (enstatite achondrite) and Bruderheim (chondrite), so that we could directly intercompare the results of both laboratories.

2. EXPERIMENTAL PROCEDURE

2.1. Mass spectrometry

The isotopic composition of Mg was determined using a programmable field mass spectrometer with digital output and with on-line data processing [11]. Previous workers have usually run Mg by thermal ionization using tungsten [9] or triple rhenium filaments [10]. Clarke et al. [1] using an electron impact source studied the use of Re filaments sintered with Ta. Rhenium, tantalum, and tungsten thermal ionization source filaments were tested by us with various size samples using flat, "V" [12] and triple filament configurations; samples were loaded with and without oxidation on these filament materials. None of these techniques yielded a high intensity ion beam.

3

It was determined that for Mg ions a high yield could be obtained using an emitter. We obtained the highest Mg intensity from samples loaded with silica gel and cemented on a Re "V" filament by 0.5N H_3PO_4. We used a zone-refined Re filament (see McHugh [3]), with dimensions of 0.0012" x 0.030". Silica gel was made from high purity SiO_2 and Na_2CO_3 and the H_3PO_4 was made by dissolving high purity P_2O_5 in quintuply distilled H_2O. The loading procedure was found to be extremely critical. The procedure adopted is as follows: The filament is outgassed in a high vacuum for two hours at 2000°C.; $MgCl_2$ (~ 1 to 6 x 10^{-7} g of Mg) is loaded into the "V" filament under a microscope from a HCl solution using size P.E. 60, Intramedic polyethylene tubing and a Hamilton micropipette control. The drop containing the sample is ~ 0.002 ml. Hydrocarbons are burned off by running a current of approximately 1.5 - 2.0 A through the filament. The current is turned off and silica gel is loaded so as to fill the "V" approximately half full. A drop of phosphoric acid (~ 0.001 ml) is added and the silica gel spread evenly with a clean tungsten carbide needle. The phosphoric acid is then evaporated by a high intensity lamp, another drop of H_3PO_4 is added and evaporated away by running a current of 0.5A through the filament. This is repeated at a current of 0.7A until the silica gel is almost dry, whereupon the current is increased gradually to 1.5A. The total amount of H_3PO_4 used is ~ 0.005 ml. At this point, the silica gel is cemented on the filament. The current is then increased until the filament glows a dull red for a few seconds. The current is

4

turned off and the filament loaded in the spectrometer. The filament is then baked in the spectrometer for 6-8 hours at 960°C (optical pyrometer) to remove most of the sodium. The filament current is carefully increased over a 4-5 hour period until the filament temperature is from 1480° to 1580°C and the ^{24}Mg ion signal becomes stable with an intensity between 1 and 2 x 10^{-11}A. The signal is very unstable until this running condition exists.

A run usually ends when the signal begins to decay and then goes very unstable and dies; sometimes, however, a sample would run until the operator quit from exhaustion.

The ionization and transmission efficiency was determined to be $\geq 4 \times 10^{-4}$ ions collected per atom on the filament. (This is a limit because it is not certain that the sample was exhausted.) This ionization efficiency and ion intensity are superior to the results obtained previously by other workers [1, 10] who had lower ionization efficiencies and achieved lower ion beam intensities. Our procedure typically permits high precision determinations on samples as small as 1 x 10^{-7} gm Mg. Clarke et al. reportedly used samples of 1-10 x 10^{-6} gm Mg and Catanzaro and Murphy used $\sim 10^{-4}$ gm Mg samples.

As shown in fig. 1, the peak half width for the slits used is 2.7 gauss and the peak top is flat for 0.8 gauss to within 2 parts in 10^4 which is comparable to ion counting statistics. The background between peaks was determined to be less than 10^{-15} amps with the ion beam on. At running conditions, the ^{23}Na peak has been baked away so that it is less than the background between Mg peaks ($\sim 10^{-6}$ of the ^{24}Mg peak). The only peak within five mass units of the Mg isotopes is ^{27}Al which has an intensity varying from 0.1 to 1.0 of the ^{24}Mg peak. The variation in the size of the ^{27}Al peak was found to have no correlation with any effects in the Mg isotopic ratios. No other peaks were

observed (including the C_2H_2 observed by Clarke et al. [1]) even when our slits were reduced such that our resolution was capable of resolving better than 0.005 mass units. Their observation of C_2H_2 was probably due to the fact that these workers used an electron impact source. Silica gel was run without loading a sample; no hydrocarbons were observed above the background ($\lesssim 10^{-15}$A).

Although in most runs we did not close the slits to look for C_2H_2, we always scanned ± 5 mass units around the Mg region and never observed any hydrocarbons nor did we ever observe any significant variation in our ratios. Source plate focusing potential settings were almost identical throughout a run and from one run to the next. When source conditions were intentionally altered outside of our standard running conditions, no change in the isotopic ratios was found. Digital voltmeter (DVM) readings were taken at the center of each peak and ± 8 gauss about the center to determine the zeroes. The separation between isotopes is 61.7 gauss. A one-second integration time was used for all DVM readings. Data was taken using a Faraday cage collector, a 10^{11} Ω resistor and a vibrating reed electrometer (model 36, Applied Physics), with ^{24}Mg on the 10V scale and ^{25}Mg and ^{26}Mg on the 1V scale of the DVM. The ^{24}Mg peak was measured in between each ^{25}Mg and ^{26}Mg reading (i.e., the sequence is 24-25-24-26-24-25- ...). This was done to decrease the interpolation interval for calculation of isotopic ratios and was found to improve the quality of the data (see [11]). A check was made of the magnetic field control during cycling, and it was found to be constant to better than 0.05 gauss in a channel through ten data cycles. Since the principal effect under

investigation would be caused by radioactive decay, it was possible to correct for isotopic fractionation following Burnett, Lippolt and Wasserburg [14]. The ratios were corrected for mass discrimination in the following manner.

The mean of a set of five ratios (μ) of $^{25}Mg/^{24}Mg$ was normalized to $(^{25}Mg/^{24}Mg)_o = 0.12663$ [15]

$$1-\epsilon = \frac{(^{25}Mg/^{24}Mg)_\mu}{(^{25}Mg/^{24}Mg)_o} \qquad (1)$$

to obtain the discrimination correction factor $(1-\epsilon)$. This was used to correct (c) <u>each</u> measured (m) $^{26}Mg/^{24}Mg$ ratio in the set

$$(^{26}Mg/^{24}Mg)_c = \frac{(^{26}Mg/^{24}Mg)_m}{(1-\epsilon)^2} \qquad (2)$$

where we have assumed that ^{26}Mg is fractionated with respect to ^{25}Mg in the same manner that ^{25}Mg is fractionated with respect to ^{24}Mg.

As long as the standard data acquisition conditions described previously held, ϵ was found to be 0.015 ± 0.001. This result was obtained both throughout an individual run and from one run to another (see Fig. 2). Note that by using the discrimimation correction of $(1-\epsilon)^2$ for the $^{26}Mg/^{24}Mg$ ratio, the enrichment

$$\Delta_{26} \equiv \frac{(^{26}Mg/^{24}Mg)_c - (^{26}Mg/^{24}Mg)_o}{(^{26}Mg/^{24}Mg)_o}$$

is independent of the standard value $(^{25}Mg/^{24}Mg)_o$. This is not exactly true for all methods of discrimination correction, in particular if $1-2\epsilon$ were used instead of $(1-\epsilon)^2$ to correct $^{26}Mg/^{24}Mg$, Δ_{26}

would have an explicit dependence on $(^{25}Mg/^{24}Mg)_o$.
Ratios used for final data analysis were all from sets of five having a standard deviation of the $^{26}Mg/^{24}Mg$ ratios of less than or equal to two parts in 1000. Tabulated results are the mean of these selected $^{26}Mg/^{24}Mg$ ratios.

The fractional random error of the mean of the $(^{26}Mg/^{24}Mg)_c$ ratios can be estimated using

$$\sigma_{mean} = \frac{1}{\sqrt{N}} \left(\sigma_6^2 + \frac{4\sigma_5^2}{n}\right)^{\frac{1}{2}} \qquad (3$$

where σ_5 and σ_6 are the standard deviations of the $^{25}Mg/^{24}Mg$ and $^{26}Mg/^{24}Mg$ ratios per set, respectively, n is the number of ratios in a set, and N is the number of ratios analyzed. The $4\sigma_5/n$ term enters from the discrimination correction. For our analysis, $n \sim 5$ and $\sigma_5 \approx \sigma_6 \equiv \sigma$; thus, $\sigma_{mean} \approx \frac{\sqrt{2}\sigma}{\sqrt{N}}$. A run typically consists of 20 to 40 sets of five ratios; thus, $N \sim 100$. If the discrimination is a constant from set to set, then it is possible to increase the size, n, of a set. It should be noted, however, that although the random error from the discrimination correction decreases with increasing n, the discrimination factor may have a time dependence which could lead to a systematic error if a large n was used. In our analyses, no such time dependences were observed (see Fig. 2); thus, a larger n could have been used.

2.2. Chemistry

The mineral samples were put into solution in the following manner. One ml concentrated HF was added to the sample and left for ~ 8 hours at room temperature; then 1 ml $HClO_4$ was added and the sample evaporated to dryness and the residue dissolved in 1N HCl.

8

An aliquot was taken and the Mg concentration determined using a Perkin-Elmer atomic absorption spectrophotometer (AAS) calibrated with solutions of known concentrations. Another aliquot was put through two consecutive cation exchange columns of the same dimensions made of fused SiO_2 (1 cm x 17 cm) using Dowex 50-X8 (100-200 mesh) resin. After each separation, the columns were stripped with 4N HCl. Mg was eluted from each column with 145 ml. 1N HCl with the last 30 ml kept as the Mg fraction. The Mg fraction was then evaporated to dryness and loaded on the filament. All evaporations were done in closed teflon "pots" under a stream of high purity dry N_2 [16]. The rest of the chemistry was performed in a closed lucite box. Total system blanks were determined by mass spectrometry using a ^{25}Mg spike. Total system blanks (excluding loading on the filament) were also determined using the AAS. A filament-loading blank was measured using the ^{25}Mg tracer and dissolution and column blanks were measured using the AAS. Measurements using the ^{25}Mg spike were carried out in an identical but separate system from that which was used for samples (e.g. separate ion exchange columns in a separate lucite box as well as separate labware to avoid ^{25}Mg contamination). The ^{25}Mg tracer samples were also run on a separate mass spectrometer from the regular samples.

The dissolution blank using 1 ml HF and 1 ml $HClO_4$ was found to be 18-20 nanograms. The most recent sample analyses were dissolved using ~ 1/3 ml HF and ~ 1/3 ml $HClO_4$. The dissolution blank for this amount of acid was found to be 10-13 nanograms. Column blanks varied from 6-12 nanograms per column yielding 12 to 24 nanograms for the two columns. The silica gel - phosphoric acid filament loading blank was found to be less than 0.5 nanograms. Total system blanks were found to be ~ 45 nanograms using 1 ml HF and $HClO_4$ for dissolution and 25 to 36 nanograms using 1/3 ml of the acids for dissolution. These total system blanks are within the range of the sum of the partial blanks. Blank corrections were made using the maximum measured blank for each operation. Blank corrections were all less than 7% with the exception of the Moore Co. I separate where a 45% correction was made due to the small sample size.

2.3. Normals

A normal solution was made by dissolving spectrographically pure MgO in 1.5N HCl. The recent normal runs were made from portions of this solution which were passed through the column in order to obtain a more stable ion beam. Earlier runs, however, were made without passing the solution through the columns.

10

Preliminary runs were made with loads from 5×10^{-8} gm to 1×10^{-4} g Mg, and it was determined that the optimum load was $1 - 6 \times 10^{-7}$ gm Mg. All normal runs shown in this report were in that range.

2.4. Enriched standards

To show explicitly how small an anomaly could be detected, a set of isotopically enriched standards was made up using mixtures of normal Mg and a tracer solution enriched in ^{25}Mg. We chose to use ^{25}Mg since any later laboratory contamination would appear as a depletion in ^{26}Mg and could therefore be detected. The gravimetric standards were prepared in 1.5 N HCl solutions using mixtures of normal MgO (spec. pure) and tracer MgO from Oak Ridge (99.21% ^{25}Mg , 0.39% ^{24}Mg , 0.4% ^{26}Mg). Aliquots of the enriched standards were passed through the ion exchange columns prior to mass spectrometric analysis in order to get more stable runs. Table 1 and Fig. 3 show the spectrometrically (S) measured enrichment for the standards compared with the gravimetric (G) values in parts in 10^4.

$$\Delta_{25}^{G,S} \equiv \frac{[(^{25}Mg/^{24}Mg)^{G,S} - (^{25}Mg/^{24}Mg)_o]}{(^{25}Mg/^{24}Mg)_o} \times 10^4 \qquad (4)$$

The standard $(^{25}Mg/^{24}Mg)_o$ ratio is taken as 0.12663 from Catanzaro et al. [15] and the $^{26}Mg/^{24}Mg$ value was taken as 0.139794 based on normal runs done up to the time of the measurements of the standards.

The mass spectrometric determination was made using our standard on-line program which normalized to the $^{25}Mg/^{24}Mg$ ratios to correct

the $^{26}Mg/^{24}Mg$ ratios for discrimination. For enrichments of $^{25}Mg/^{24}Mg$ the result after the discrimination correction is a lower value of $^{26}Mg/^{24}Mg$ relative to the normal. These corrected (c) $^{26}Mg/^{24}Mg$ values are then used to calculate the implied $^{25}Mg/^{24}Mg$ enrichment.

$$\Delta^S_{25} = \left[\sqrt{\frac{(^{26}Mg/^{24}Mg)_o}{(^{26}Mg/^{24}Mg)_c}} - 1 \right] \times 10^4 \qquad (5)$$

Note that this method (eq. 5) yields results equivalent to measuring the $^{25}Mg/^{24}Mg$ ratio and correcting it for discrimination by normalizing the $^{26}Mg/^{24}Mg$ value; however, we wished to analyze the $^{26}Mg/^{24}Mg$ ratios from the enriched standards in the same manner as we analyzed the samples so that the propagation of errors from the discrimination correction would be identical (see eq. 3).

From examining the data, we see that deviations from the 45^o line are less than 5 parts in 10^5. From Fig. 3 we see that an enrichment of $\sim$ 2.5 parts in 10^4 over the normal $^{25}Mg/^{24}Mg$ value could be resolved easily.

Throughout the rest of this work, the ratio of interest is $(^{26}Mg/^{24}Mg)_c$. To convert the resolution in Δ^S_{25} to the resolution capability in $(^{26}Mg/^{24}Mg)_c$, note that we have calculated Δ^S_{25} by first calculating $(^{26}Mg/^{24}Mg)_c$ and then taking the square root (following eq. 5). The resolution in Δ^S_{25} is therefore a factor of two better than the resolution in $(^{26}Mg/^{24}Mg)_c$. The resolution in $(^{26}Mg/^{24}Mg)$ is thus $\sim$ five parts in 10^4.

12

2.5. Terrestrial feldspars

Various terrestrial feldspars were analyzed, both to verify the agreement of the isotopic ratios with normal reagents and to determine the Mg concentration in high purity feldspars. The minimum Mg concentration attainable in a feldspar separate is, or course, the amount of Mg actually substituting in the feldspar crystal. The magnesium concentrations of several terrestrial feldspars were determined using the AAS. To determine if these Mg concentrations were due to impurities or to Mg in the feldspar itself, electron microprobe analyses were carried out on 100-200 grains using a beam site of ~ 1 micron. If Mg "hot spots" (generally greater than ~ 1/2% Mg) were found, this would indicate Mg-rich impurities. If no hot spots were found, this indicates that the observed Mg concentration was probably in the feldspar lattice.

The magnesium concentration in the feldspar ranged from 5 ppm (with hot spots) in an orthoclase to 990 ppm in a high temperature Bytownite (see table 2). In this Bytownite, large crystal fragments, as well as several hundred small grains, were analyzed with the microprobe and no hot spots were found, indicating that the Mg is actually in the feldspar.

It is apparent from these results that many feldspars do contain Mg, and thus lower limits on Mg concentrations in feldspar mineral separates will be limited not only by impurities but also by the feldspar itself. The Mg content of the feldspars may be a reflection of their temperature of formation.

Also given in table 2 are the isotopic analysis of those terrestrial feldspars which were run on the mass spectrometer. The deviation Δ_{26} has been calculated relative to the normal spec. pure MgO reagent runs (see table 4). Within the precision of our data, terrestrial feldspars yield identical Mg isotopic ratios with those of the reagent Mg.

2.6. Mineral separates

With the exception of the Colomera potassium-feldspar, all mineral separates were done using the following basic procedure (with minor variations): 1) gentle grinding of rocks; 2) handpicking out feldspar when possible; 3) coarse grinding ($\lesssim 75\mu$); 4) density separation by centrifuging in methylene iodide and acetone solution of appropriate density; 5) handpicking out impurities; 6) regrinding to $\sim$ 10-20μ; 7) repeat density separation (density of solution ~ 0.01 gm/cm^3 greater than that of feldspar; 8) handpicking to remove impurities; 9) electron microprobe analysis to determine purity

14

of separate, determine the feldspar composition, and to check if any SiO_2 phase is present, and check for Mg "hot spots". Grinding of the feldspar was done using an agate mortar and pestal under acetone.

2.7. Colomera

Twelve milligrams of a large single crystal potassium-feldspar inclusion C5 [17] in the iron meteorite Colomera were handpicked for subsequent analysis. The grains when picked were covered with rust. These grains were gently crushed, and the rust was removed by washing in warm 4N HCl and rinsing with H_2O and acetone. The grains were then water clear.

A microprobe analysis showed the separate to be 98% alkali-feldspar Or_{89}, 1% plagioclase and 1% other phases. An aliquot of 3.2×10^{-7} gm of Mg was run on the mass spectrometer.

2.8. Moore County

Two feldspar separates were made from the achondrite Moore Co. The feldspars contained some pyroxene inclusions and some small black inclusions. Rust spots were also noticed on some crystals.

Separate I was prepared from 16 mg of handpicked crystals. It was first rinsed in warm 2N HCl for about 3-5 minutes and then rinsed in H_2O and acetone. This procedure removed the rust spots. This separate was then put through our basic mineral separation and gave a final yield of 1.6 mg of feldspar with / about 11% of SiO_2 polymorphs. The Moore County I sample run on the mass spectrometer was $\sim 1 \times 10^{-7}$ gm of Mg.

Separate II started from 100 mg of handpicked plagioclase and yielded a final separate of 32 mg sample. A 9.5 mg fraction of this feldspar separate was then dissolved and aliquots taken for concentration and mass spectrometric analysis. Approximately 3.6×10^{-7} gm of Mg from Moore Co. II were run on the mass spectrometer.

A microprobe analysis for both Moore Co. I and II determined that the plagioclase was An_{92}. No free SiO_2 was found in the Moore Co. II feldspar separate. No Mg hot spots were found in either separate.

2.9. Juvinas

Forty milligrams of feldspar were handpicked from a feldspar-rich part of the specimen and subjected to the separation procedure. A microprobe analysis showed that the plagioclase feldspar was An_{91}, and that some grains had Mg-rich inclusions. Reprocessing did not decrease the Mg concentration. The final separate weighed 4.5 mg. No SiO_2 phase was found. Aliquots containing 4.3×10^{-7}g of Mg from this separate were run on the mass spectrometer.

16

2.10. Pasamonte

The achondrite Pasamonte, in which fission Xe has been observed [18] was also investigated. Twenty-one milligrams of feldspar were handpicked from the coarse-grained portion (darker than the fine-grained matrix). The final plagioclase (An_{86}) separate consisted of 9.0 mg of $\leq$ 20μ size grains. The final separate was determined to contain 4% of SiO_2 impurities. The weight dissolved was 4 mg. An aliquot with 4.3×10^{-7} g Mg was run on the mass spectrometer.

2.11. St. Severin

St. Severin is of interest because both excess fission tracks and fission type Xe as well as a ^{129}Xe anomaly have been observed in this meteorite [19, 20, 35]. The starting point for this feldspar separate was a feldspar-rich fraction left over from previous separates obtained from St. Severin in this laboratory [19]. It had been sieved such that it ranged in grain size from 70μ to 25μ and had floated in 2.70 density liquid. An AAS analysis yielded a Mg concentration of 6200 ppm for this material. A fraction of this material

17

(163.2 mg) was then ground under acetone until grain size was ~ 10μ. This was then centrifuged in 2.75 density methylene iodide and acetone. The floats were then centrifuged in 2.70 density liquid. The remaining 27.0 mg of floats were then centrifuged in 2.67 density liquid handpicked and reprocessed through 2.67 density liquid. A 3.0 mg aliquot of the remaining 17.1 mg of sample was dissolved in the normal manner. With such small grain size, some particles tended to remain in the acetone during washing and decanting. The particles that remained in the wash of the 2.70 floats were allowed to settle out overnight and found to weigh 16.2 mg. These extremely fine grains were then centrifuged in 2.67 density liquid and the floats handpicked for impurities yielding a final weight of 12.7 mg. A microprobe analysis of these hyperfines was made and was found to be $Ab_{88}An_{12}$ with no free SiO_2 observed. Some Mg hot spots were found indicating Mg-rich impurities. An aliquot (5.5×10^{-7} g Mg) of these extremely fine grains was analyzed on the mass spectrometer.

2.12. Lunar rock 12064-26

This is a coarse-grained, gabbroic rock from Apollo 12. Twenty mg of plagioclase were handpicked from the gently crushed rock and then purified. A microprobe analysis showed the plagioclase to be An_{85} with less than 5% free SiO_2. No Mg hot spots were found. The final separate weighed 2.6 mg. An aliquot of 5.1×10^{-7} g of Mg was run on the mass spectrometer.

2.13. Guareña

Excess fission tracks as well as fission-type Xe and anomalous ^{129}Xe have been observed [21] in the chondrite Guareña.

The starting point for this separate was a feldspar-rich separate left over from earlier separates in this laboratory on Guareña [21] . This 60 to 100 μ starting material was found to have 44,000 ppm Mg. Approximately 50 mg of this material were put through the standard mineral separation procedure. In the final processing, the grains were ground until the particle size was less than 5μ. (It was necessary to centrifuge the acetone suspension to work with the separate).

This fine material was then centrifuged in 2.67 g/cm^3 liquid and handpicked to remove impurities. A microprobe analysis showed plagioclase to be $\sim Ab_{85}\ An_{15}$. Hot spots of Mg were found. No evidence of any free SiO_2 phases was found.

The final separates of 1.9 mg of feldspar were dissolved using 1/3 ml. Hf and 1/3 ml $HClO_4$ and put through the chemical processing. An aliquot of 5.6×10^{-7} g Mg was analyzed on the mass spectrometer.

2.14. Lunar rock 12013,10

This sample was from a few milligrams of feldspar left over from previous mineral separates performed in this laboratory on lunar rock 12013 [33]. It had been crushed to less than 75 μ grain size , and the floats were taken from centrifuging in 2.65 g/cm^3 liquid twice.

From a microprobe analysis, it was found that the separate had many Mg-rich impurities. It was also found that the sample was made up of several feldspar phases ranging from almost pure K feldspar to plagioclase with wide variations in Ca. The remainder of the sample (1.9 mg) was dissolved using 1/3 ml HF and 1/3 ml $HClO_4$.

An aliquot containing 5.8×10^{-7} g Mg was run on the mass spectrometer.

2.14a. Lunar rock 10024, 24

This is a fine-grained, high-K rock from Apollo 11. After crushing, the material was centrifuged in 2.40 g/cm^3 liquid, and the sinks from this were centrifuged in 2.70 g/cm^3 liquid. A portion (1.9 mg) of the floats were dissolved using 1 ml HF and 1 ml $HClO_4$ and processed for analysis. A microprobe analysis indicated some Mg-rich impurities and ~ 10% cristobalite.

20

2.15. Samples from Clarke et al.

Due to the tremendous significance of the result reported by Clarke et al. [1], it was important that a direct comparison be made with samples which were run at McMaster University. To aid in this, Clarke, de Laeter, Schwarcz and Shane were kind enough to give us some of their samples. These were fractions of their feldspar separates, Khor Temiki, Bruderheim III and Bruderheim IV. In addition, an aliquot of the Mg solution separated from Khor Temiki which was used by Clarke for analysis (which did not require further chemical preparation) was also provided to us. In order to establish if the chemical preparation had any effect on the results, an aliquot of this Mg solution was also put through one of our ion exchange columns before running. An estimate of the Mg concentration of the Khor Temiki solution was given to us by Clarke. From this, we estimated the blank correction for the aliquot which was passed through only one column to be only ~ 1.3%, and the blank correction for the aliquot which was loaded directly on to the filament is estimated to be only ~ 0.1% due to the filament loading blank.

The three feldspar separates were dissolved and put through our standard chemistry. The Mg concentrations measured by our atomic absorption spectrophotometer are in reasonable agreement with those determined by Clarke et al. using isotope dilution.

The mass spectrometric isotopic results corrected for blanks are shown in table 3. It is immediately apparent that our results do not substantiate the ^{26}Mg anomalies reported by Clarke et al.

3. ANALYTICAL RESULTS

The results of all normal Mg runs are shown in table 4. The data from the early runs (38-46) was combined as if all were from one run since the early runs did not yield sufficient data individually to provide a satisfactory analysis. Run numbers are given to show the chronological order in which the analyses were made and to therefore demonstrate the lack of any time-dependent effect. The data from all normal runs was combined and processed as one run to yield the mean $(^{26}Mg/^{24}Mg)_c$ ratio of 0.139805 for normal Mg with a fractional 2σ error of 9.6 parts in 10^5.

One interesting side light of our analysis is that our $^{26}Mg/^{24}Mg$ normal ratio is 0.139805 ± 0.000013 which is 3.5 ‰ greater than 0.13932 ± 0.00026 reported by Catanzaro, Murphy, Garner and Shields [15], even though we normalized our $^{25}Mg/^{24}Mg$ data to their value of 0.12663 and used that normalization to calculate the mass discrimination correction. (Clarke et al. [1] obtained a $^{26}Mg/^{24}Mg$ normal ratio 2.6 ‰ higher than Catanzaro et al.[15]). This difference in normal $^{26}Mg/^{24}Mg$ values can, of course, have no effect with regard to whether an anomaly exists. We believe the present values for $^{26}Mg/^{24}Mg$ normal to be a more precise estimate compatible with the absolute $^{25}Mg/^{24}Mg$ ratio used for normalization.

22

Table 5 is a summary of the isotopic results for all extraterrestrial samples other than those obtained from Clarke et al. (which were shown in table 3). The Δ_{26} values given have been corrected for the estimated blank. The estimated error $2\sigma_\Delta$ in Δ_{26} is calculated as the linear sum of $2\sigma_{sample} + 2\sigma_{normal}$ (in units of 10^4) where $2\sigma_{normal}$ is 9.6×10^{-5}. This is a liberal error estimate so that the absolute value of $\Delta_{26} \pm 2\sigma_\Delta$ is a rather strict upper limit to any ^{26}Mg anomaly. Fig. 4 shows the results of all Mg runs with the exception of the enriched standards. It is immediately obvious that they all overlap. In fact, with the exception of run #66 (which is Khor Temiki Mg solution from Clarke et al. passed through one of our columns and is slightly negative and was repeated as run #87) all runs intersect the mean of all normals 0.139805 ± 0.000013. Since it is expected from statistics that approximately one point in 20 will be outside the 2σ error bars, it can be stated that <u>there is no ^{26}Mg anomaly within our limits of detection.</u>

From Fig. 4 we see that no values of $|\Delta_{26}|$ are found greater than three parts in 10^4 which can be taken as the upper limit of any effect. However, to be conservative and to state a firm upper limit for each sample, we will use throughout the rest of this discussion $|\Delta_{26} \pm 2\sigma_\Delta|$ for our upper limit.

Negative anomalies are treated as statistical fluctuations which could just as well have been positive and are analyzed as such. A true negative anomaly with respect to the terrestrial normal would require more complex mechanisms operating in the solar system than will be considered in this work.

4. LIMITS AND IMPLICATIONS REGARDING THE EARLY SOLAR SYSTEM

From the upper limit on Δ_{26} of $|\Delta_{26} \pm 2\sigma_{\Delta}|$, along with the Mg and Al concentrations in the feldspar, one can obtain the upper limit on the $^{26}Al/^{27}Al$ ratio at the time when the feldspar finally crystallized. When more than one sample of a particular feldspar was analyzed, the upper limit comes from the analysis which yielded the lowest $|\Delta_{26} \pm 2\sigma_{\Delta}|$ value. The values obtained are shown in table 6 for all the extraterrestrial feldspars investigated. The upper limit on the amount of primordial ^{26}Al in the meteorite can be taken relative to Si by multiplying the upper limit on the $^{26}Al/^{27}Al$ by the Al/Si ratio in the meteorite as shown in table 7. It is important to note that the relative sizes of the maximum upper limits on $^{26}Al/Si$ obtained for our samples depend strongly on the Mg concentration we were able to obtain in the feldspar separate and the Al/Si ratio in the extraterrestrial object. Thus, a high upper limit for a sample <u>does not imply</u> that the sample was more primitive.

Table 7 also summarizes some of the relevant information on each sample; the existence of ^{129}Xe anomalies, R (an unknown nucleus which fits prescription; presumably ^{244}Pu, although this has not been proven) fission xenon, and excess R fission tracks.

Having determined the upper limit on the $^{26}Al/Si$ ratio at the time of solidification, a limit on the heat output from ^{26}Al at the time of solidification of the feldspar can be calculated in the following manner. The energy released from ^{26}Al available for heating is

$$E(MeV) = 1.83\ MeV(\gamma) + (0.85) \times (0.42) \times (1.16)\ MeV(\beta^{+}) + (1.7) \times (0.511)\ Mev(e^{\pm})$$
$$+ (0.04) \times (1.12)\ MeV(\gamma) = 3.16\ MeV,$$

24

where the decay scheme and energies are from Ferguson [22] and the electron capture energy is neglected since the neutrino carries most of it away, and thus it does not contribute to any heating. The fraction of the β energy contributing to the heating was taken as 0.42 β_{max} from the calculation of Marinelli, Brinckehoff and Hine [23] which included the coulomb correction but neglected forbiddenness. The accuracy of this approximation is shown in the Kurie plot of Ferguson [22]. We will also assume that primordial solar system material had chondritic composition and thus was $\sim$ 17% Si [24]. Using the above estimates, the rate of heat production at the time of crystallization in terms of ^{26}Al/Si is:

$$H_o = 0.00048\ (^{26}\text{Al/Si})$$

where the units of H_o are cal/gm/yr and ^{26}Al/Si is normalized to Si = 10^6. Thus, by assuming the upper limit on the ^{26}Al/Si ratio from a particular extraterrestrial sample represents ^{26}Al/Si in primordial matter, one obtains a limit on H_o. This calculation of the upper limit on the heat output from ^{26}Al is shown in table 7 for each sample.

The maximum central temperature (T_c) of an object due to ^{26}Al decay can be estimated from the case where all the heat output goes into heating up the body and none escapes through surface cooling (infinite radius object).

For this limit

$$T_c \approx \frac{H_o}{\lambda C_p} + T_o \qquad (6)$$

where $\lambda = 1/\tau_{mean}$ is the decay constant of ^{26}Al, T_o is the initial temperature and C_p is the specific heat of the object. The actual central temperature for a finite-sized object depends on the rate that heat diffuses from the center. The crucial parameter in studying the heat diffusivity of a sphere is

$$\eta \equiv \frac{\pi^2 Kt}{\rho C_p a^2} \qquad (7)$$

where K is the thermal conductivity of the media ; ρ is the density of the media; a is the radius of the object and t is the time after formation. For $\eta << 1$ and $t > 1/\lambda$, the center of the body is effectively insulated and heat will not flow out and $T_c - T_o \approx H_o/\lambda C_p$.

Detailed calculations using the solution to the temperature diffusion equation with a radioactive heat source and appropriate boundary conditions given by Urey [25] were found to agree with results found from the estimates given by eq. 6 and eq. 7.

26

Calculations have been performed using reasonable estimates for $\rho \approx 3.3$ g/cm^3, $C_p \sim 0.2$ cal/g/deg, $K \sim 0.007$ (cal/cm/deg/sec) and $T_o \sim 100^\circ$K. For these parameters, the central temperature due to ^{26}Al is at or near its maximum ($\eta << 1$) for all objects with a radius ≥ 100 km for $t \approx 10^7$ yrs. Thus, for a given H_o, if the core of a 100 km object will melt, so will the core of a 1000 km object and vice versa; however, if a 100 km object's core is just at the melting point, then the cores of all smaller objects will require a larger heat output to melt. The H_o which just yields the melting temperature for 100 km is then the minimum H_o necessary to melt objects. The minimum H_o from ^{26}Al necessary to raise the temperature near to the melting point of stony objects is $\sim 2 \times 10^{-4}$ cal/gm/yr. Since our parameter estimates probably yield a solution good only to within a factor of two, we can state this as a firm limit of at least 10^{-4}cal/gm/yr[37] from ^{26}Al would be necessary to melt the cores of objects. In terms of ^{26}Al/Si this means it takes ^{26}Al ≥ 0.2 atoms on a Si = 10^6 scale to melt objects. The maximum possible central temperature due to ^{26}Al heating, using the above-mentioned parameter values, has been calculated for each sample making the assumption that the ^{26}Al/Si value

from that sample was representative of the primordial solar system material. This maximum possible central temperature is shown in table 7. It is apparent that none of the meteoritic samples studied had enough ^{26}Al at the time of solidification of the feldspars to have produced any melting in the core of a planetary object. This, of course, does not rule out the possibility that ^{26}Al was melting cores in objects prior to the solidification time of these feldspars but had subsequently decayed down to below our limits of observation by the time of solidification. In fact, it is possible that some of our meteoritic samples solidified less than a million years after ^{26}Al was melting the cores of planetary objects. The strictest limits can be placed on the achondrite Moore County which had to solidify at least three million years after ^{26}Al was capable of any melting.

No ^{26}Al effects were observed in the lunar sample either. Of course, it would be difficult to find traces of primordial ^{26}Al in lunar samples since these rocks are the order of a billion years younger than the meteoritic samples. The lunar samples did, however, yield higher limits on $^{26}Al/Si$ due to the high Mg concentrations in the feldspar separates combined with high Al/Si ratios in the rocks.

The problems of nucleosynthesis of ^{26}Al have been discussed many times, estimates for the relative production rates for ^{26}Al relative to Si (on 10^6 scale)range from 100 [5] to 0.56 atoms [7]. This implies that the feldspars studied solidified at least one and one-half million years after the nucleosynthesis of ^{26}Al, and the strictest limit from Moore County yields at least four million years between nucleosynthesis of ^{26}Al and the solidification of that meteorite.

28
PP The effects of cosmic rays are below the limits of detection in the samples we investigated since, as pointed out by Clarke et al. [1] for the example of Bruderheim, the amount of $^{26}Al/(10^6$ atoms Si) produced by cosmic rays and integrated for the cosmic ray exposure age is 2.6×10^{-4}, which is far below our limit for Bruderheim of 0.1 $^{26}Al/(10^6$ atoms Si). However, for a feldspar separate similar in Mg/Al to our Moore Co. separate, where our best limits are obtained, an integrated cosmic ray exposure age of $\geq 1.5 \times 10^9$ years could be detected by our method.

5. CONCLUSIONS

The results of our enriched standards showed that five parts in 10^4 in the $^{26}Mg/^{24}Mg$ ratio can clearly be resolved. A wide range of extraterrestrial feldspar separates were analyzed including samples run by Clarke et al. (1) and found by them to have effects of 4-6 parts in 10^3. No resolvable effects were found. Thus, at present there is no positive experimental evidence for the existence of ^{26}Al in the early solar system. It therefore follows that there is no observational evidence which requires models of nucleosynthesis which produce ^{26}Al near the time of formation of the solar system. From our results, it can be stated that at the time of solidification of the feldspars which we analyzed, there could not have been enough ^{26}Al to melt the cores of a stony planetary object or to contribute significantly to their heating. However, because of its short mean life the possibility that ^{26}Al was melting objects a few million years prior to the solidification of the feldspars cannot be ruled out.

ACKNOWLEDGEMENT

We are extremely grateful to W. B. Clarke, J. R. deLaeter, H. P. Schwarcz and K. C. Shane for generously giving us their samples from Bruderheim and Khor Temiki.

The Lunatic I was kept in running condition for this work through constant pampering by P. C. Young, U. Derksen, A. Massey and C. Bauman. Additional pampering of the Lunatic as well as enlightening comments on the research was provided by D. A. Papanastassiou.

Encouragement to carry out this work was provided by W. A. Fowler. Helpful comments were made by all members of the Lunatic Asylum, especially D. S. Burnett, J. C. Huneke, A. L. Albee and G. P. Russ.

Aid on the mineral separations was obtained from J. Brown. We would also like to thank Lily Ray for doing an infinite number of time-consuming jobs without which this work would have been impossible. The microprobe analyses were performed by A. Chodos. V. Debelak did an amazing job in turning hieroglyphics into a finished manuscript.

One of us (DNS) was supported in part by an NDEA fellowship. This work was supported by NSF grants GP-15911, GP-9114 and GP-19887. The mass spectrometric facilities used in this work were developed under NSF grant GP-9114.

REFERENCES

[1] W. B. Clarke, J. R. de Laeter, H. P. Schwarcz, and K. C. Shane, Aluminum 26 - magnesium 26 dating of feldspar in meteorites, J. Geophys. Res. 75 (1970) 448.

[2] H. C. Urey, The cosmic abundances of potassium, uranium and thorium and the heat balances of the earth, the moon, and mars, Proc. Nat. Acad. Sci., 41 (1955) 127.

[3] H. C. Urey, The early history of the solar system as indicated by meteorites, Proc. Chem. Soc. (1958) 67.

[4] H. C. Urey, Evidence regarding the origin of the earth, Geochim. Cosmochim. Acta 26 (1962) 1.

[5] R. A. Fish, G. G. Goles and E. Anders, The record in the meteorites, Astrophys. J. 132 (1960) 293.

[6] W. A. Fowler, J. L. Greenstein, F. Hoyle, Nucleosynthesis during the early history of the solar system, Geophys. J. Roy. Astron. Soc. 6 (1962) 148.

[7] H. Reeves and J. Audouze, Early heat generation in meteorites, Earth Planet. Sci. Lett. 4 (1968) 135.

[8] G. J. Wasserburg, D. N. Schramm and J. C. Huneke, Nuclear chronologies for the galaxy, Astrophys. J. 157 (1969) L91.

[9] A. C. Daughtry, D. Perry, and M. Williams, Magnesium isotopic distribution in dolomite, Geochim. Cosmochim. Acta 26 (1962) 857.

[10] E. J. Catanzaro and T. J. Murphy, Magnesium isotope ratios in natural samples, J. Geophys. Res. 71 (1966) 1271.

[11] G. J. Wasserburg, D. A. Papanastassiou, E. V. Nenow, C. A. Bauman, A programmable magnetic field mass spectrometer with on-line data processing. Rev. Sci. Instr. 40 (1969) 288.

[12] F. A. White, T. L. Collins, F. M. Rourke, Search for possible naturally occurring isotopes of low abundance, Phys. Rev. 101 (1956) 1786.

[13] J. A. McHugh, Surface ionization -- the rhenium V-type single filament, Int. J. Mass Spectrom., Ion Phys. 3 (1969) 267.

[14] D. S. Burnett, H. J. Lippolt and G. J. Wasserburg, The relative isotopic abundance of K^{40} in terrestrial and meteoritic samples, J. Geophys. Res. 71 (1966) 124.

[15] E. J. Catanzaro, T. J. Murphy, E. L. Garner, W. R. Shields, Absolute isotopic abundance ratios and atomic weight of magnesium, J. Res. N.B.S. 70A (1966) 453.

[16] H. G. Sanz and G. J. Wasserburg, Determination of an internal ^{87}Rb - ^{87}Sr isochron for the Olivenza chondrite, Earth Planet. Sci. Lett. 6 (1969) 335.

[17] G. J. Wasserburg, H. G. Sanz, A. E. Bence, Potassium-feldspar phenocrysts in the surface of Colomera, an iron meteorite, Science 161 (1968) 684.

[18] M. W. Rowe and P. K. Kuroda, Fissiogenic xenon from the Pasamonte meteorite, J. Geophys. Res. 70 (1965) 709.

[19] G. J. Wasserburg, J. C. Huneke, D. S. Burnett, Correlation between fission tracks and fission-type xenon from an extinct radioactivity, Phys. Rev. Lett. 22 (1969) 1198.

[20] F. A. Podosek, The abundance of ^{244}Pu in the early solar system, Earth Planet. Sci. Lett. 8 (1970) 183.

[21] J. C. Huneke, D. S. Burnett, D. N. Schramm and G. J. Wasserburg, Correlation between fission tracks and fission-type xenon in the meteorite Guareña. In preparation (1970).

[22] J. Ferguson, Al^{26} decay scheme, Phys. Rev. 112 (1958) 1238.

[23] L. D. Marinelli, R. F. Brinckerhoff and G. J. Hine, Average energy of beta-rays emitted by radioactive isotopes, Rev. Mod. Phys. 19 (1947) 25.

[24] H. C. Urey and H. Craig, The composition of the stone meteorites and the origin of the meteorites, Geochim. Cosmochim. Acta 4 (1953) 36.

[25] H. C. Urey, The planets, their origin and development, Oxford Press: London (1952).

[26] W. R. Van Schmus and J. A. Wood, A chemical-petrologic classification for the chondritic meteorites, Geochim. Cosmochim. Acta, 32 (1969) 1327.

[27] M. Hey and A. J. Easton, The Khor Temiki meteorite, Geochim. Cosmochim. Acta 31 (1967) 1789.

[28] L. Loveland, R. A. Schmitt, and D. E. Fisher, Aluminum abundances in stony meteorites, Geochim. Cosmochim. Acta 33 (1969) 375.

[29] Lunar Sample Preliminary Examination Team, Preliminary examination of lunar samples from Apollo 12, Science 167 (1970) 1325.

[30] C. M. Hohenberg, F. A. Podosek, J. H. Reynolds, Xenon-iodine dating: sharp isochronism in chondrites, Science 156 (1967) 233.

[31] J. H. Reynolds, Plutonium-244 in the early solar system, Nature 218 (1968) 1024.

[32] O. Eugster, P. Eberhardt and J. Geiss, Isotopic analysis of krypton and xenon in fourteen stone meteorites, J. Geophys. Res. 74 (1969) 3874.

[33] Lunatic Asylum, Mineralogic and isotopic investigations on lunar rock 12013, Earth Planet. Sci. Lett. 9 (1970) 137.

[34] R. L. Fleischer, P. B. Price and R. M. Walker, Spontaneous fission tracks from extinct Pu^{244} in meteorites and the early history of the solar system, J. Geophys. Res. 70 (1965) 2703.

[35] Y. Cantelaube, M. Maurette, P. Pellas, Traces d'Ions Lourds dans les Mineraux de la Chondrite de St. Severin, Radioactive dating and methods of low level counting, Int. Atomic Energy Agency, Vienna, (1967) 213.

[36] J. A. Maxwell, S. Abbey, W. H. Champ, Oxygen, silicon, and aluminum in lunar samples by 14 MeV neutron activation, Science 167 (1970) 528.

[37] E. Anders, Origin, age and composition of meteorites, Space Sci. Rev. 3 (1964) 583.

Table 1

Enriched standards

Standard	Δ^{G}_{25}	Δ^{S*}_{25}	Run #	$(^{26}Mg/^{24}Mg)_c$	2σ x 10^4
0	0.0	0.0	**	0.139794	0.9
I	2.22	1.92	63	0.139740	1.2
	2.22	1.88	74***	0.139741	1.3
II	4.55	5.00	62	0.139654	1.8
III	9.08	9.38	61	0.139532	1.9
	9.08	9.98	88****	0.139546	2.9
IV*****	22.27	22.77	53	0.139158	4.0

* Calculated from

$$\Delta^{S}_{25} = \left[\sqrt{\frac{(^{26}Mg/^{24}Mg)_o}{(^{26}Mg/^{24}Mg)_i}} - 1\right] \times 10^4$$

** Combination of all normal runs up to the running of the enriched standards (run #'s 38-46, 50, 56; see table 4).

*** This run was done as a check after several meteoritic runs were made to make sure the standards were still reproducible. This point is not included in Fig. 3.

**** This sample went through the entire chemistry including 1/3 ml HF and 1/3 ml $HClO_4$ and has been corrected for the blank accordingly. (It is not included in Fig. 3).

***** This standard was not put through the ion exchange column and thus did not run as stably as the others.

Table 2

Terrestrial feldspars

Sample	Description	Mg Concentration (ppm)+	Mg "hot spots"	Run # (Chronological order of runs)	$\Delta^{*}_{26} \pm 2\sigma_{\Delta}$
Kragero, Norway Andesine	Single crystal	26	No	47	+ 1.5 ± 4.5
India, Orthoclase	Single crystal	5	Yes	No mass spectrometry	
Lakeview, Oregon Bytownite	Single crystal	490	No	48	- 1.7 ± 4.7
Louis Lake, Wyoming Microcline	Min. separate	630	No	51	+ 1.3 ± 3.3
Grenville Front, Canada Microcline	Min. separate	780	Yes	No mass spectrometry	
Clear Lake, Oregon Bytownite	Single crystal	990	No	83 91	0.0 ± 8.2 +1.2 ± 2.6

+ Corrected for dissolution blank.

* $$\Delta_{26} = \left[\frac{(^{26}Mg/^{24}Mg)_s - (^{26}Mg/^{24}Mg)_o}{(^{26}Mg/^{24}Mg)_o}\right] \times 10^4$$

and $(^{26}Mg/^{24}Mg)_o = 0.139805$ (see table 4)

$2\sigma_{\Delta} = 2(\sigma_s + \sigma_o)$ where $2\sigma_o = 9.6 \times 10^{-5}$.

Table 3

Samples received from Clarke et al. [1]

Sample	Mg concentration Clarke et al. [1] (ppm)	Mg concentration atomic absorption (ppm) +	$\Delta_{26} \pm 2\sigma_\Delta$ Clarke et al. [1]	Run #	$\Delta_{26}^{*} \pm 2\sigma_\Delta$	$\lvert\Delta_{26} \pm 2\sigma_\Delta\rvert$
Khor Temiki Feldspar						
a) Mg soln.				73	-1.3 ± 4.1	5.4
b) Mg soln. through column	3120 ± 200	3120 ± 310	41 ± 18	66	-2.4 ± 2.3	4.7
				87	+0.3 ± 4.3	4.6
c) Mineral grains				78	-0.5 ± 3.5	4.0
Bruderheim III Feldspar	Not given	3230 ± 320	60 ± 26	69	+0.1 ± 4.2	4.3
Bruderheim IV Feldspar	3660 ± 490	4830 ± 490	43 ± 18	76	+1.2 ± 3.7	4.9

+ Corrected to dissolution blank.

* $$\Delta_{26} = \frac{\left[\left(^{26}Mg/^{24}Mg\right)_s - \left(^{26}Mg/^{24}Mg\right)_o\right]}{\left(^{26}Mg/^{24}Mg\right)_o} \times 10^4$$

$2\sigma_\Delta = 2\sigma_s + 2\sigma_o$. $\left(^{26}Mg/^{24}Mg\right)_o = 0.139805$. $2\sigma_o = 9.6 \times 10^{-5}$

Clarke et al.'s errors have been converted from their published ~ 1σ errors to 2σ errors for comparison with our errors.

Table 4

Normal Mg standard

Run #	($^{26}Mg/^{24}Mg$) Mean	$2\sigma \times 10^4$	Comments
38 - 46	0.139794	5.97	Early data
50	0.139791	3.03	
56	0.139822	2.77	
67	0.139812	2.35	
70	0.139795	3.00	Through column
71	0.139831	1.56	Through column
77	0.139823	1.87	Through column
85	0.139815	1.81	Through column

Mean of data from all normal runs = 0.139805 with a fractional 2σ error of 9.6 parts in 10^5.

Normalized to $^{25}Mg/^{24}Mg = 0.12663$ [15].

Table 5

Extraterrestrial samples

(other than those received from Clarke et al. [1])

Sample	Run #	$\Delta_{26} \pm 2\sigma_\Delta^*$	$\lvert\Delta_{26} \pm 2\sigma_\Delta\rvert$
Bruderheim	52	-1.1 ± 5.3	6.4
Whole rock	89	-2.6 ± 2.8	5.4
Colomera			
Feldspar inclusion	64	+ 0.7 ± 2.7	3.4
Guareña			
Feldspar separate	86	-1.1 ± 3.5	4.6
Juvinas	80	-2.3 ± 4.6	6.9
Feldspar separate	84	-0.5 ± 2.6	3.1
Lunar rock 10024			
Feldspar separate	92	+0.8 ± 3.0	3.8
Lunar rock 12064			
Feldspar separate	79	+ 2.3 ± 2.4	4.7
Lunar rock 12013	90	-2.1 ± 2.8	4.9
Feldspar separate			
Moore Co. I	68	+ 2.3 ± 2.5	4.8
Feldpsar separate			
Moore Co. II	75	-1.3 ± 2.9	4.2
Feldspar separate			
Pasamonte	82	-1.0 ± 3.1	4.1
Feldspar separate			
St. Severin	81	-0.3 ± 2.6	2.9
Feldspar separate			

* $$\Delta_{26} = \left[\frac{(^{26}Mg/^{24}Mg)_s - (^{26}Mg/^{24}Mg)_o}{(^{26}Mg/^{24}Mg)_o} \right] \times 10^4$$

$2\sigma_\Delta = 2(\sigma_s + \sigma_o)$

$(^{26}Mg/^{24}Mg)_o = 0.139805$ and $2\sigma_o = 9.6 \times 10^{-5}$ (see table 4).

The mean of all extraterrestrial Δ_{26} values shown in this table is -4.8×10^{-5}.

Table 6

Upper limits on ^{26}Al in extraterrestrial feldspar

Feldspar	$\lvert\Delta_{26} \pm 2\sigma_{\Delta}\rvert$ (parts in 10^4)	Mg^+ Concentration (ppm)	Al Concentration (%)	$(^{26}Al/Mg)^{max}$ solidification (units of 10^{-6})	$(^{26}Al/^{27}Al)^{max}$ solidification (units of 10^{-6})
Bruderheim III	4.3	3230	9.7	48	1.6
Bruderheim IV	4.9	4830	9.7	55	2.7
Colomera Inclusion	3.3	213	9.8	37	0.081
Guareña	4.6	1890	11.7	51	0.83
Juvinas	3.1	1400	18.6	35	0.26
Khor Temiki	4.0	3120	10.6	44	1.3
Lunar rock 10024	3.8	2350	~11	43	0.91
Lunar rock 12064	4.6	1190	18.0	52	0.34
Lunar rock 12013	4.9	4500	~12	55	2.1
Moore Co. I	4.7	144	16.6	53	0.046
Moore Co. II	4.2	248	18.7	47	0.063
Pasamonte	4.1	915	17.4	45	0.24
St. Severin	2.9	2000	11.4	33	0.57

+ Corrected for blank

Table 7

Upper limits on heating from ^{26}Al at the time of solidification of the feldspars

Sample	Type	^{129}Xe anomaly	R fission Xe	Excess Fission Tracks	(Al/Si) (2)	$(^{26}Al/Si)^{Max}$ Solidification on scale Si = 10^6 atoms	H_o Units of 10^{-4} cal/gm/yr	Max.change in central temp. $T_c - T_o$ (deg. K)
Bruderheim[3,6]	Chondrite (L6)[1]	Yes	Yes		0.062	0.10	0.48	260
Colomera	Iron							
Guareña[5]	Chondrite (H6)[1]	Yes	Yes	Yes	0.061	0.05	0.24	130
Juvinas[8,3]	Ca-rich achondrite (eucrite)	Yes	Yes		0.29	0.08	0.36	190
Khor Temiki[3,7]	Ca-poor enstatite achondrite (aubrite)	Yes	No		0.015	0.02	0.09	50
Lunar rock 10024	High-K basalt				0.22	0.20	0.96	(510)
Lunar rock 12064	Gabbroic				0.34	0.12	0.56	(300)
Lunar rock 12013	Luny rock 2	No	No	No	0.22	0.45	2.18	(1170)
Moore Co.[3,6,9]	Ca-rich achondrite (eucrite)	Yes	Yes	Yes	0.29	0.01	0.06	30
Pasamonte[6]	Achondrite	Yes	Yes		0.29	0.07	0.33	180
St. Severin[10,11]	Chondrite (LL6)	Yes	Yes	Yes	0.061	0.03	0.16	90

1. Chondrite classification, Van Schmus and Wood [26].

2. Data for Khor Temiki from Hey and Easton [27] and for other meteorites from Loveland et al. [28]. Apollo 12 data from LSPET [29], Apollo 11 data from Maxwell et al. [36].

3. Limits from analysis which yielded lowest $^{26}Al/^{27}Al$ for that object.

4. ^{129}Xe results from Hohenberg, Podosek and Reynolds [30].

5. Xe and track results on Guareña from Huneke, Burnett, Schramm, and Wasserburg [21].

6. Xe results from Reynolds [31].

7. Xe results from Eugster et al. [32].

8. Xe and track results from Lunatic Asylum [33].

9. Track results from Fleischer, Price, and Walker [34].

10. Xe results from Wasserburg, Huneke and Burnett [19].

11. Track results from Cantelaube et al. [35].

* Parameters used; $\rho = 3.3$ g/cm^3, $C_p = 0.2$ cal/g/deg, $K = 0.007$ cal/cm/deg/sec, $T_o = 100°K$.

FIGURE CAPTIONS

Fig. 1. Typical peak shape for ^{24}Mg under standard running conditions is shown with expanded view of the peak top, demonstrating that the peak top is flat within calculated 2σ ion statistics. The plotted points are DVM measurements. The variation in magnetic field (0.05g) in cycling is compared with the peak width. Source slit was 0.2 mm and collector slit 0.64 mm.

Fig. 2. Discrimination factor (1-ε) is shown for sets of five ratios taken throughout a run from two different mass spectrometer runs. This demonstrates that the discrimination factor is approximately a constant (to within ± 1 part in 1000) within a run and from one run to another. Points for run 76 are from the entire period that running conditions existed until the sample started to die; run 80 ran for much longer and the final points are not shown.

Fig. 3. Correlation of enrichments (Δ_{25}) in $^{25}Mg/^{24}Mg$ calculated from gravimetry (G) and from mass spectrometry (S). Results fof four measurements are shown. The lowest (zero) standard is used for normalization. It can be seen that ~ 2.5 parts in 10^4 can be clearly resolved for Δ_{25}, thus five parts in 10^4 could be easily resolved for $^{26}Mg/^{24}Mg$.

Fig. 4. Mass spectrometer measurements (excluding enriched standards of $^{26}Mg/^{24}Mg$ (without blank corrections) plotted as parts in 10^4 deviation from the normal value of 0.139805 ± 0.000013. The analyses are shown in the chronological order in which the measurements were made. For calculated Δ_{26} values corrected for blanks, see tables 2, 3, 4 and 5 (blank corrections are all less than 7% with the exception of the Moore County I separate).

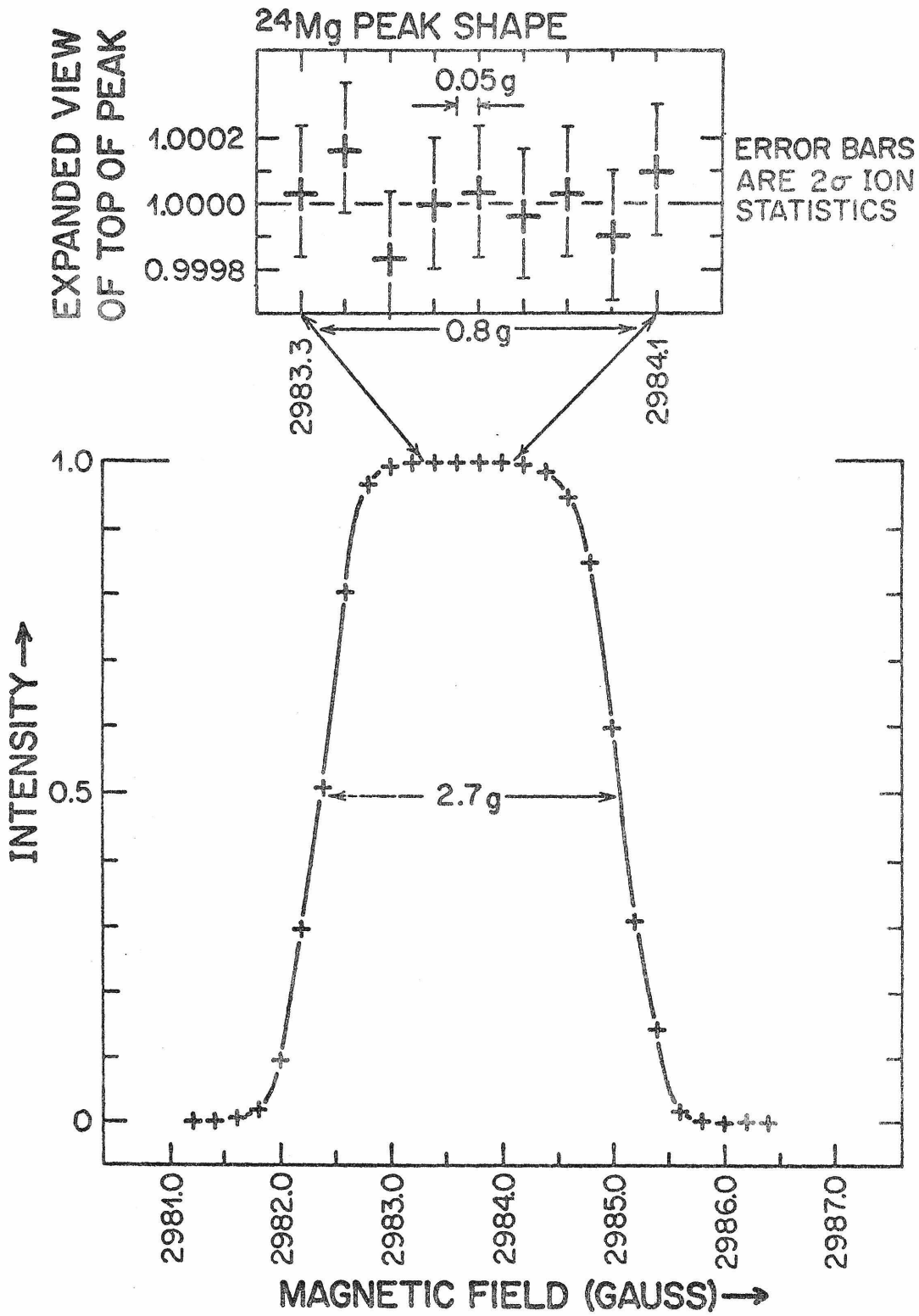

FIG. 1
SCHRAMM, TERA, WASSERBURG

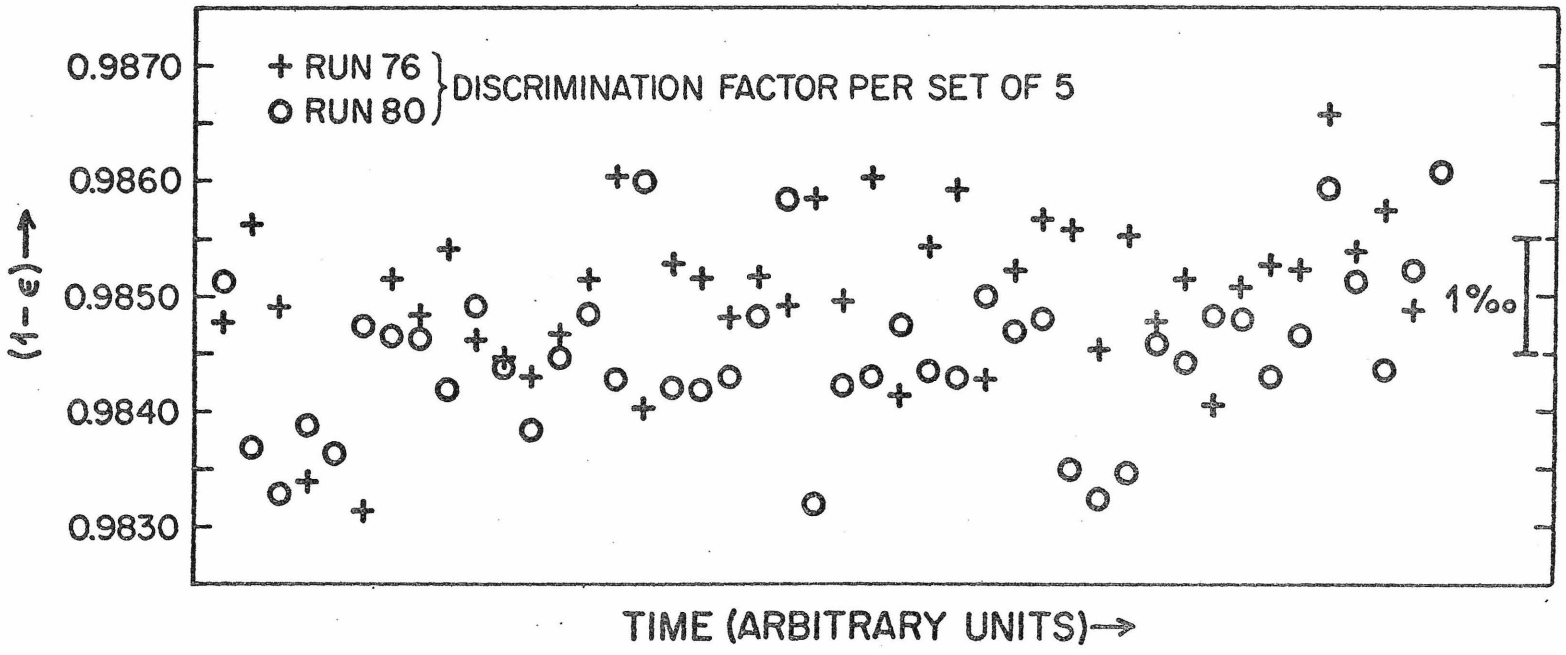

FIG. 2
SCHRAMM, TERA, WASSERBURG

FIG. 3
SCHRAMM, TERA, WASSERBURG

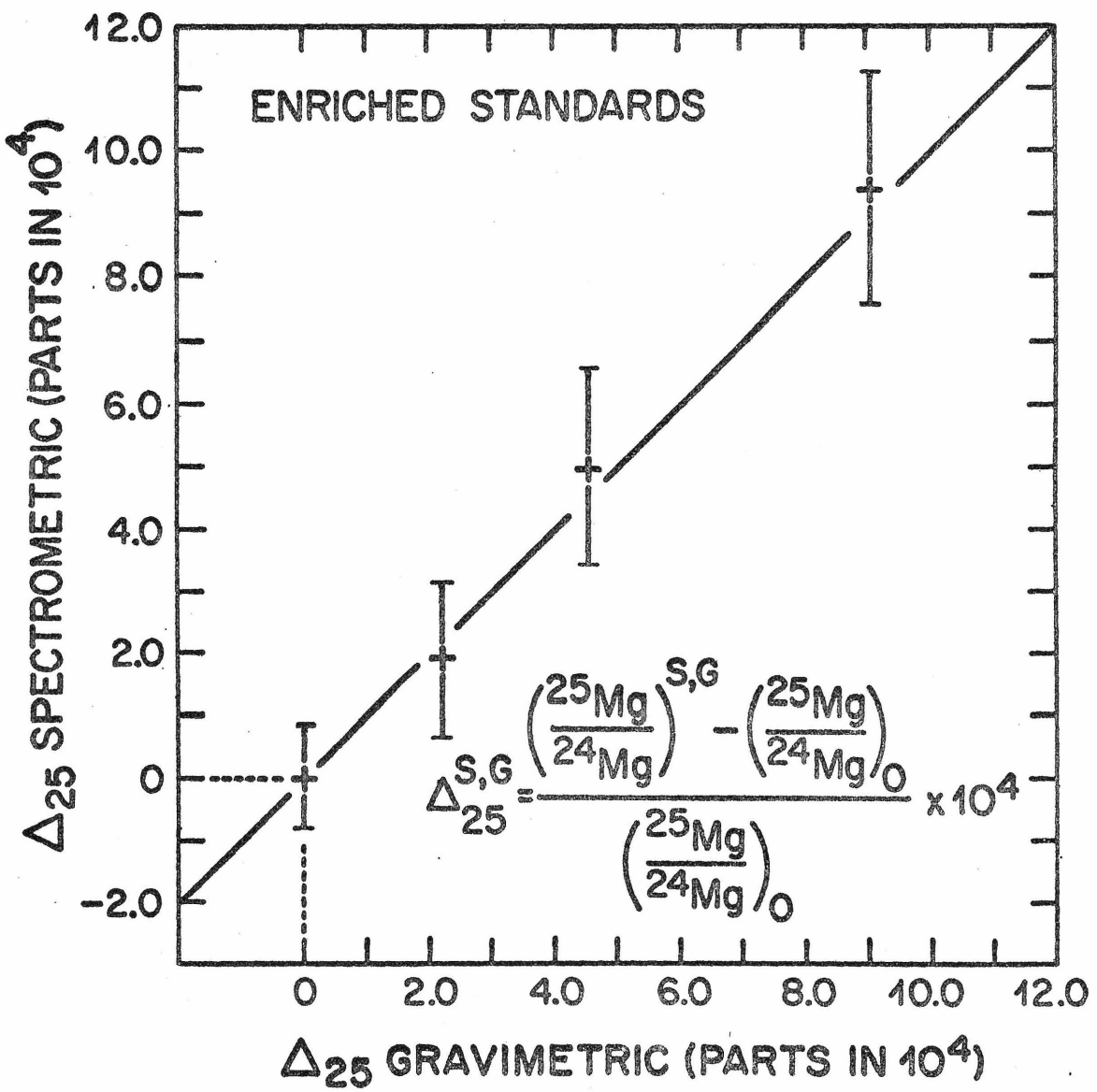

FIG. 4

SCHRAMM, TERA, WASSERBURG